

UM-HSRI-81-19-5

PROPERTIES OF ANTILOCK SYSTEMS

C.C. MacAdam  
P.S. Fancher

DESCRIPTIVE PARAMETERS USED IN ANALYZING THE BRAKING  
AND HANDLING OF HEAVY TRUCKS

Volume 5

May 1981

Technical Report Documentation Page

1. Report No. UM-HSRI-81-19-5	2. Government Accession No.	3. Recipient's Catalog No.	
4. Title and Subtitle DESCRIPTIVE PARAMETERS USED IN ANALYZING THE BRAKING AND HANDLING OF HEAVY TRUCKS  Properties of Antilock Systems		5. Report Date May 1981	
		6. Performing Organization Code (361507) 361912	
7. Author(s) C. C. MacAdam and P.S. Fancher		8. Performing Organization Report No. UM-HSRI-81-19-5	
9. Performing Organization Name and Address Highway Safety Research Institute The University of Michigan Huron Parkway & Baxter Road Ann Arbor, Michigan 48109		10. Work Unit No.	
		11. Contract or Grant No. MVMA Proj. 1196	
12. Sponsoring Agency Name and Address Motor Vehicle Manufacturers Association 300 New Center Building Detroit, Michigan 48202		13. Type of Report and Period Covered Final 7/1/77-4/30/81	
		14. Sponsoring Agency Code	
15. Supplementary Notes			
<p>16. Abstract</p> <p>This volume is one of a set of five volumes being prepared under support from the Motor Vehicle Manufacturers Association. The set of volumes is entitled "Descriptive Parameters Used in Analyzing the Braking and Handling of Heavy Trucks." The volumes address the acquisition of data on (1) steering and suspension systems, (2) inertial properties, (3) tires, (4) brakes, and (5) antilock systems.</p> <p>In this volume, results of laboratory tests performed on five commercial air brake antilock systems are discussed. A hybrid computer has been used to simulate wheel dynamics and to control test sequencing. Test results for each system under a variety of simulated test conditions have been digitized and stored on magnetic tape.</p>			
17. Key Words Antilock, antiskid, brakes, braking performance, tests, data, wheel dynamics		18. Distribution Statement  UNLIMITED	
19. Security Classif. (of this report) NONE	20. Security Classif. (of this page) NONE	21. No. of Pages 89	22. Price

## ACKNOWLEDGEMENTS

The work described in this report was supported by the Motor Vehicle Manufacturers Association. The cooperation of the following people associated with the various MVMA member companies and antilock manufacturers is appreciated: Mr. Ray Murphy, Freightliner; Mr. M.L. Hutchins, Bendix Heavy Vehicle Systems Group; Mr. Clark Lowman and Mr. George Megginson, Kelsey-Hayes Research and Development Center; Mr. Yudh Vir Rajput, B.F. Goodrich; Mr. Richard Bueler, Wagner Electric; and Mr. Hal Reigner, Eaton Research.

## TABLE OF CONTENTS

1.	INTRODUCTION . . . . .	1
2.	DESCRIPTION OF TESTING . . . . .	2
	2.1 Hardware - Computer Test Setup . . . . .	3
	2.2 Special Logic Module Tests . . . . .	9
3.	DISCUSSION OF RESULTS . . . . .	13
	3.1 Antiskid System Characteristics . . . . .	13
	3.2 Antiskid Digital Library . . . . .	26
	3.3 Special Logic Module Test Results . . . . .	30
4.	GENERAL OBSERVATIONS AND CONCLUSIONS . . . . .	44
5.	REFERENCES . . . . .	47
6.	APPENDIX A . . . . .	48
7.	APPENDIX B . . . . .	79

## 1.0 INTRODUCTION

Past research by HSRI relating to antilock braking performance of commercial vehicles has indicated a need to define in detail the range and variety of current antilock system performance. The purpose of MVMA Project #1.37 was to collect data suitable to those needs for further study of commercial vehicle antilock braking performance. The results obtained in Project #1.37 are reproduced in this report.

The first portion of this report, Section 2.0, describes the work performed in testing of each system, followed by a discussion in Section 3.0 of the test results. General observations and conclusions are presented in Section 4.0.

Sample time histories, illustrating the performance of each antilock system, are given in Appendix A. Appendix B contains an example-analysis showing how a mathematical representation of a system's control logic can be derived from test data.

## 2.0 DESCRIPTION OF TESTING

Five air-brake antiskid systems were acquired for testing during the course of this project. Each of these systems is listed in Table 1 by manufacturer and model number.

---

Table 1. Antiskid Systems Tested.

<u>Manufacturer</u>		<u>Model/Part No.</u>
Bendix	Logic Module	EC-1 289359
	Air Valve	M-6 289614
B.F. Goodrich	Logic Module	1800-6C
	Air Valve	65328-C
Eaton	Logic Module	670002
	Air Valve	600000
Kelsey-Hayes	Logic Module	KH095470006 ASSY 1088
	Air Valve	09869704
Wagner	Logic Module	AF-97781-1227
	Air Valve	02178

---

The general operational features displayed by these systems cover a variety of characteristics: single/double solenoid air valves, pneumatic logic, and high-frequency pulse-rate solenoid modulation. As will be shown, these differences in hardware and control strategies can result in significantly different wheel speed cycling behavior during antiskid operation.

## 2.1 Hardware - Computer Test Setup

The general test setup is shown in the block diagram of Figure 1. The antiskid hardware (air valve and logic module) was located in a laboratory area and connected by trunk lines to a hybrid computer (Figure 2). Single wheel dynamics were simulated on the analog computer and generated the required wheel speed signal to the antiskid logic module. Brake pressure was transduced from the brake cans connected to the antiskid air valve and returned to the analog computer for the calculation of brake torque. The digital computer was responsible for program control and test sequencing by altering parameters on the analog computer between tests, initiating each test, and recording the digitized variables on magnetic tape during each run. The data recorded on magnetic tape resulted in a digital library of time histories for each antiskid system.

The matrix of simulated test conditions, represented by parameters on the analog computer, included three repeats for each variation in wheel load, wheel inertia, tire-road friction, and initial velocity. Table 2 lists the specific values of each parameter variation used in the test matrix, totaling 288 tests for each system.

Table 3 lists the variables recorded during each test and stored as a digital time history at 0.01-second intervals on magnetic tape. A sample test result showing time histories for the Kelsey-Hayes system is given in Figure 3.

Each test was initiated by a signal from the hybrid computer which actuated a solenoid-controlled valve applying a nominal 100 psi at the pilot port of the antiskid air valve. Completion of each test was determined by the simulated vehicle velocity falling below 10 ft/sec. The time base used in the digitized data was referenced to the time of application of pilot port pressure.

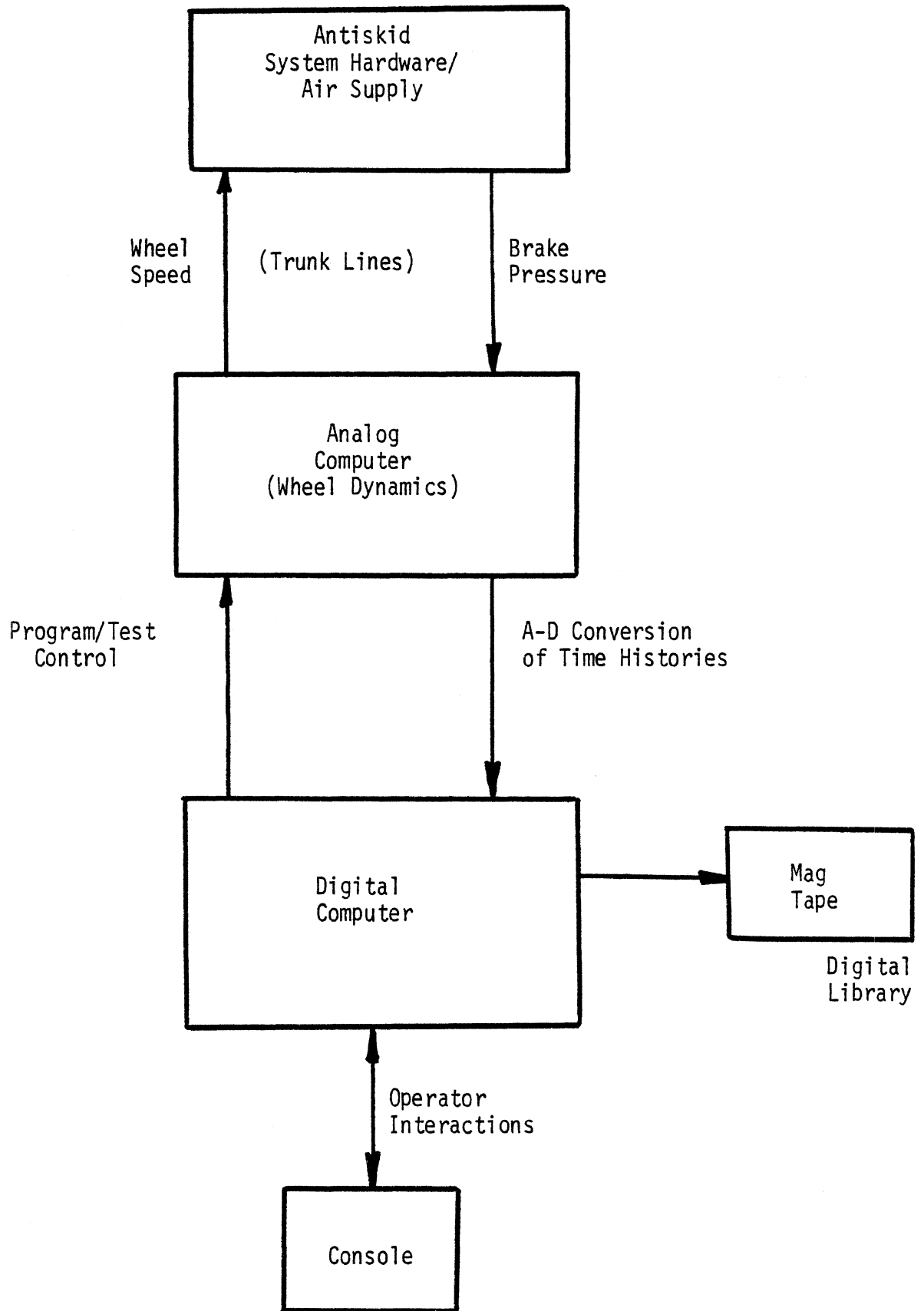


Figure 1. Antiskid test setup



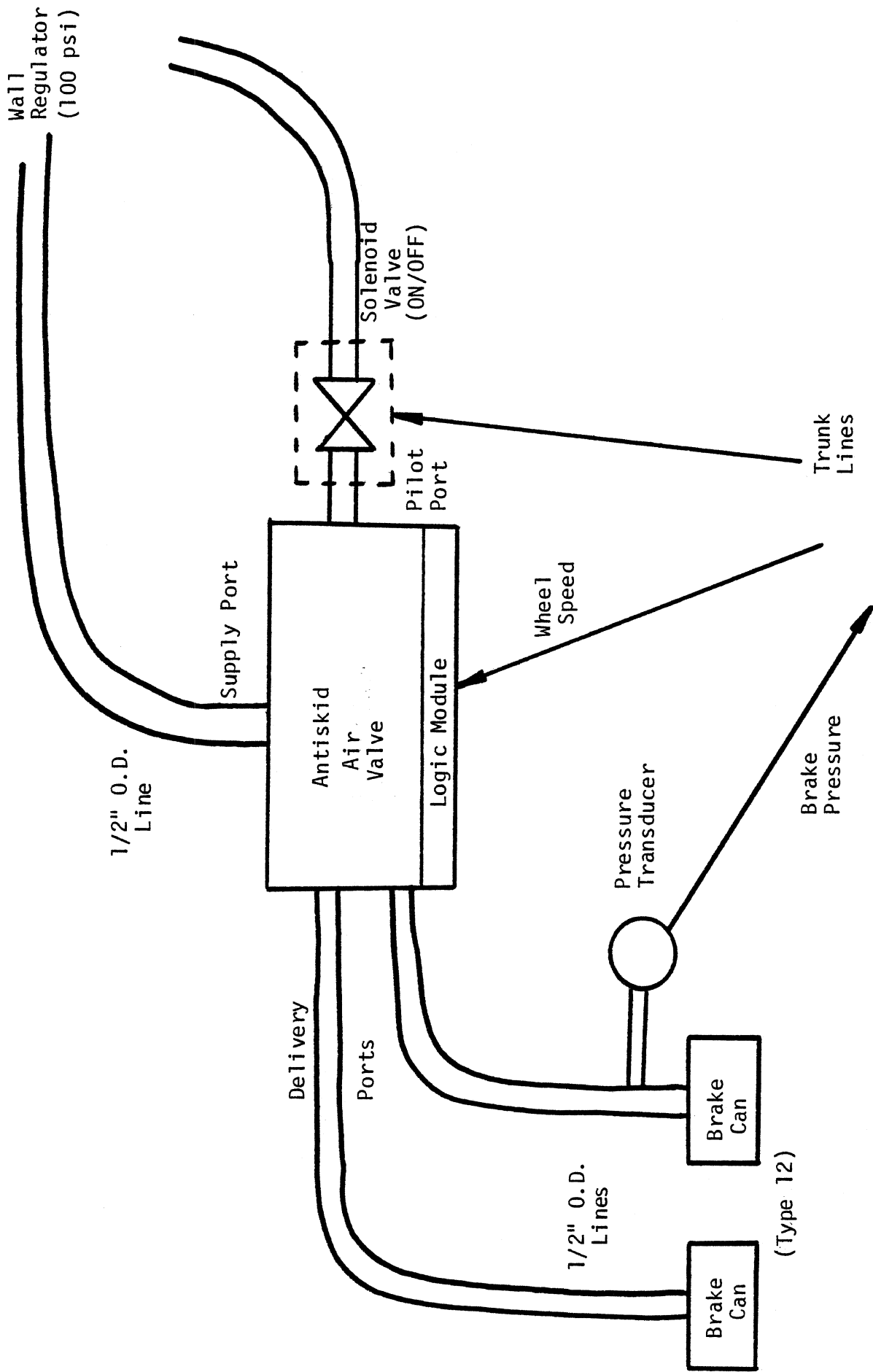


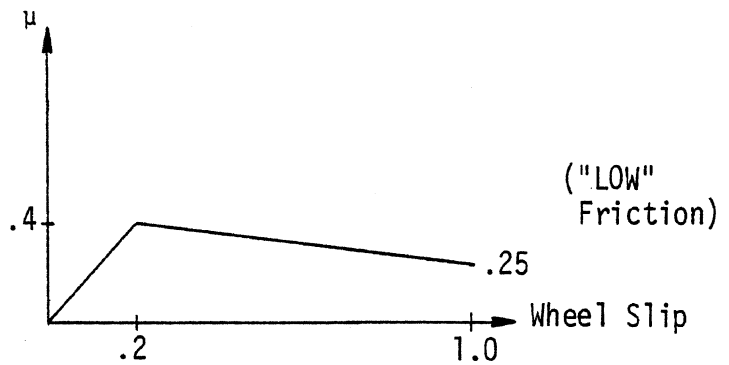
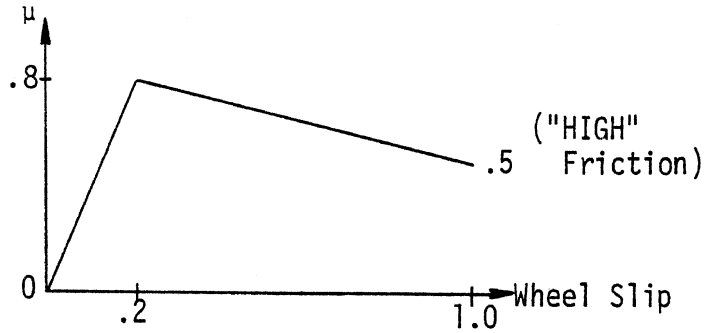
Figure 2. Antiskid hardware setup.

Table 2. Parameter Variations.

Wheel Load: 2500, 5000, 7500 lbs

Wheel Inertia: 50, 75, 100, 150, 200, 300, 400, 500 in-lb-sec<sup>2</sup>

Tire-Road Friction:



Initial Velocity: 60 mph (88 ft/s) , 30 mph (44 ft/s)

Repeats: 3

Table 3. Recorded Variables.

<u>Variable</u>	<u>Units</u>
Wheel Speed	(rad/sec)
Wheel Acceleration	(rad/sec <sup>2</sup> )
Vehicle Velocity	(ft/sec)
Brake Pressure	(psi)
Wheel Slip	(percent)
Friction Coefficient ( $\mu$ )	-----
Antiskid Solenoid Signal(s)	(volts)

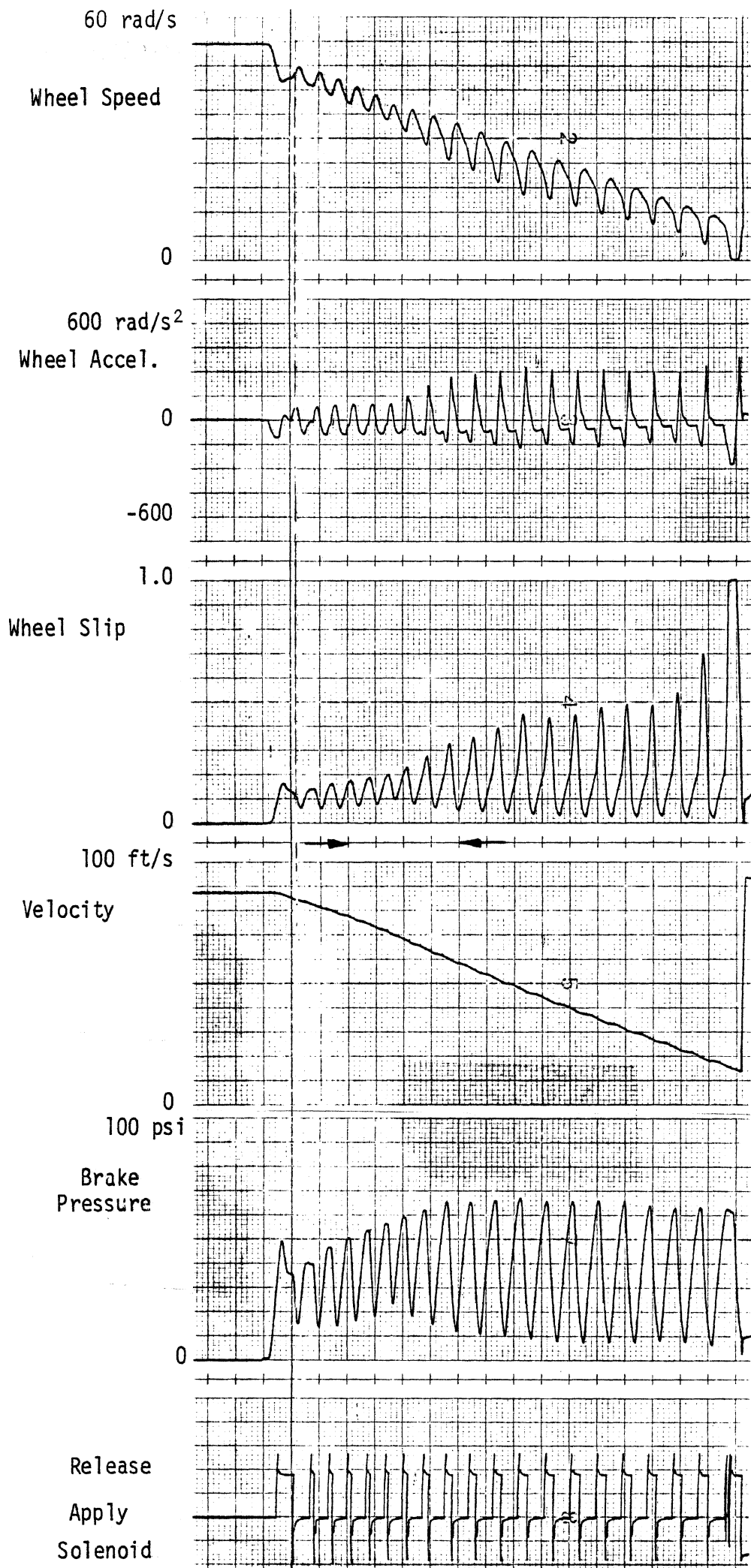


Figure 3. Kelsey-Hayes System

## 2.2 Special Logic Module Tests

In addition to the tests just described, a series of special tests were performed on the Kelsey-Hayes logic module to study the feasibility of identifying the control logic employed under specific conditions. The basic test arrangement is shown in Figure 4. Each test was initiated by a simulated treadle step input of 100 psi to a first-order filter simulating a representative brake pressure response, as shown in Figure 5. The simulated wheel speed signal was used as input to the antiskid logic module. At the occurrence of the antiskid brake release solenoid signal, the analog computer was placed in the HOLD mode and values of  $\omega = \omega_{\text{off}}$ ,  $\dot{\omega} = \dot{\omega}_{\text{off}}$ , and  $t = t_{\text{off}}$  were recorded. Plots of each  $(\dot{\omega}_{\text{off}}, \omega_{\text{off}})$  pair were also recorded on an X-Y recorder for each test. Following the recording and plotting of these variables, wheel inertia or brake pressure application rate was altered and the above test repeated. After ten or fifteen such variations and corresponding tests, a partial mapping in the  $\omega - \dot{\omega}$  plane of the first-cycle pressure-release switching curve was obtained. Figure 6 shows such a curve obtained for the Kelsey-Hayes logic module for a first-cycle, high- $\mu$ , 60-mph initial velocity condition. By including time ( $t = t_{\text{off}}$ ) values as a third coordinate axis, the two-dimensional curve extends to a three-dimensional switching locus. As will be demonstrated in Section 3.3, regression analyses can be performed on this three-dimensional data to yield an equation representing the switching surface involving these variables. This expression could then be used to approximate the anti-skid control logic under these same, or similar, operating conditions.

Identical logic module test sequences were performed for a lower initial velocity and a reduced tire-road friction coefficient. Tests were also conducted for second-cycle operation. Wheel spin-up conditions following the first cycle were used as the start or reference condition for the second-cycle tests. These results are discussed in Section 3.3. A similar example analysis, using the digital library data, is provided in Appendix B.

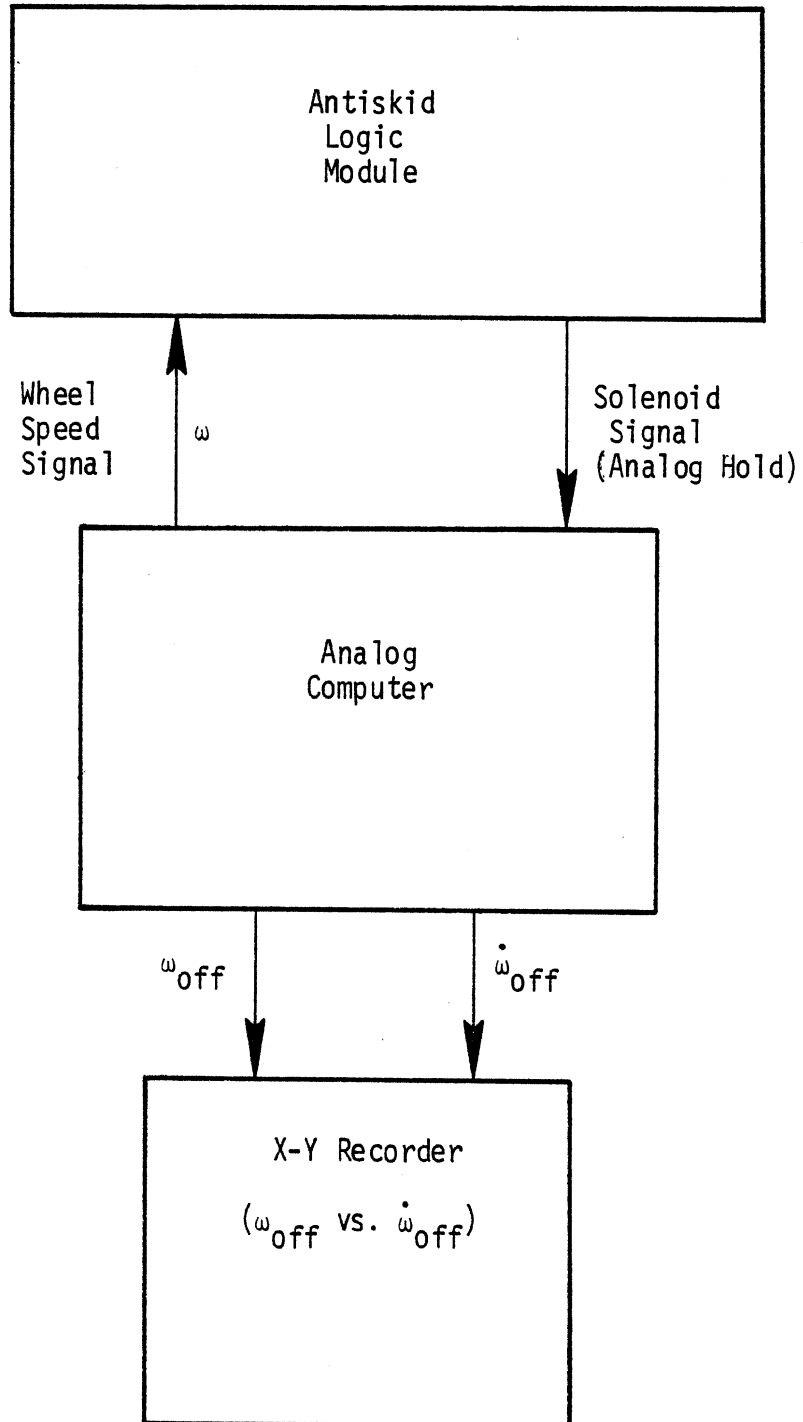


Figure 4. Logic module test setup.

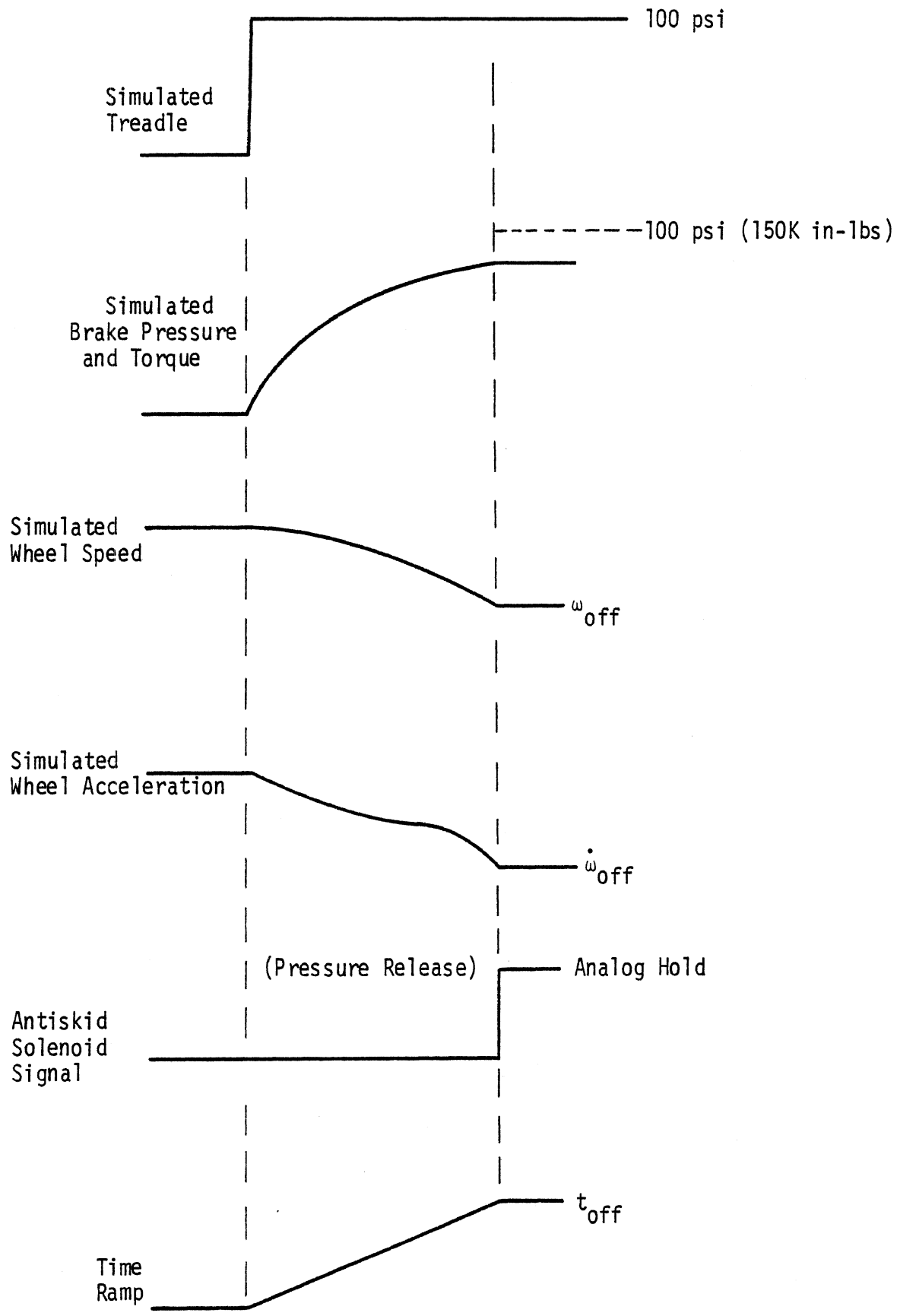


Figure 5. Typical logic module test (1st cycle).

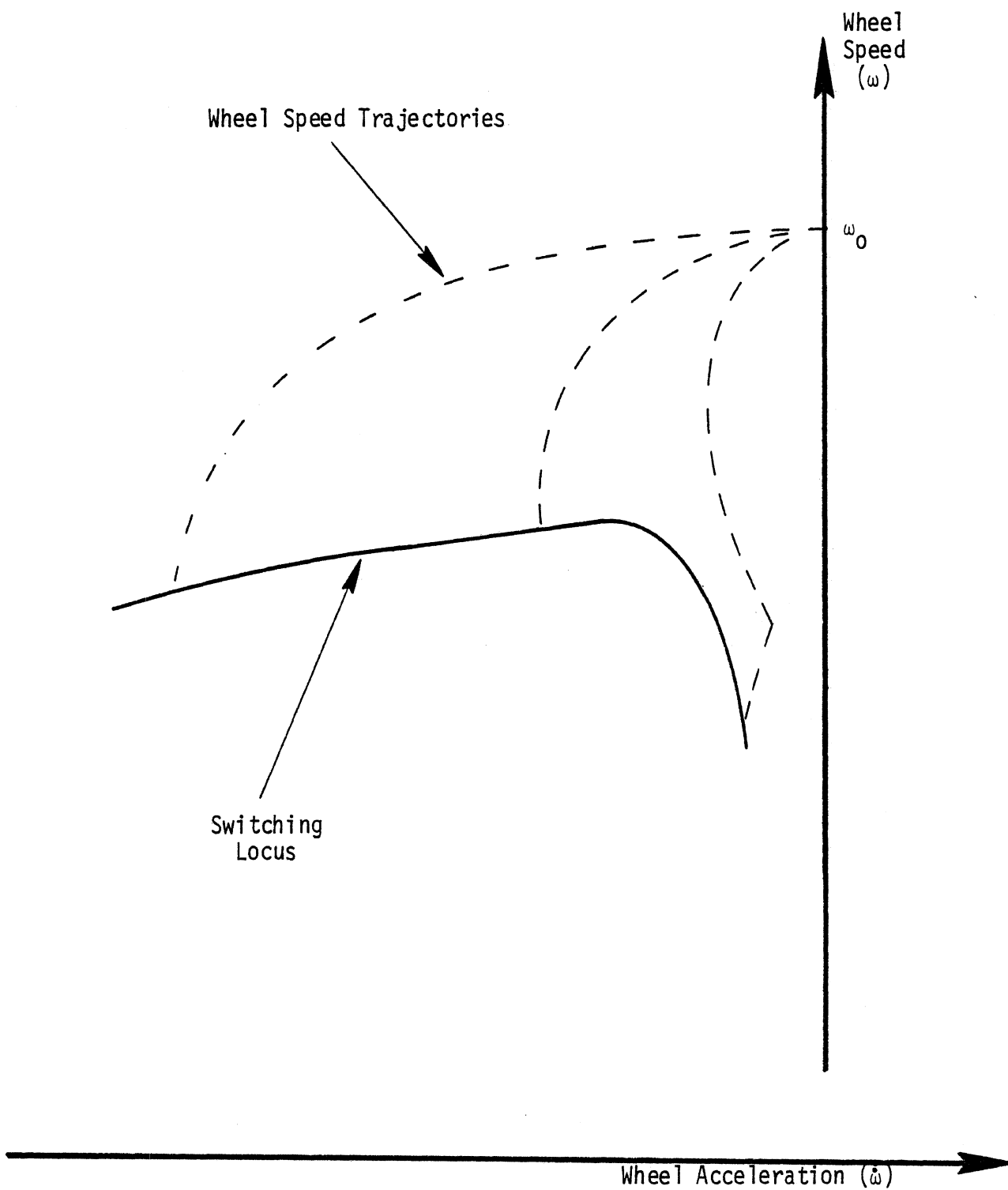


Figure 6. Logic module test result (K-H system).



### 3.0 DISCUSSION OF RESULTS

The first portion of this section is devoted to a discussion of features characteristic of each antiskid system using analog time histories to document these remarks. The majority of these time histories appear in Appendix A for various operating conditions. Simulation of the basic features for each system with the Phase III digital computer program are also outlined in this section. Following this discussion, the antiskid digital library tape and output format will be described and documented with example printouts. Finally, in Section 3.3, results of the special analog logic module tests described in Section 2.2 will be examined.

#### 3.1 Antiskid System Characteristics

3.1.1 Bendix Antiskid System. The most characteristic feature of the Bendix system is the rapid on-off sawtooth modulation of brake chamber pressure appearing during an application cycle. This is achieved by variable rate pulsing of the high frequency solenoid valve controlling the pilot (treadle) air. The pilot air modulation acts as an effective secondary, internal electronic treadle valve which limits the demanded pilot air, thereby lowering the rate at which brake chamber pressure is permitted to increase. Typical pulse widths are 15 milliseconds long with solenoid-pressure delays on the order of 20 milliseconds. Figure 7 provides an example of the brake pressure and solenoid signals (lower two traces) measured by HSRI during the testing described in Section 2.1. Typical cycling frequencies for the Bendix system ranged between 2 and 4 Hz.

The Bendix logic module generates the appropriate solenoid signal by comparing the measured wheel speed (lowest) with an internal reference speed signal. Figures 8 and 9, provided by Bendix, describe the basic system operation and valve assembly. No pneumatic logic is employed with the Bendix system.

Aside from a few adverse operating conditions involving low friction and light loads, control of wheel slip over a variety of conditions

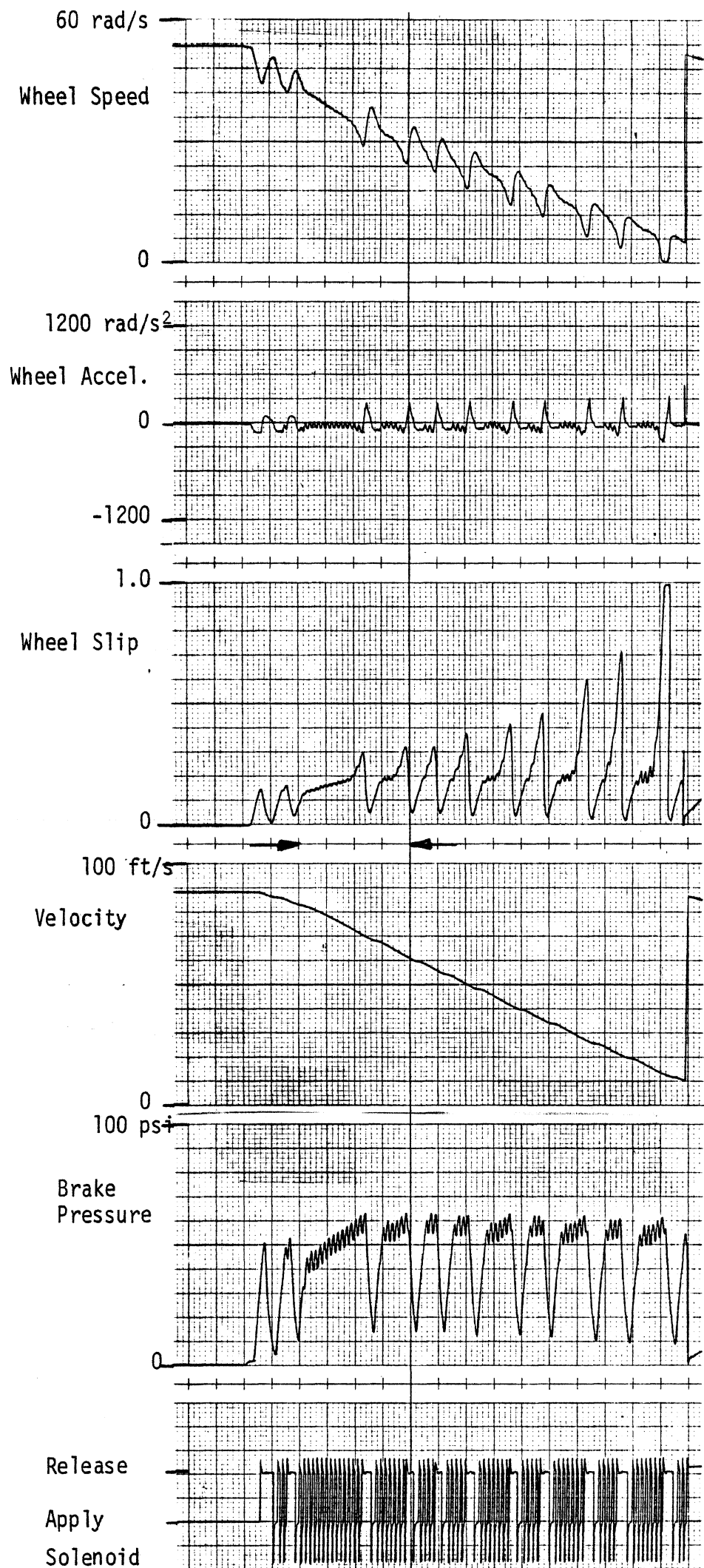


Figure 7. Bendix System

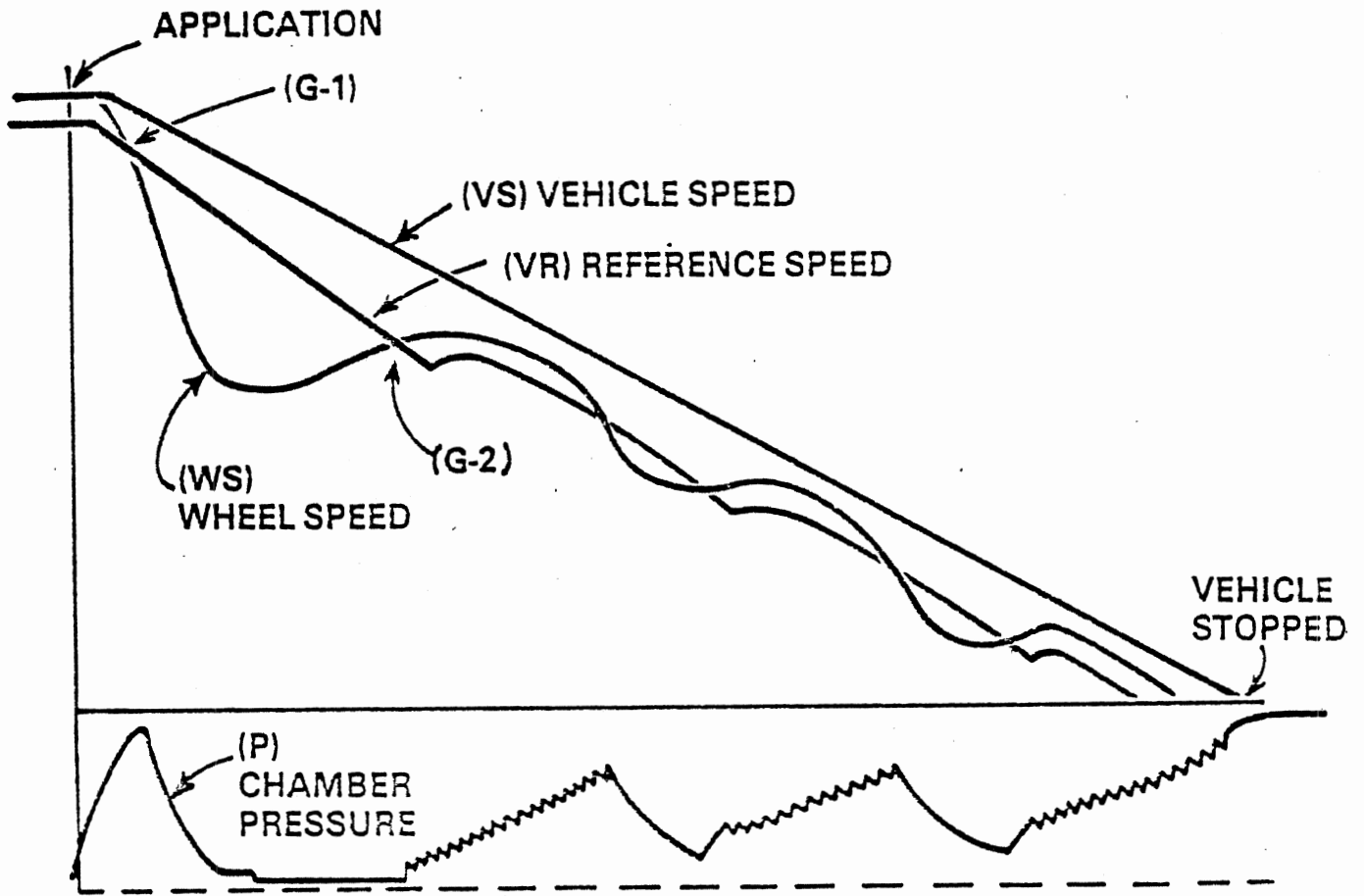


Figure 8. Bendix antiskid system operation.

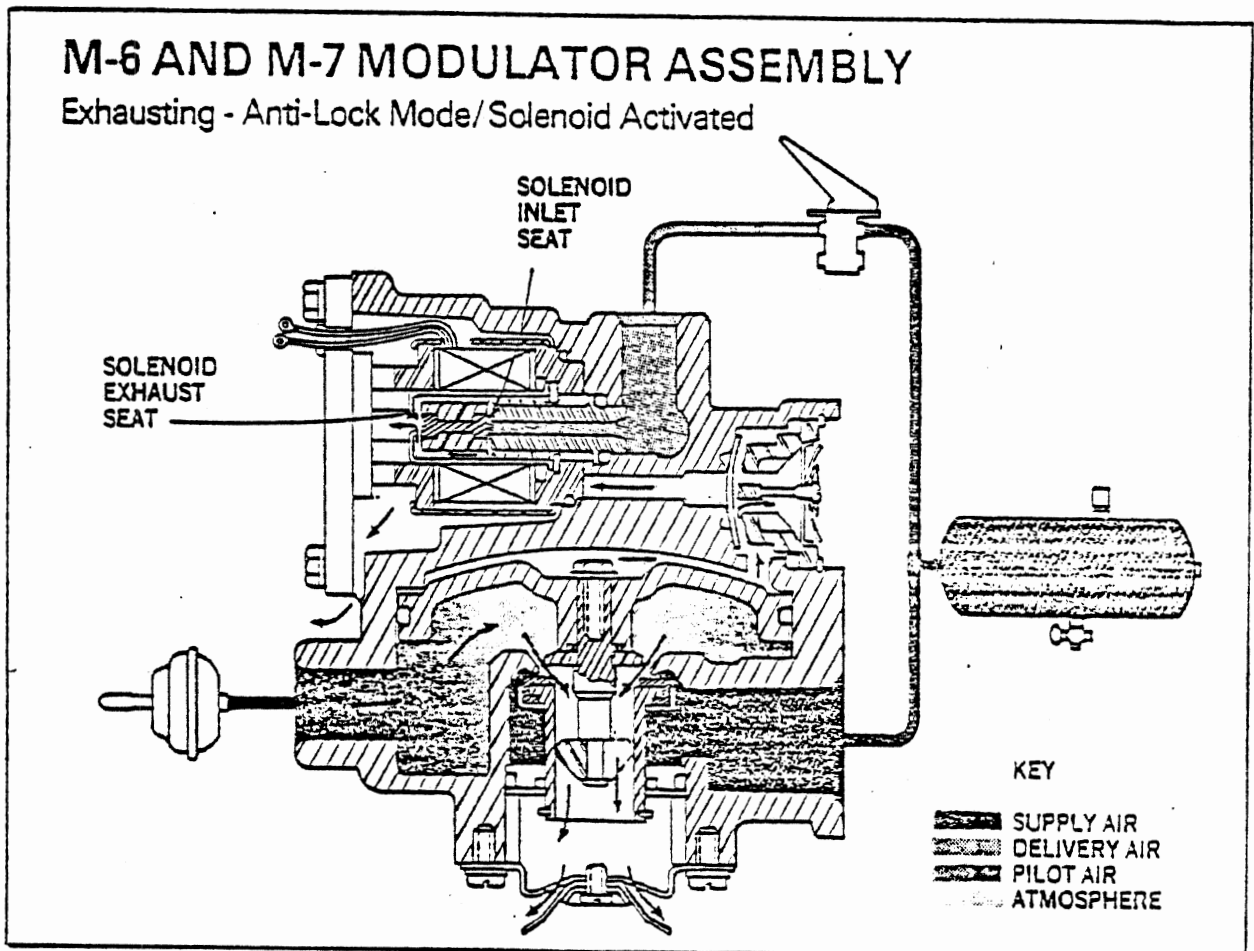


Figure 9. Bendix air valve assembly.

is quite good, as evidenced by the time histories of Appendix A and the digital library data. Most of the data for the Bendix system demonstrates a preferred operation within the low- and mid-wheel slip regimes. It should, of course, be noted that the ideal operating conditions (static load, simplified brake torque-pressure characteristics, etc.) of these tests will enhance, in most cases, the overall operating performance of each of the systems appearing in this study.

For purposes of modeling the characteristics of the Bendix system, the Phase III antiskid digital computer program [1] appears to be quite capable of simulating its basic behavior. Addition of a pulse-rate modulation option within the Phase III antiskid program would facilitate simulation of the actual system's pilot pressure modulation. Modulation of the computer program pulse rate could depend, for example, upon the error between the simulated wheel speed and an internal reference wheel speed; the latter defined to operate in the same fashion as the actual one depicted in Figure 8.

3.1.2 Kelsey-Hayes Antiskid System. A unique feature of the Kelsey-Hayes system is its use of pneumatic logic. Generally, this feature is displayed in an antiskid pressure time history as a slowly increasing linear pressure ramp (approximately 50 psi/second). Its basic purpose is similar to that provided by the pulse-rate pilot pressure modulation in the Bendix system; namely, to limit the rate of brake pressure application. A sample time history for the Kelsey-Hayes system is shown in Figure 10. The pneumatic logic pressure ramp can be seen during the second pressure application cycle.

Most of the Kelsey-Hayes data collected during this study displayed little of the pneumatic logic operation. This is apparently due to a requirement or characteristic of the Kelsey-Hayes system which limits operation of the pneumatic logic to cycling frequencies less than 2-3 Hz. The bulk of data collected on this system showed typical cycling frequencies between 3 and 4 Hz, somewhat above the threshold for more frequent operation of the pneumatic logic feature. In actual

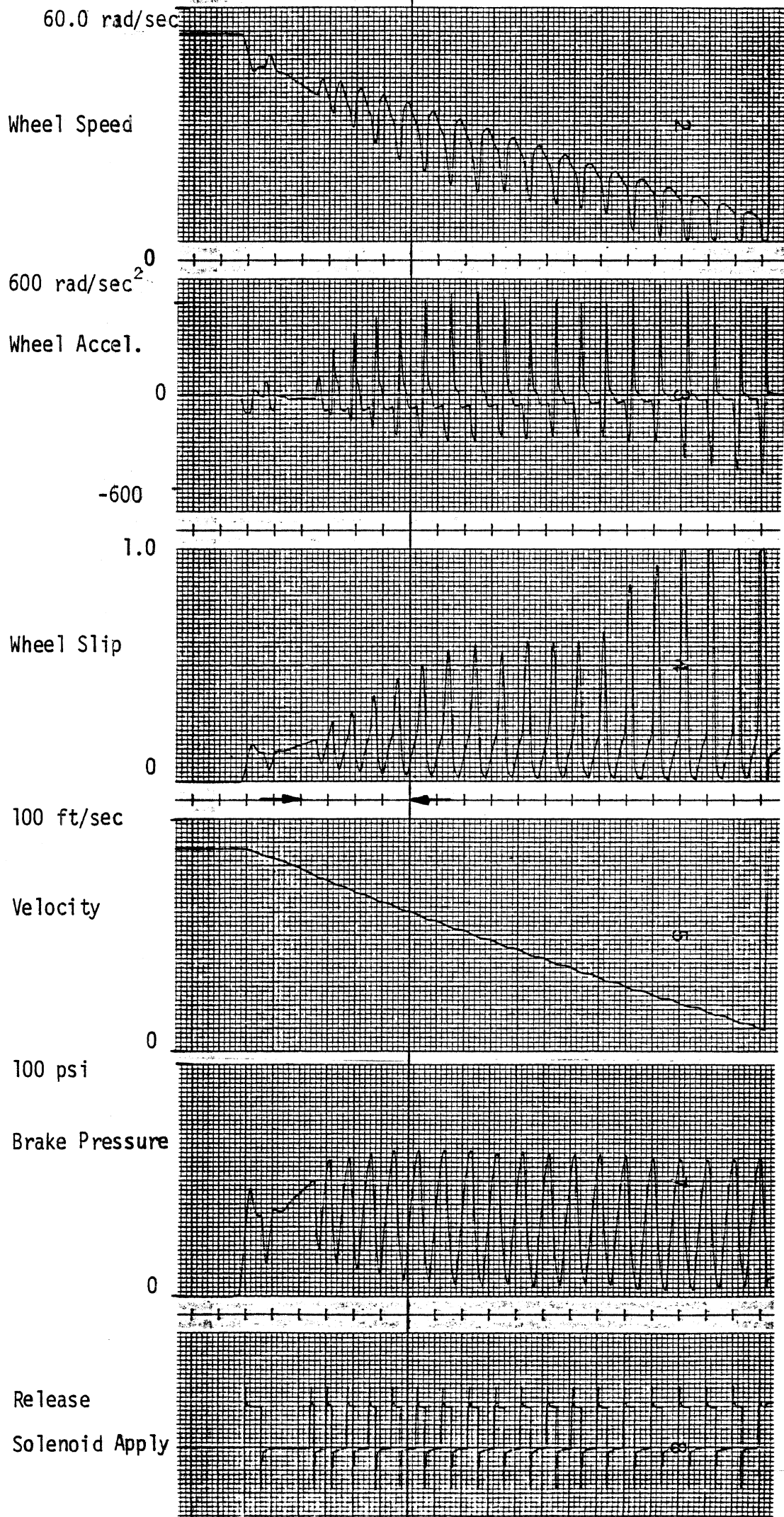


Figure 10. Kelsey-Hayes system.

vehicle use, additional delays and timing variations would derive from wheel load variations, non-ideal pressure-torque brake characteristics (hysteresis, fade), and wheel sensor delays thereby producing somewhat lower antiskid cycling frequencies and more frequent pneumatic logic operation.

Another characteristic exhibited by the Kelsey-Hayes system is the release of brake pressure, during the first cycle only, to a level equal to about 1/3 of the demanded (pilot) pressure. Full release follows after a short delay if certain wheel recovery conditions are not satisfied. Solenoid-pressure time lags on the order of 0.040 second were noted for first-cycle releases, while subsequent cycles displayed much smaller release lags of about 0.015 second. Application delays averaged about 0.025 second.

The Kelsey-Hayes solenoid commands are primarily derived from a comparison of the lowest measured wheel speed and an internal reference wheel speed signal. An example of the Kelsey-Hayes control logic derived from the series of special logic module tests is presented in Section 3.3.

Like the Bendix system, the Kelsey-Hayes system tended to favor the low- and mid-wheel slip regimes. However, it appears that the Kelsey-Hayes system spends a shorter percentage of its time within the pressure application portion of each cycle. This is no doubt due to the aforementioned reduction in pneumatic logic operation of the Kelsey-Hayes valve which would normally promote longer periods of operation within the pressure application portion of each cycle. Deep wheel excursions for first cycles were also noted for most combinations of low friction and light load.

Computer modeling of the Kelsey-Hayes system has been performed in previous MVMA research using the Phase III antilock digital simulation. Control logic used to simulate an earlier Kelsey-Hayes version and very similar to that identified for this system is contained in Reference [2]. Detailed modeling of the pneumatic logic operation was also done in conjunction with the 1977 validation study involving the White truck equipped with the same Kelsey-Hayes system.

3.1.3 B.F. Goodrich Antiskid System. The B.F. Goodrich system employs a dual-solenoid operation in its air valve modulation of brake pressure. Actuation of the first, second, or both solenoids permits pressure increases to 1/3, 2/3, or full apply levels demanded at the pilot port. Figure 11 and those appearing in Appendix A show a staircase-like pressure signal during the application portion of each cycle. Apparently, the main purpose of the staircase behavior is to limit brake pressure application levels and rates during each cycle based on information obtained from previous cycles. The first, or first two, cycles of each test typically tend to produce deep wheel speed excursions which possibly serve as learning cycles attempting to identify operating conditions. In some cases, the severity of these initial wheel speed excursions and their subsequent recovery could seemingly hasten the onset of undesirable pitching and bouncing characteristics inherent in the antiskid braking dynamics of many heavy vehicles.

In general, the B.F. Goodrich system tests tended to display initially aggressive wheel slip excursions which quickly diminish to slip cycles operating in the low- and mid-slip range. Cycling frequencies ranging between 2 and 7 Hz were fairly typical. Time lags of about 0.025 second were measured between the solenoid and pressure responses.

Operation of the logic module for the B.F. Goodrich system is somewhat more complicated than the two systems just discussed in that two solenoid signals are generated. Although it is not known, it is assumed that the control logic used to actuate each of the two solenoids in the B.F. Goodrich system is probably similar in nature to the other systems, utilizing internal reference wheel speed signals and wheel acceleration conditions.

Simulation of the basic valve characteristics could be modeled within the current Phase III antiskid program. The air valve operation could be simulated using the treadle pressure modulation option and two general-purpose or one-shot variables representing the two solenoid

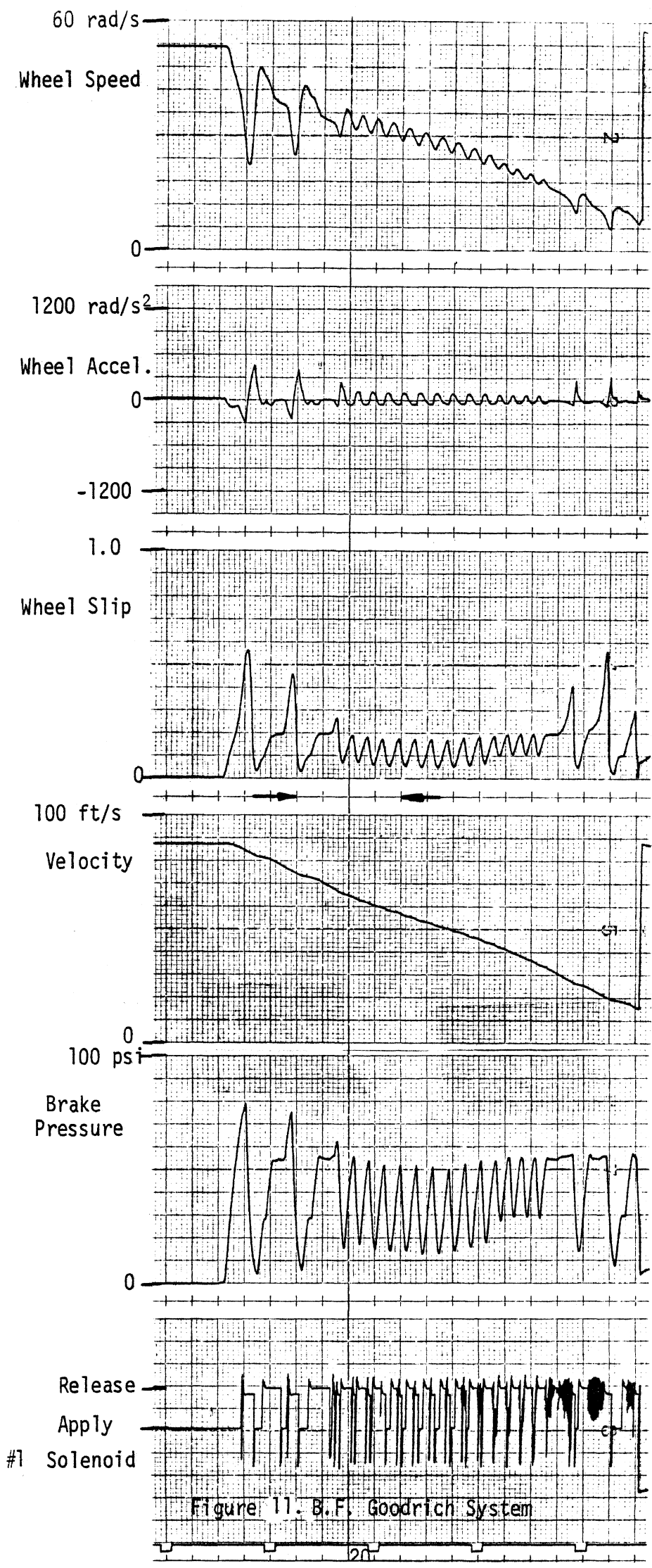


Figure 11. B.F. Goodrich System



signals. By associating one of the solenoid variables with the 1/3 pressure application condition and the remaining variable with the 2/3 pressure application, summation of these two variables in the treadle pressure modulation option should duplicate the general valve operation. Suitable control logic to generate the two solenoid signals would, of course, be needed.

3.1.4 Eaton Antiskid System. The Eaton system employs pneumatic logic in a manner similar to that used in the Kelsey-Hayes system. Initiation of the Eaton pneumatic logic was generally delayed during most of these tests until the third cycle and only occurred during the brake pressure application mode of each cycle (Figure 12). The reduced pressure rates, in Figure 12, occurring in the vicinity of 60 psi during the third and subsequent cycles reflect the operation of the pneumatic logic. The enlarged scale of Figure 13 demonstrates this in greater detail. For the high friction, large wheel load condition, the pneumatic logic was evident during the first cycle, occurring at about the 85% level of the demanded pressure. Overall operation of the Kelsey-Hayes and Eaton systems appear to be very similar, with the Eaton system cycling at a somewhat slower rate (1.5-3.5 Hz) and spending greater percentages of time in the pressure application portion of each cycle.

Interestingly, the Eaton system was the only system of the five tested which was not confused by the most adverse operating conditions (light wheel load, low tire-road friction coefficient, and large wheel inertia). Each of the other systems erroneously concluded that the vehicle velocity had fallen to near zero several seconds too soon and therefore reverted to "normal" system operation prematurely with full pressure and a locked wheel. This behavior could suggest that the Eaton system does not employ estimates of vehicle velocity usually derived from local, cycle-to-cycle wheel speed spin-up conditions (e.g., use of wheel acceleration conditions only). However, a more likely answer is the Eaton system simply allows greater time during some or all cycles for the wheel to recover, thereby achieving better estimates of vehicle

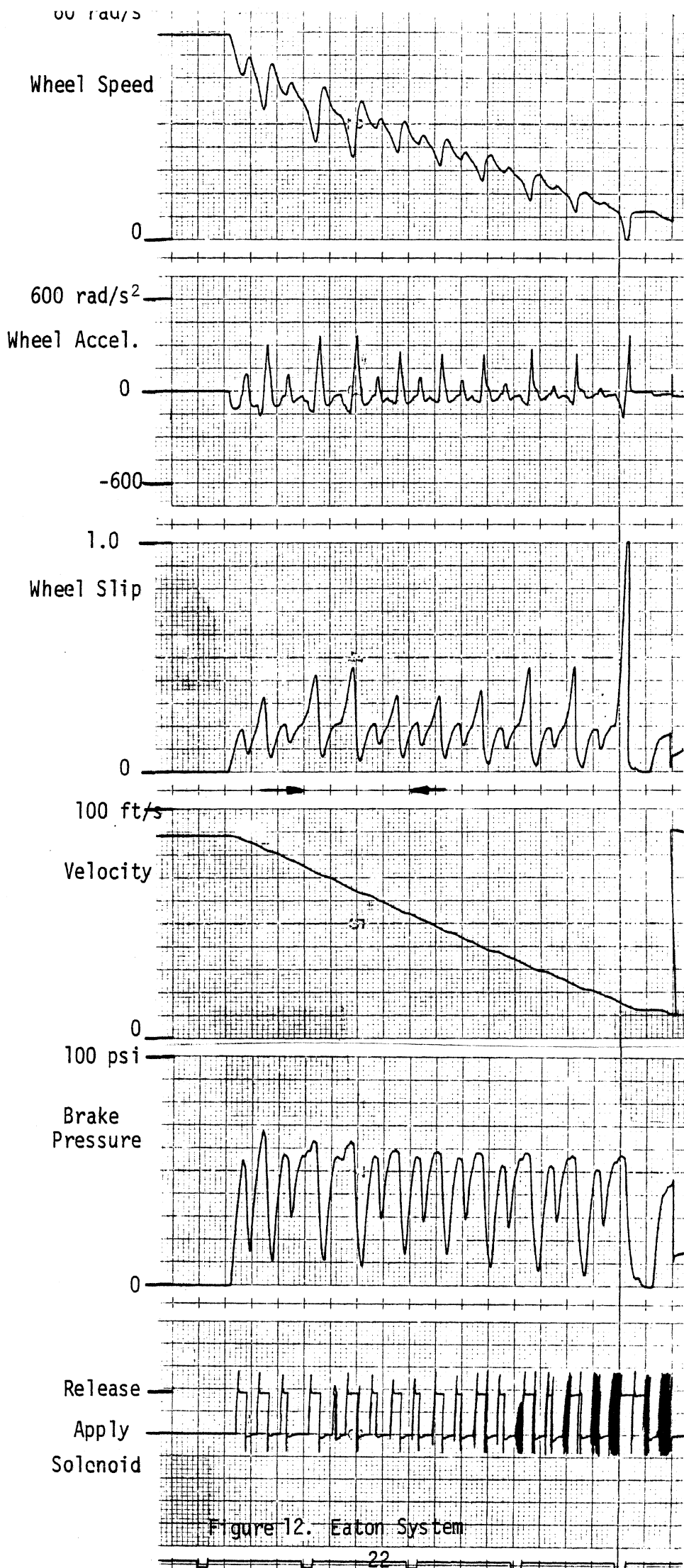
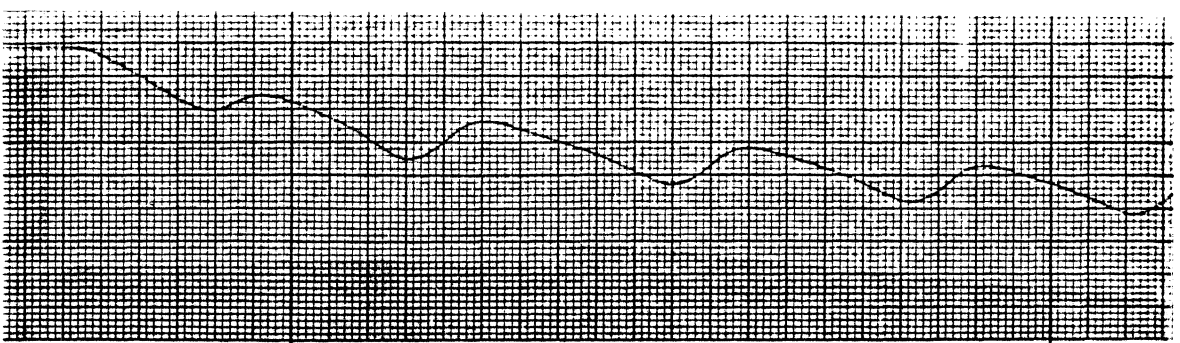
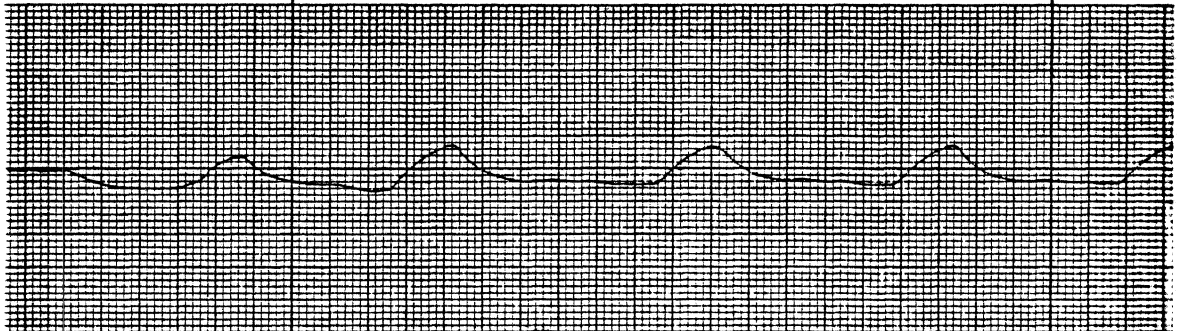


Figure 12. Eaton System

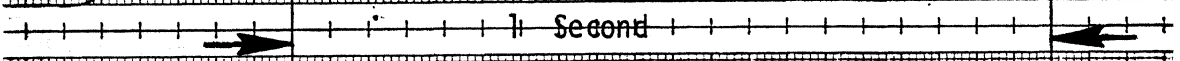
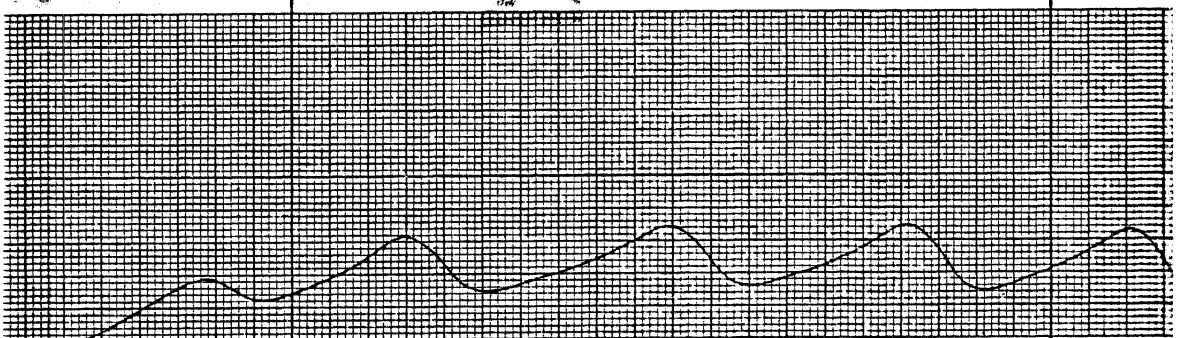
Wheel Speed



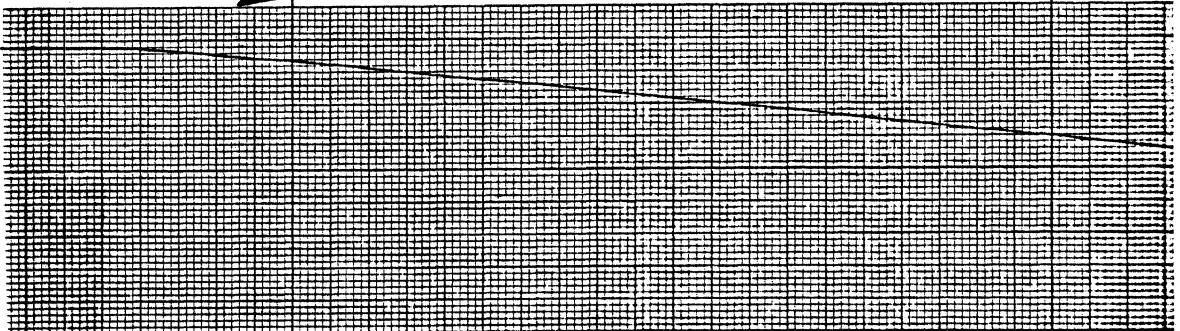
Wheel Accel.



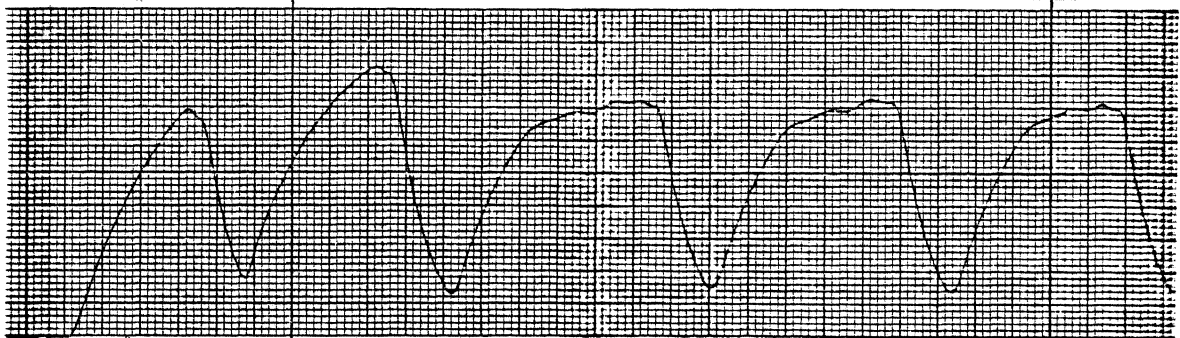
Wheel Slip



Velocity



Brake Pressure



Solenoid

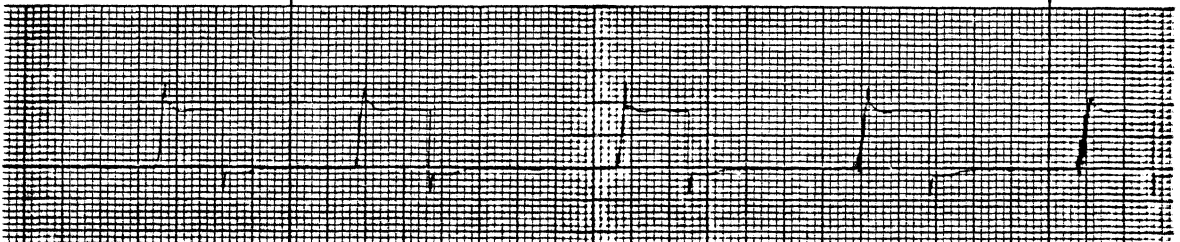


Figure 13. Eaton system.

velocity. Typical solenoid-pressure response time lags exhibited by the Eaton system were 30 milliseconds.

Simulation of the Eaton system using the Phase III program would appear to be quite similar to that of the Kelsey-Hayes system. Principal differences would presumably lie in the control logic.

3.1.5 Wagner Antiskid System. The Wagner system differs from the other systems tested in that it provides for two different rates for the release of brake pressure and one for the application of pressure. This is achieved by a dual solenoid operation which activates one solenoid for moderate exhaust rates and increases the exhaust rate with a second release valve operational under more severe wheel slip or wheel acceleration conditions. Although the dual solenoid operation was difficult to detect from observation of most pressure time history traces, its operation is clearly visible in the individual solenoid time histories contained on the digital library tape.

Figure 14 shows a representative set of time histories for the Wagner system. In general, the Wagner system tended to prefer lower wheel slip operation than the other systems tested. Its overall operation also seemed to be very regular, operating with a nearly constant cycling frequency during each test. The range of cycling frequencies for varying operating conditions fell between 3 and 5 Hz. Solenoid-pressure release time lags for one solenoid averaged about 50 ms, with a reduction to about 20 ms for any secondary solenoid actuations. Solenoid-pressure application lags averaged about 30 ms.

Simulation of the basic Wagner system could be modeled with the Phase III antiskid program. The dual solenoid valve action would be approximated in a fashion similar to that suggested for the B.F. Goodrich system, using two one-shot variables and combining these in the exponential pressure model. Appropriate control logic dependent upon wheel speed and acceleration conditions would be required.

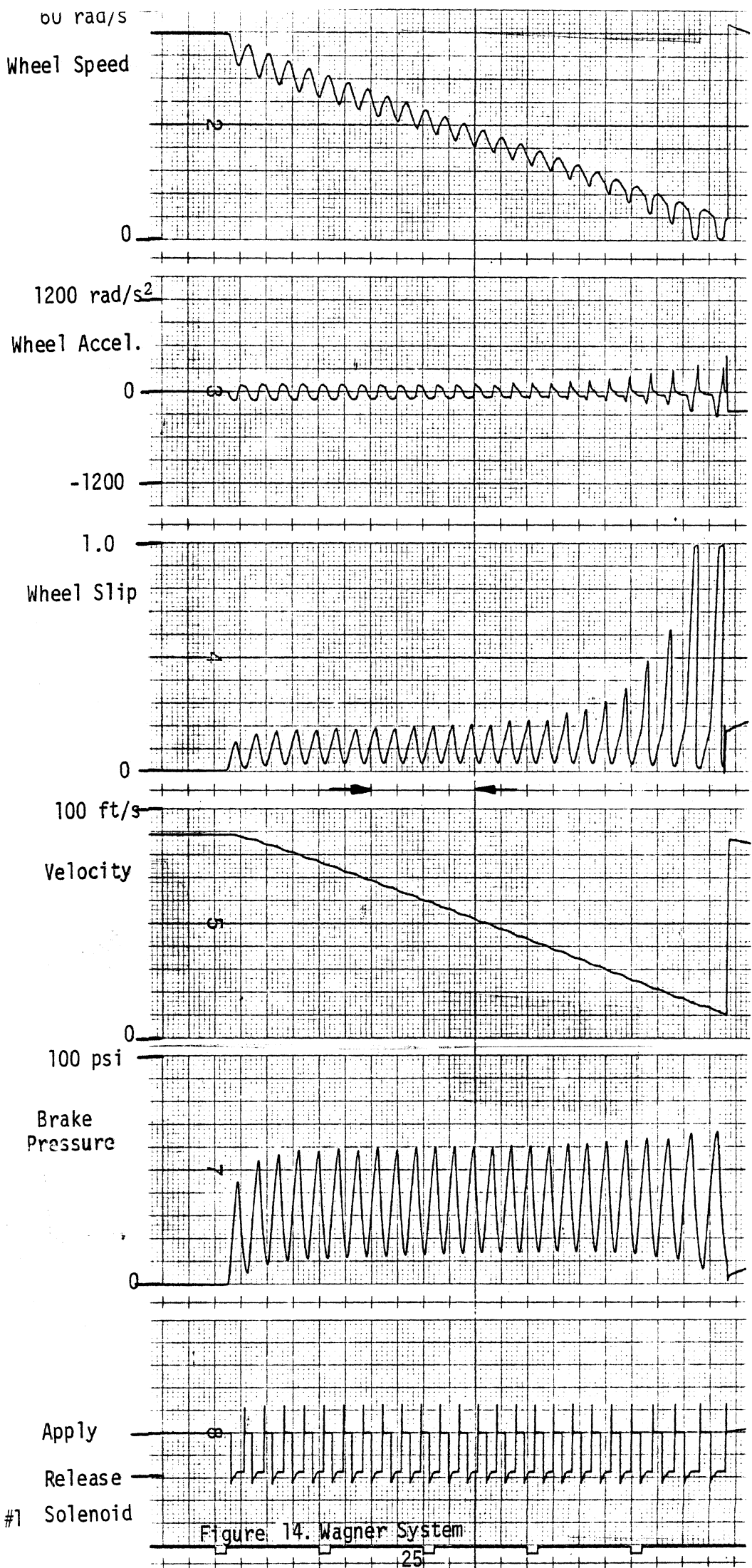


Figure 14. Wagner System

3.1.6 Time Constants and Time Lags. A summary of approximate time constants (exponential-like pressure rise and fall characteristics) and linear rise rates (pneumatic logic operation) measured for each of the systems tested appear in Table 4. Type 12 brake cans and 1/2-inch brake lines were used during the testing. Also included in Table 4 are the approximate solenoid-pressure release/apply time lags measured for each system.

### 3.2 Antiskid Digital Library

During the course of testing described in Section 2.1, a data bank of 288 digital time histories was created for each system corresponding to the test matrix given in Table 2. Of these 288 time histories, 108 were selected and formatted for inclusion on a final digital magnetic tape known as the antiskid digital library. The reduced number of time histories appearing on the final formatted tape simply reflects three of the original eight wheel inertia values appearing in the test matrix of Table 2 (75, 150, and 300 in-lb-sec<sup>2</sup>). These three values are seen as adequately representing the influence of wheel inertia variation on antiskid performance while also permitting a significant reduction in size of the final antiskid library.

The output format for a typical time history stored in the antiskid library is shown in Tables 5 and 6 for the Kelsey-Hayes system. The first page, Table 5, lists the name of the system and simulated operating conditions. MU-PEAK and MU-LOCK refer to the values of tire-road friction coefficient at 20% and 100% wheel slip. The test repeat number and linear brake torque-pressure gain are also shown on this page. Subsequent pages conform to the format shown in Table 6. The first column is time with increments of 0.01 second and referenced to the time of application of the treadle pressure. Columns 2 and 3 show wheel speed and acceleration in units of rad/sec and rad/sec<sup>2</sup> for an assumed constant wheel radius of 20 inches. Brake pressure (psi), wheel slip (percent), vehicle velocity (ft/sec), and current tire-road friction coefficient are listed in columns 4-7. Column 8 shows the

Table 4. Pressure Release/Apply Rates and Solenoid-Pressure Time Lags.

<u>System</u>	<u>Pressure Time Constants/Rate</u>	<u>Solenoid-Pressure Time Lag (sec)</u>
Bendix	0.045 sec (Release)	0.025
	0.11 sec (Full Apply)	Release and Apply
	Variable (Pulse Rate Modulation)	
Kelsey-Hayes	0.040 sec (Release)	0.040 1st Cycle Release
	0.11 sec (Full Apply)	0.015 Subsequent Cycle
	50 psi/sec (Pneumatic Logic)	0.025 Apply
B.F. Goodrich	0.035 sec (Release)	
	0.11 sec (Full Apply)	0.0250
	Variable (1/3, 2/3, Full Application)	Release and Apply
Eaton	0.040 sec (Release)	0.030
	0.11 sec (Full Apply)	Release and Apply
	50 psi/sec (Pneumatic Logic)	
Wagner	0.080 sec (Single Solenoid Release)	.050
	0.040 sec (Both Solenoid Release)	.020
	0.11 sec (Full Apply)	.030

Table 5. Sample Printout from the Digital Library Tape

\*\*\* KELSEY-HAYES ANTISKID SYSTEM \*\*\*

INITIAL VELOCITY = 88 FT/SEC      LOAD = 5000 LBS

WHEEL INERTIA = 150 INCH-LBS-SEC<sup>2</sup>      MU-PEAK = .80      MU-LOCK = .50

REPEAT #3      BRAKE GAIN = 1500 INCH-LBS/PSI



Table 6.

\*\*\* KELSEY-HAYES ANTISKID SYSTEM \*\*\*

TIME (SEC)	WHEEL SPEED (RAD/S)	WHEEL ACCEL (RAD/S <sup>2</sup> )	BRAKE PRESS (PSI)	WHEEL SLIP (PCT)	VELOC (FT/S)	FRICT COEFF	SOL 1 (VOLTS)	SOL 2
0.0	52.79	4.6	0.0	0.2	88.00	0.006	0.08	0.0
0.01	52.74	-1.9	0.9	0.3	88.00	0.009	0.08	0.0
0.02	52.72	-5.8	1.4	0.3	88.00	0.011	0.06	0.06
0.03	52.70	-1.6	0.7	0.3	87.98	0.012	0.08	0.04
0.04	52.70	1.1	0.8	0.3	87.98	0.013	0.06	-0.02
0.05	52.69	1.0	0.8	0.4	87.98	0.013	0.08	0.0
0.06	52.68	-0.4	1.0	0.4	87.98	0.014	0.08	-0.02
0.07	52.60	-16.6	3.9	0.5	87.98	0.019	0.06	0.04
0.08	52.31	-44.6	7.2	1.1	87.96	0.042	0.06	0.02
0.09	51.79	-59.6	11.4	2.0	87.94	0.080	0.08	0.04
0.10	51.06	-80.8	17.0	3.4	87.92	0.133	0.08	0.04
0.11	50.15	-93.6	22.7	5.0	87.84	0.199	0.08	0.04
0.12	49.14	-101.4	28.4	6.9	87.78	0.273	0.08	0.04
0.13	48.10	-104.8	34.7	8.7	87.66	0.348	0.08	0.02
0.14	47.00	-106.4	39.1	10.7	87.54	0.425	10.86	0.0
0.15	45.92	-104.9	44.0	12.6	87.38	0.502	9.78	0.04
0.16	44.89	-96.5	47.9	14.4	87.22	0.573	8.98	-0.02
0.17	43.99	-69.7	49.2	15.9	87.02	0.633	8.64	0.06
0.18	43.51	-28.7	47.0	16.6	86.84	0.662	8.78	0.0
0.19	43.39	5.3	43.7	16.6	86.60	0.663	8.86	-0.02
0.20	43.56	23.0	40.1	16.1	86.38	0.642	8.78	0.06
0.21	43.85	31.9	37.7	15.3	86.20	0.612	8.74	0.04
0.22	44.15	27.7	36.1	14.6	86.00	0.582	8.78	-0.02
0.23	44.36	18.6	35.1	14.0	85.82	0.557	8.80	0.04
0.24	44.50	9.2	35.1	13.6	85.62	0.540	8.80	-0.02
0.25	44.53	1.8	36.1	13.3	85.44	0.529	8.78	0.02
0.26	44.53	-0.5	35.0	13.1	85.30	0.523	8.76	0.04
0.27	44.51	-3.5	35.0	13.1	85.12	0.519	8.80	0.0
0.28	44.52	20.9	32.0	12.8	84.96	0.510	8.78	0.06
0.29	44.89	55.3	26.1	11.9	84.78	0.473	-3.60	0.0
0.30	45.56	70.2	20.4	10.5	84.64	0.415	-3.74	0.04
0.31	46.34	79.1	15.4	8.8	84.54	0.349	-0.10	-0.02
0.32	47.00	48.0	14.7	7.4	84.44	0.292	0.02	0.04
0.33	47.26	1.8	17.8	6.8	84.34	0.268	0.06	-0.02
0.34	47.03	-40.8	23.0	7.1	84.24	0.282	0.08	0.0
0.35	46.45	-66.8	28.3	8.2	84.14	0.324	0.08	0.04
0.36	45.68	-80.5	33.5	9.5	84.02	0.380	0.08	-0.02
0.37	44.83	-83.2	37.8	11.1	83.90	0.442	0.06	0.04
0.38	44.05	-69.5	40.2	12.5	83.74	0.498	0.08	0.0
0.39	43.48	-42.5	40.1	13.5	83.58	0.537	0.38	0.04
0.40	43.12	-27.2	39.9	14.0	83.38	0.557	0.08	0.04
0.41	42.88	-18.5	39.8	14.3	83.20	0.570	0.10	0.02
0.42	42.72	-9.5	39.3	14.4	83.04	0.574	0.06	-0.02
0.43	42.62	-10.0	39.3	14.4	82.86	0.574	0.08	0.02
0.44	42.53	-3.7	38.9	14.4	82.68	0.574	10.40	0.06
0.45	42.43	-9.4	39.2	14.4	82.48	0.574	9.70	0.04
0.46	42.49	27.0	34.8	14.1	82.30	0.562	8.86	0.0
0.47	42.96	64.9	27.9	13.0	82.10	0.517	-0.18	-0.02
0.48	43.70	77.2	21.9	11.3	81.96	0.449	-3.76	0.02
0.49	44.53	85.7	16.4	9.4	81.84	0.374	-0.98	0.0

recorded solenoid voltage in the case of a single solenoid system. For systems employing additional solenoids (Wagner, B.F. Goodrich), the first solenoid voltage is shown in Column 8, the second in Column 9.

The antiskid library tape format is file structured. Each file contains a set of time histories corresponding to a single test. Table 7 is the index for the antiskid library tape which identifies the operating conditions and particular antiskid system with a specific file number on the library tape. For example, the third test repeat of the Kelsey-Hayes system with a wheel inertia of 300 in-lb-sec<sup>2</sup>, 2500 lb load, 88 ft/sec initial velocity, and "HIGH" friction condition, is contained in file number 126. Table 8 describes the tape format information required by most computer installations for reading the antiskid library tape.

### 3.3 Special Logic Module Test Results

As described in Section 2.2, a series of special tests were conducted on the Kelsey-Hayes logic module using the analog computer. All tests were performed for either first cycle or second cycle brake release conditions. (No brake application switching conditions were recorded or analyzed using this technique.) The results are presented in Figures 15 through 20 in the form of wheel speed at brake release ( $\omega_{\text{off}}$ ) versus wheel acceleration at brake release ( $\dot{\omega}_{\text{off}}$ ), and time of brake release,  $t_{\text{off}}$ , plots. Each locus represents the switching condition coincidental with brake release obtained for various combinations of wheel inertia and rate of pressure application. The locus of measurements is presumed to lie within a "switching surface" which approximates the control law logic. By performing a regression analysis upon the data set:  $(\omega_{\text{off}_i}, \dot{\omega}_{\text{off}_i}, t_{\text{off}_i}; i=1, \dots, N)$ , a mathematical expression can be obtained which represents a three-dimensional switching surface. For example, the linear regression of  $\omega_{\text{off}}$  on  $\dot{\omega}_{\text{off}}$  and  $t_{\text{off}}$  would be of the form

Wheel Inertia (in-lb-sec <sup>2</sup> )	Vertical Load (lbs)	Initial Velocity (ft/sec)	Friction Coefficient	Repeat #	Table 7. Antiskid Digital Tape Library Index.					
					Bendix	Kelley-Hayes	Eaton TAPE FILE #		Wagner	B.F. Goodrich
150	5000	88	HIGH	1	1	109	217	325	433	
				2	2	110	218	326	434	
				3	3	111	219	327	435	
				75	1	4	112	220	328	436
					2	5	113	221	329	437
					3	6	114	222	330	438
				300	1	7	115	223	331	439
					2	8				
					3	9				
150	2500			1	10	118	226	334	442	
				2	11					
				3	12					
75				1	13	121	229	337	445	
				2	14					
				3	15					
300				1	16	124	232	340	448	
				2	17					
				3	18					
150	7500			1	19	127	235	343	451	
				2	20					
				3	21					
75				1	22	130	238	346	454	
				2	23		239			
				3	24		240			
300				1	25	133	541	349	457	
				2	26		542			
				3	27		543			
150	5000		LOW	1	28	136	244	352	460	
				2	29		245			
				3	30		246			
75				1	31	139	247	355	463	
				2	32					
				3	33					
300				1	34	142	250	358	466	
				2	35					
				3	36					

Wheel Inertia	Vertical Load	Initial Velocity	Friction Coefficient	Repeat #	Table 7. (Cont.)				
					Bendix	Keisley-Hayes	Eaton	Wagner	B. F. Goodrich
OPERATING CONDITIONS					TAPE FILE #				
150	2500	88	LOW	1	37	145	253	361	469
				2	38				
				3	39				
75				1	40	148	256	364	472
				2	41				
				3	42				
300				1	43	151	259	367	475
				2	44				
				3	45				
150	7500			1	46	154	262	370	478
				2	47				
				3	48				
75				1	49	157	265	373	481
				2	50				
				3	51				
300				1	52	160	268	376	484
				2	53				
				3	54				
150	5000	44	HIGH	1	55	163	271	379	487
				2	56				
				3	57				
75				1	58	166	274	382	490
				2	59				
				3	60				
300				1	61	169	277	385	493
				2	62				
				3	63				
150	2500			1	64	172	280	388	496
				2	65				
				3	66				
75				1	67	175	283	391	499
				2	68				
				3	69				
300				1	70	178	286	394	502
				2	71				
				3	72				

Wheel Inertia	Vertical Load	Initial Velocity	Friction Coefficient	Repeat #	Table 7. (Cont.)					
					Bendix	Kelsey-Hayes	Eaton		Wagner	B.F. Goodrich
<u>OPERATING CONDITIONS</u>							<u>TAPE FILE #</u>			
150	7500	44	HIGH	1	73	181	289	397	505	
				2	74					
				3	75					
75				1	76	184	292	400	508	
				2	77					
				3	78					
300				1	79	187	295	403	511	
				2	80					
				3	81					
150	5000		LOW	1	82	190	298	406	514	
				2	83					
				3	84					
75				1	85	193	301	409	517	
				2	86					
				3	87					
300				1	88	196	304	412	520	
				2	89					
				3	90					
150	2500			1	91	199	307	415	523	
				2	92					
				3	93					
75				1	94	202	310	418	526	
				2	95					
				3	96					
300				1	97	205	313	421	529	
				2	98					
				3	99					
150	7500			1	100	208	316	424	532	
				2	101					
				3	102					
75				1	103	211	319	427	535	
				2	104					
				3	105					
300				1	106	214	322	430	538	
				2	107				539	
				3	108				540	

Table 8. Antiskid Library Tape Format.

9 Track

1600 bpi

Unlabeled

Blocking: FBS(4200, 70)

Fixed length records: 70 bytes

Maximum block size: 4200 bytes

EBCDIC characters

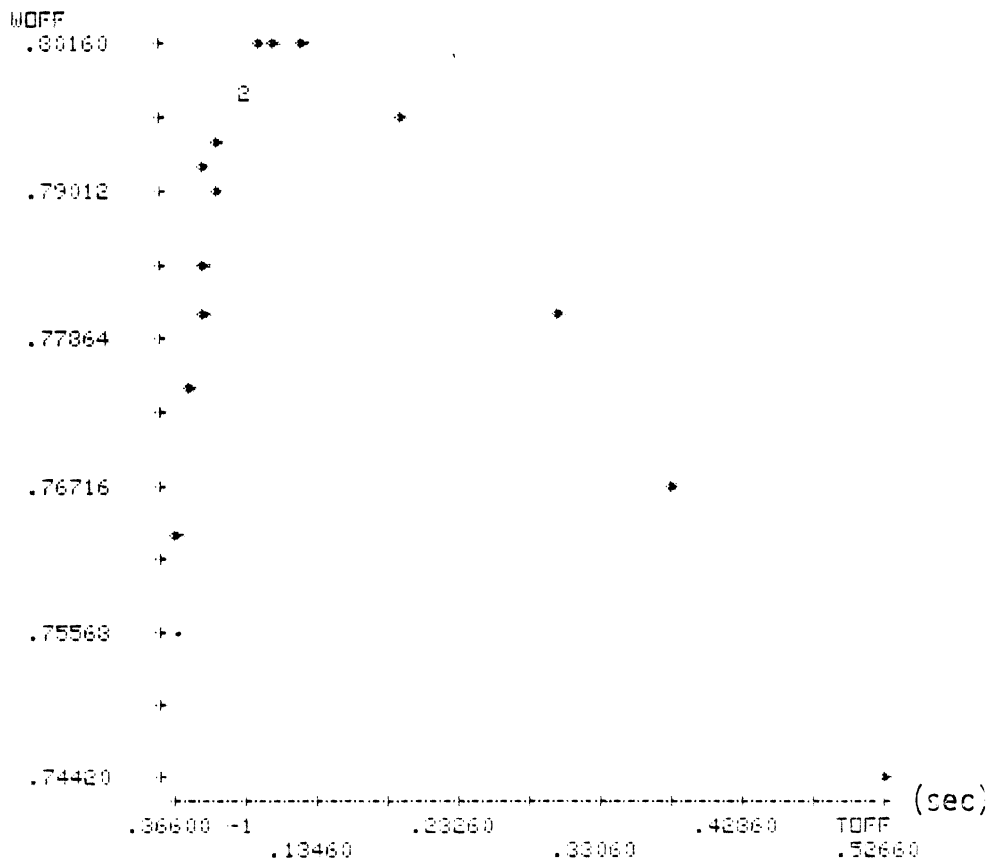
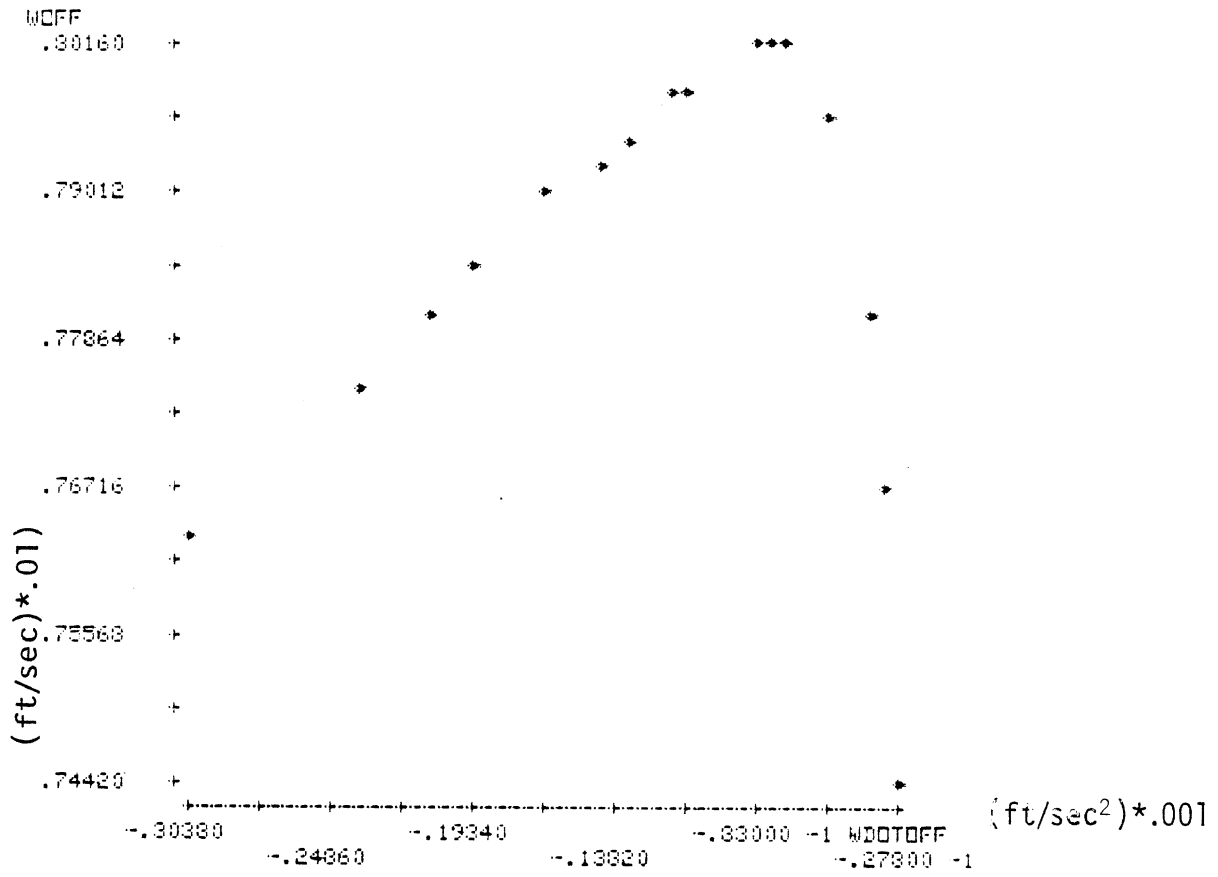


Figure 15. Logic module test result (K-H);  $\omega_0=88$ , high  $\mu$ , 1st cycle.

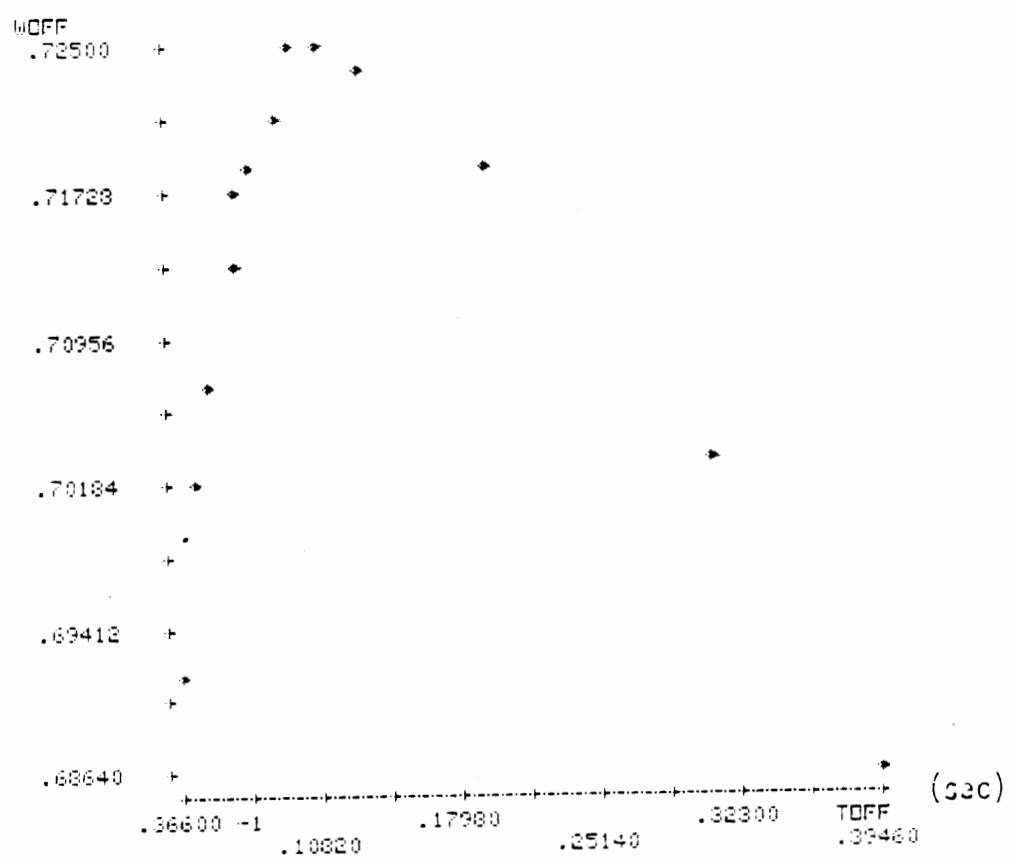
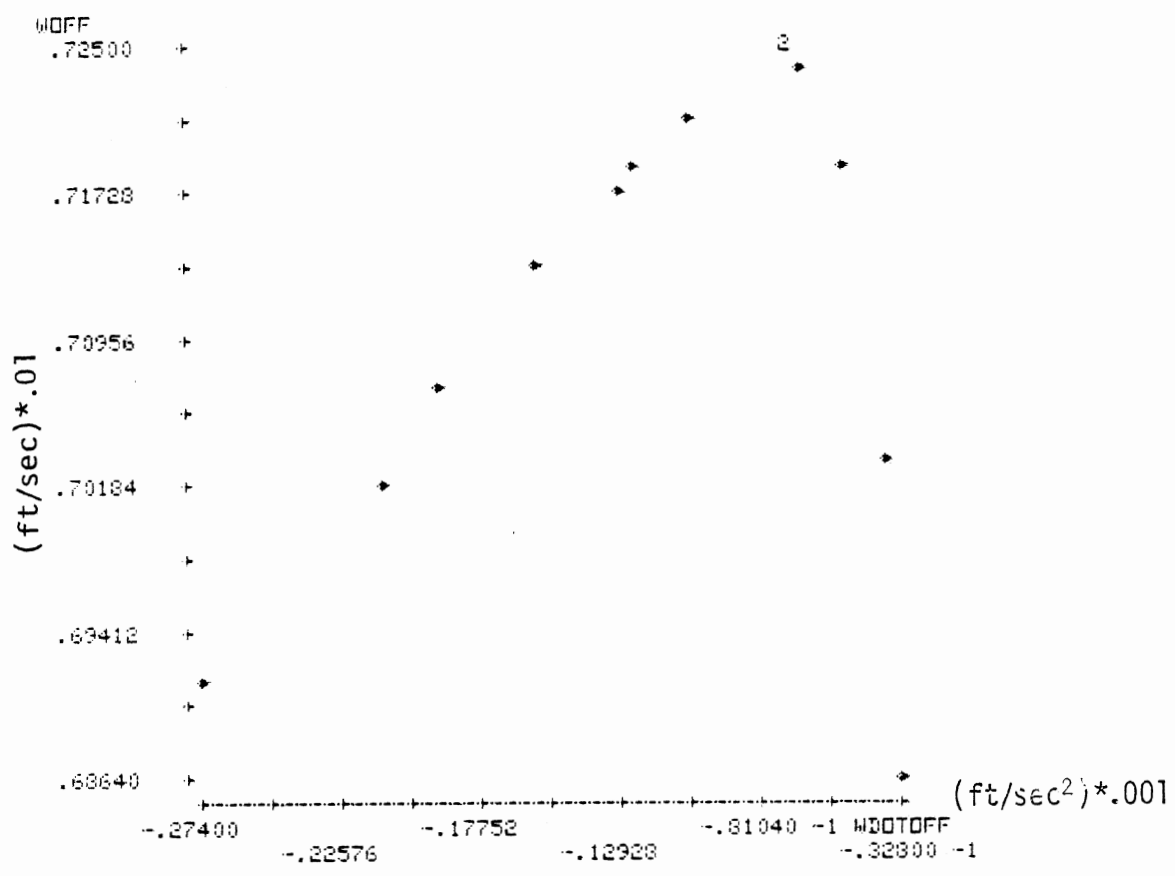


Figure 16. Logic module test result (K-H);  $\omega_0=80$ , high mu, 1st cycle.



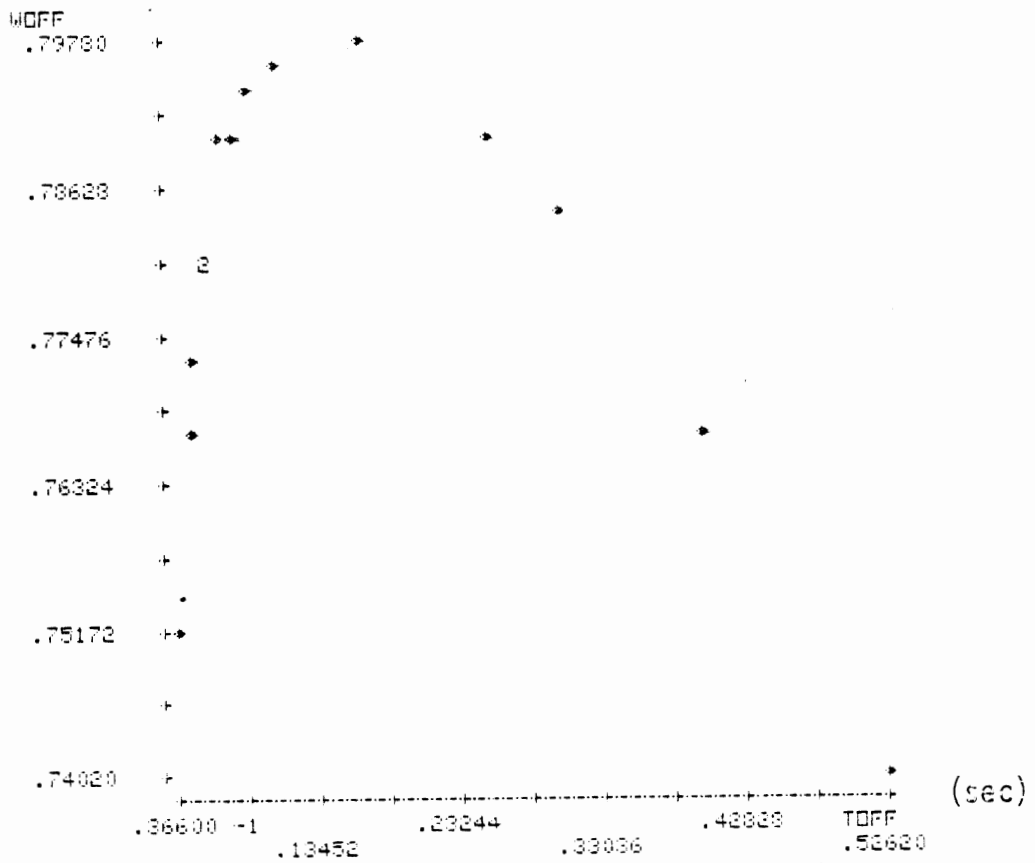
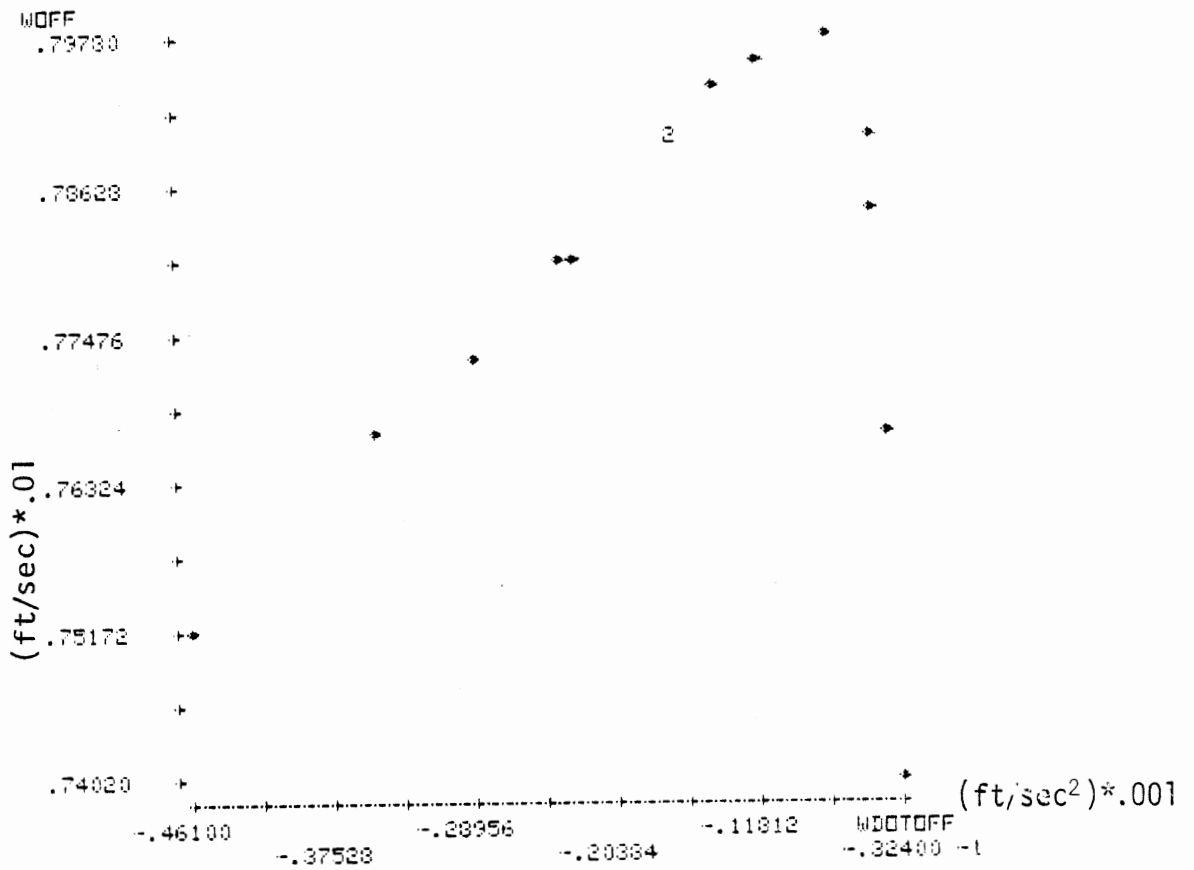


Figure 17. Logic module test result (K-H);  $\omega_0=88$ , low  $\mu$ , 1st cycle.

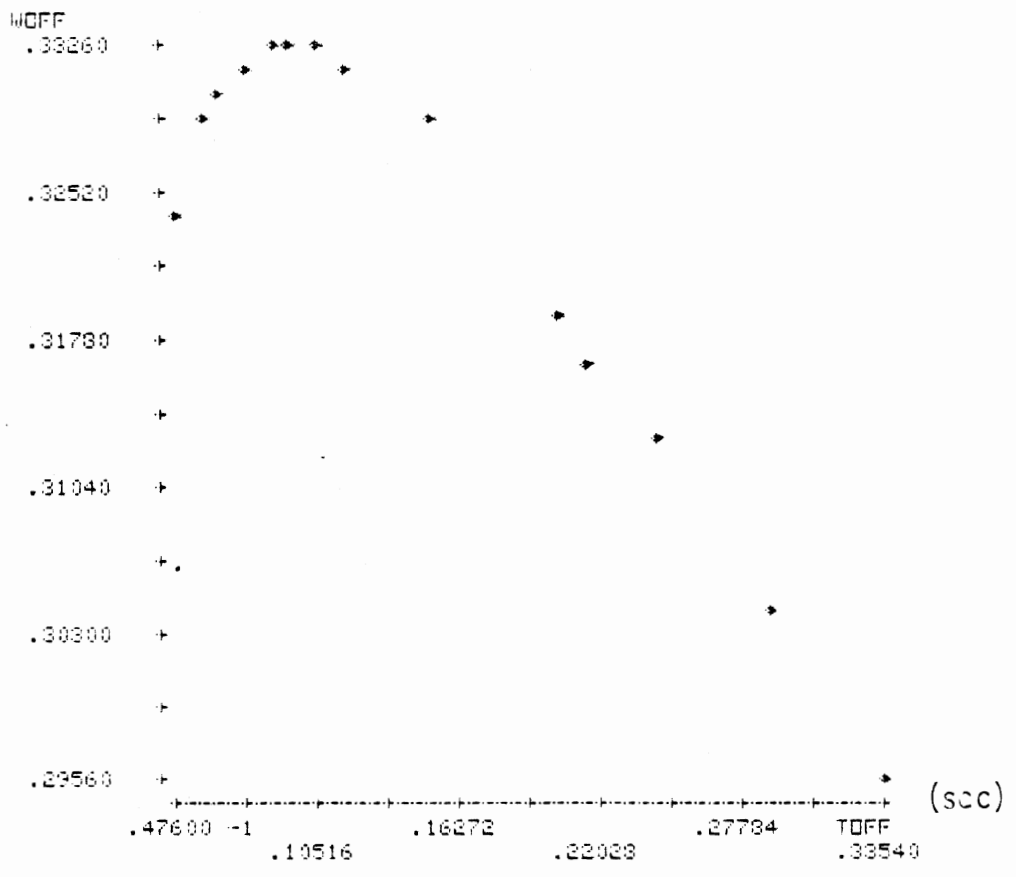
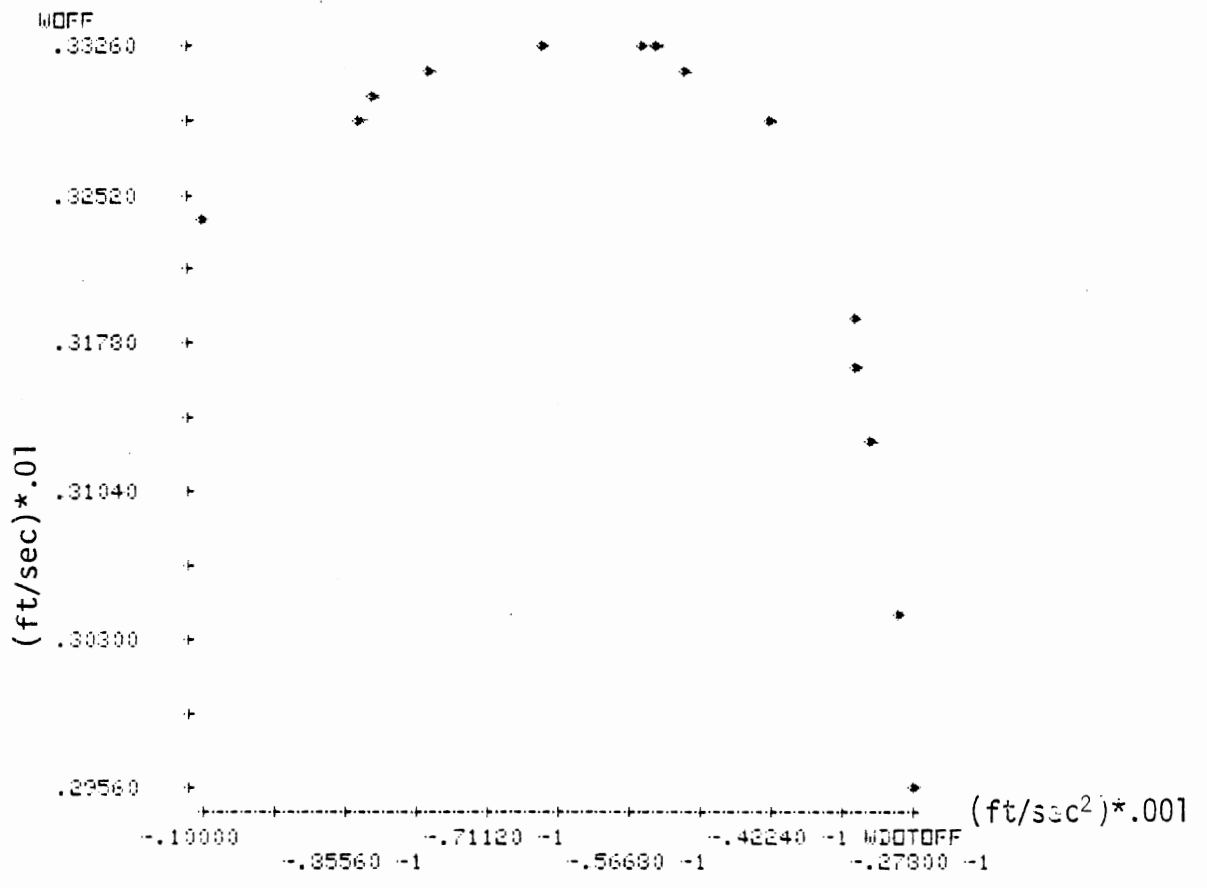


Figure 18. Logic module test result (K-H);  $\omega_0=40$ , high  $\mu$ , 1st cycle.

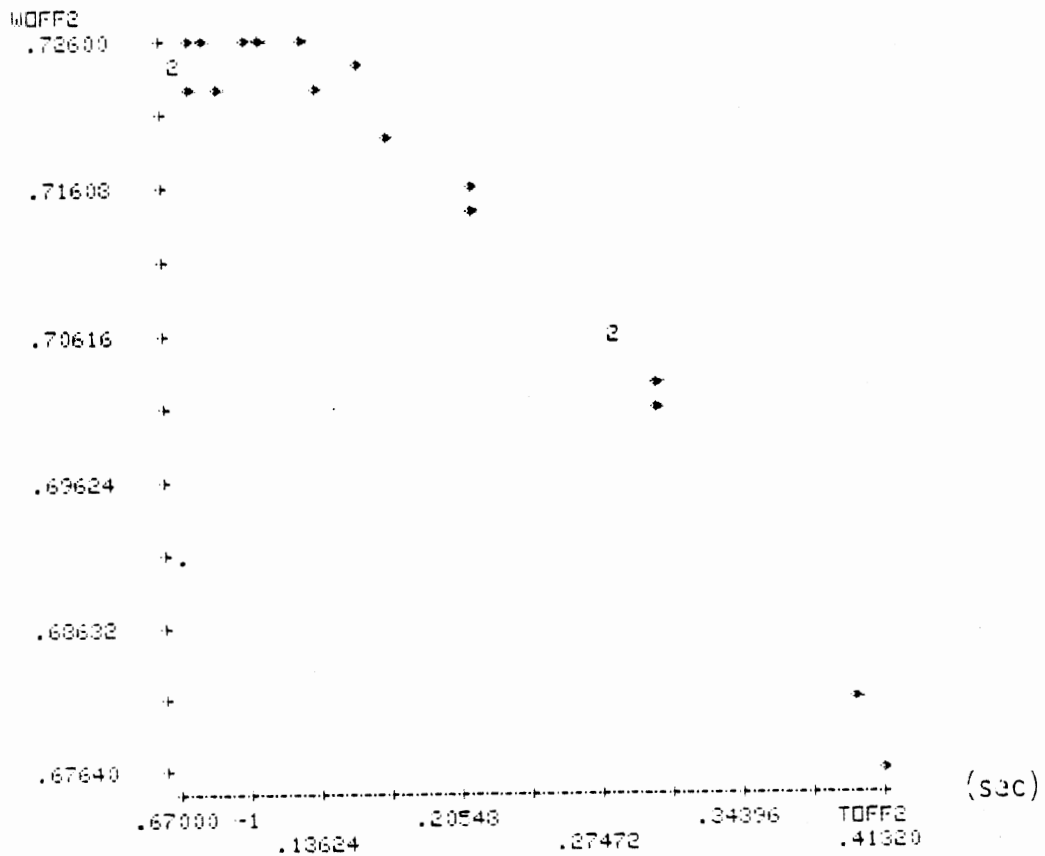
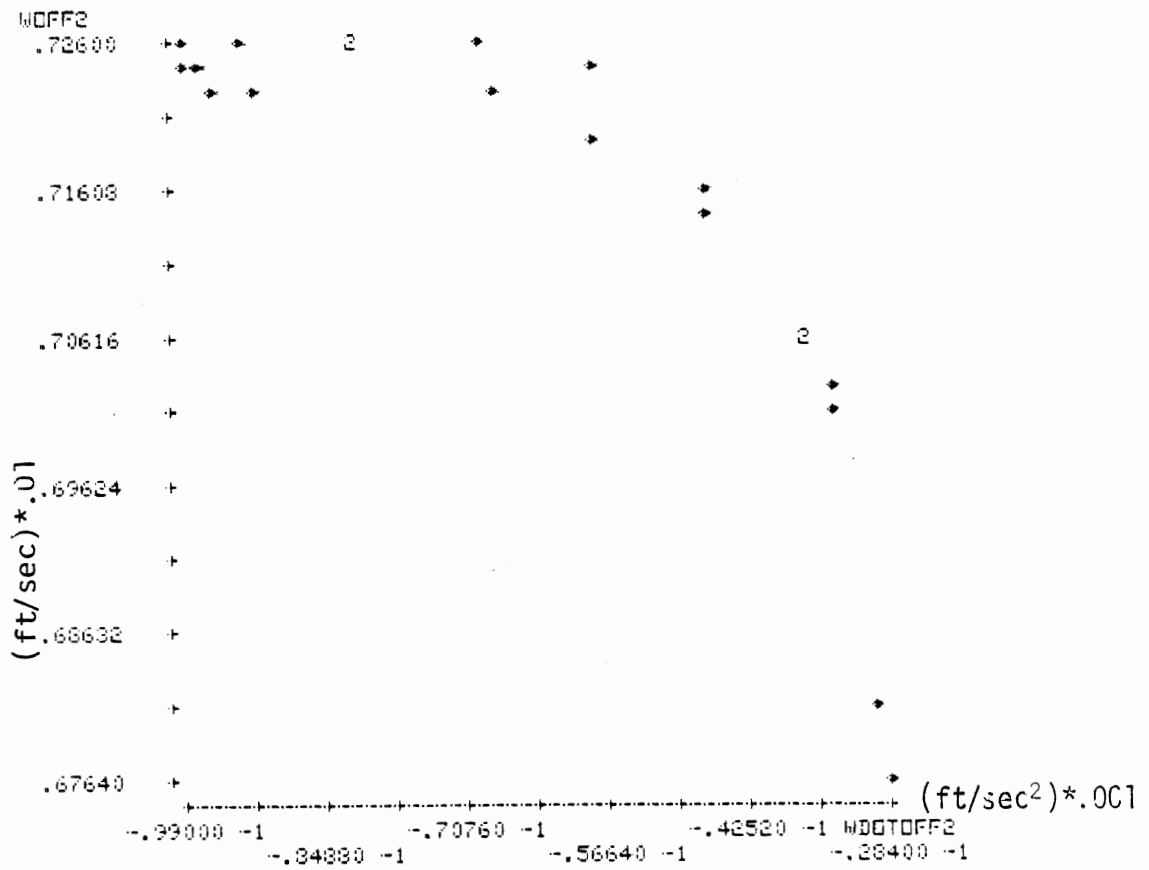


Figure 19. Logic module test result (K-H);  $\omega_0=88$ , high mu, 2nd cycle.

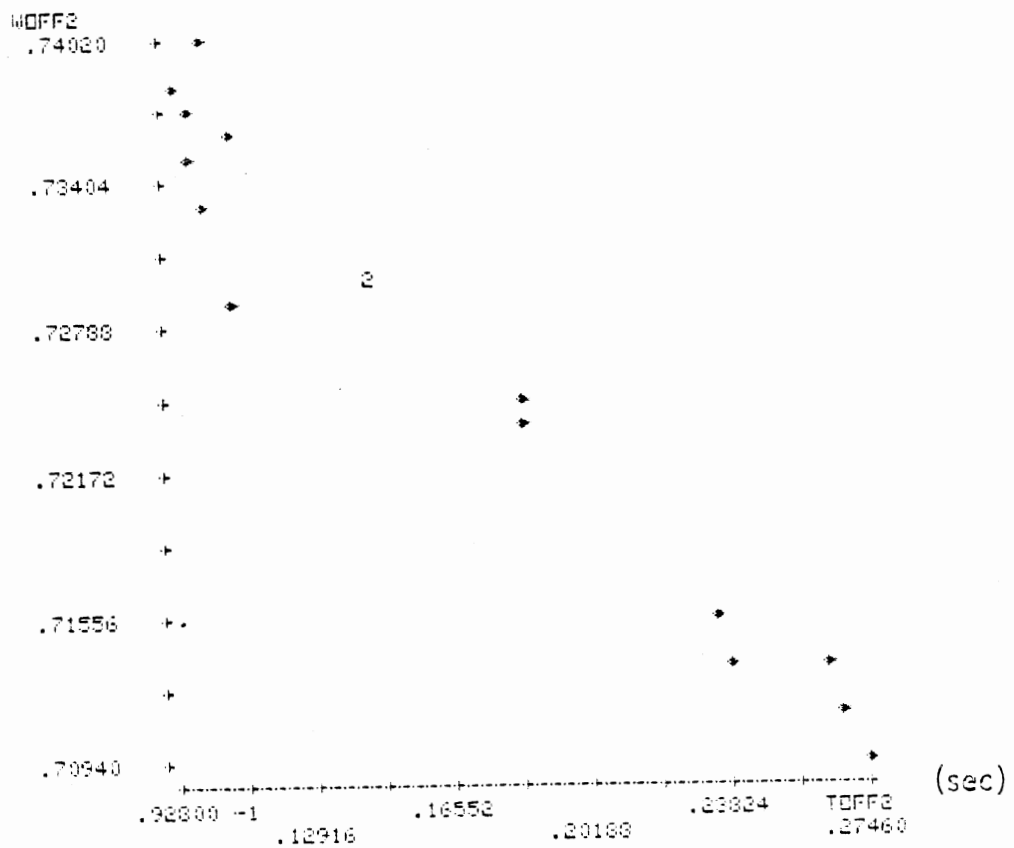
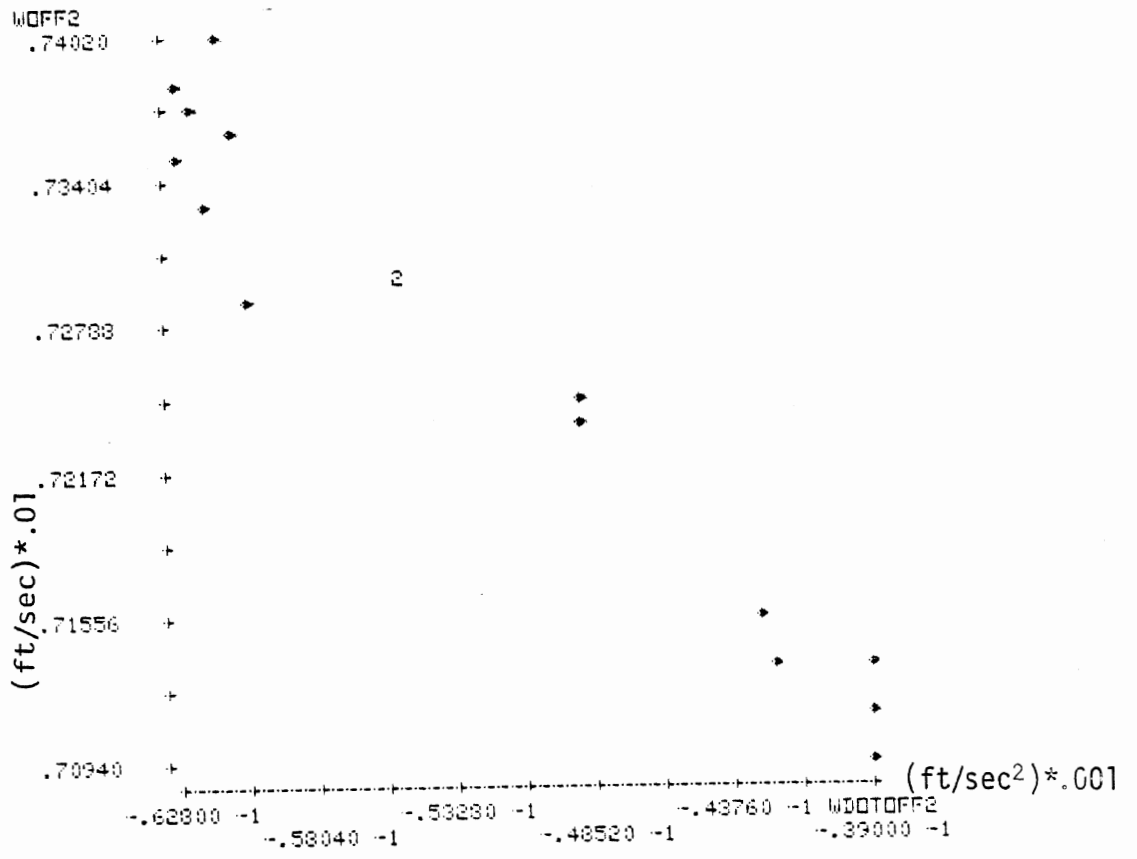


Figure 20. Logic module test result (K-H);  $\omega_0=88$ , high mu, 2nd cycle, slow apply.

$$\omega_{\text{off}} = A + B \dot{\omega}_{\text{off}} + C t_{\text{off}} \quad (1)$$

where A, B, and C are constants obtained from the regression process and provide the "best" fit (least squares) to the specified data set.

Table 9 lists the parameter values A, B, and C obtained for regression analyses of this form performed on the data shown in Figures 15-20. Also shown for each regression is the coefficient of determination,  $R^2$ , which indicates the degree of variability accounted for by the regression. In each case,  $R^2$  is about 0.9 or greater, indicating excellent matching between the measurement locus and the linear regression form of Equation (1).

The regression results for the first cycle tests suggest a basic switching condition involving a reference wheel speed ramp which starts at 95% of the initial velocity and decays at about 16 ft/sec, as shown in Figure 21. The  $\dot{\omega}$  term indicates the presence of some delay effect possibly deriving from input filtering or an intentionally programmed delay. The regression would also indicate an increased delay effect and greater slope for the reference wheel speed signal at lower velocities.

Also included in Table 9 are the regression results for two second-cycle tests, differing only by the rate of pressure application used in each sequence. Two regressions were performed for each of these test sequences. The first regression includes the effect of  $\dot{\omega}$ , while the second ignores its influence. Both regressions for the slow-apply test sequence agree quite closely, indicating little or no dependence upon the  $\dot{\omega}$  term, while suggesting  $\omega_0$  and  $t_{\text{off}}$  terms very similar to those obtained for the first-cycle tests. The regression results for the higher-apply rate sequence are similar though somewhat more scattered than the slow-apply results. Further tests and analyses are probably needed to help clarify these differences.

In general, it appears that if enough tests of this nature are performed, reasonable approximations to the actual control logic can be obtained. However, the work involved becomes progressively more difficult as additional cycles, conditions, and variables are included. A sample analysis similar to that just discussed, but using the digital library data instead is included in Appendix B.

Table 9. Regression Coefficients.

Test Condition	A	B	C	R <sup>2</sup>	
1st cycle $\omega_0 = 88$ HIGH MU (Fig. 15)	$0.951\omega_0$	0.022	-16.0	0.990	
1st cycle $\omega_0 = 80$ HIGH MU (Fig. 16)	$0.948\omega_0$	0.023	-15.8	0.985	
1st cycle $\omega_0 = 88$ LOW MU (Fig. 17)	$0.947\omega_0$	0.018	-15.4	0.961	
1st cycle $\omega_0 = 40$ HIGH MU (Fig. 18)	$0.938\omega_0$	0.040	-20.6	0.990	
2nd cycle $\omega_0 = 88$ HIGH MU (Fig. 19)	a.	$0.983\omega_0$	0.048	-23.4	0.977
	b. (ignoring $\dot{\omega}$ )	$0.921\omega_0$	0.0	-12.7	0.897
2nd cycle $\omega_0 = 88$ HIGH MU Slow Apply (Fig. 20)	a.	$0.936\omega_0$	0.006	-15.0	0.929
	b. (ignoring $\dot{\omega}$ )	$0.942\omega_0$	0.0	-15.8	0.929

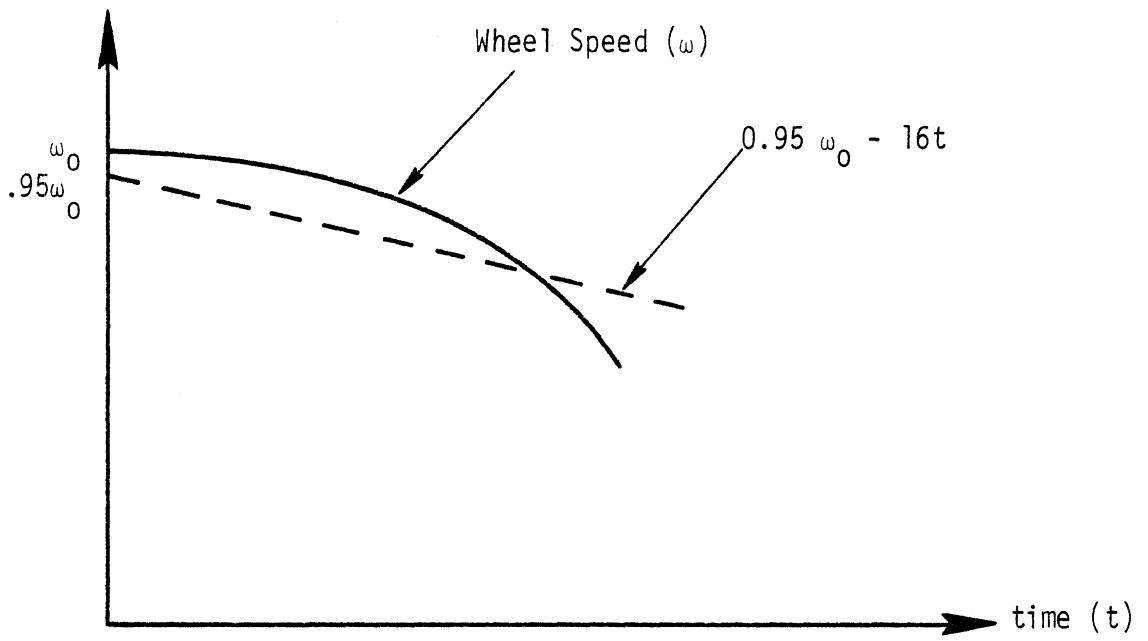


Figure 21. Example wheel speed reference signal (K-H); 1st cycle.

#### 4.0 GENERAL OBSERVATIONS AND CONCLUSIONS

The different hardware and control strategies used by each of these systems can produce significant differences in wheel speed cycling behavior. Very often these differences in cycling behavior can account for or help explain differences in overall system performance, as reflected in stopping distance or average deceleration measures. However, it is not necessarily true that the differences in cycling behavior which exist under one set of operating conditions will hold at another. To illustrate this, average decelerations were calculated for each system under three different operating conditions and are listed in Table 10. The initial velocity is 60 mph in each case, with wheel inertia, vertical load, and tire-road friction differences defining the three operating conditions. As seen, significant differences can occur for a specific system, as well as between different systems, when operating conditions are changed. This, of course, is especially true for the transition from laboratory tests such as these to actual vehicle conditions where vertical loads and brake system characteristics are continually changing.

For systems with basically similar cycling characteristics, detailed examination of the wheel slip time histories can often uncover significant differences. Frequently, two systems may cycle with the same frequency and across the same range of wheel slip, and therefore appear to be quite similar. However, percentage of time spent in various regions of the slip cycle may differ considerably, thereby suggesting significantly different antiskid braking performance capabilities.

The temptation to conjecture and draw conclusions about braking performance of vehicles equipped with such systems, on the basis of laboratory antiskid tests alone, is clearly speculative. Heavy vehicle pitch and bounce dynamics, productive of large vertical load oscillations, coupled with brake system lags, hysteresis, and side-to-side imbalances, often determine the timing and cycling characteristics of an antiskid system during the course of a heavy vehicle antiskid stop. What



Table 10. Average Deceleration Measure for Three Different Operating Conditions.

<u>System</u>	<u>Average Deceleration (g's)</u>	<u>Operating Condition</u>
Bendix	0.62	
Eaton	0.60	Wheel Inertia = 150 in-lb-sec <sup>2</sup>
B.F. Goodrich	0.59	High Mu
Kelsey-Hayes	0.53	Wheel Load = 5000 lbs
Wagner	0.50	
Eaton	0.60	
B.F. Goodrich	0.59	Wheel Inertia = 300 in-lb-sec <sup>2</sup>
Bendix	0.57	High Mu
Kelsey-Hayes	0.57	Wheel Load = 7500 lbs
Wagner	0.50	
Bendix	0.32	
Wagner	0.30	Wheel Inertia = 75 in-lb-sec <sup>2</sup>
Eaton	0.30	Low Mu
Kelsey-Hayes	0.29	Wheel Load = 2500 lbs
B.F. Goodrich	0.29	

might be described as "timid" antiskid performance during laboratory tests could conceivably transform to "aggressive" under more typically adverse vehicle operating environments.

A general feature shared by most of the antiskid systems is the recurrent philosophy of slow brake pressure application and quick release. The degree of design originality present in each system and which most separates system from system appears to be centered about those different mechanisms (pneumatic logic, pulse-rate modulation, 1/3-2/3 pressure application) which serve to achieve this common pressure modulation philosophy. The basic strategy can be explained on the basis of wheel slip dynamics. Since it is easier to control wheel slip on the low and dynamically stable side of the  $\mu$ -slip curve, usually encountered during brake pressure applications, it is likewise easier to promote longer periods of time within advantageous slip regimes during this portion of a cycle.

Finally, it should be clear that the antiskid data base generated during this project can be useful in contributing to further studies of antiskid braking performance of heavy vehicles. Use of this data to approximate and represent antiskid system performance within large-scale vehicle simulations, such as [1], will unquestionably aid in any such effort.

## 5.0 REFERENCES

1. Winkler, C.B., et al. "A Computer Program for Predicting the Braking Performance of Trucks and Tractor-Trailers." Phase III Technical Report, The Univ. of Michigan, Highway Safety Research Institute, Ann Arbor, Mich., June 15, 1975.
2. Fancher, P.S. and MacAdam, C.C. "Computer Analysis of Antilock System Performance in the Braking of Commercial Vehicles." Conference on Braking of Road Vehicles, Inst. of Mech. Engrs., London, March 23-25, 1976, pp. 113-123.

## APPENDIX A

### SAMPLE TIME HISTORIES

This appendix contains sample time histories for the antiskid system tests described in Section 2.1. Six time histories are shown for each system covering three vertical loads and two friction conditions. All test results included here are for 60 mph initial velocities and 150 inch-lb-sec<sup>2</sup> wheel inertias.

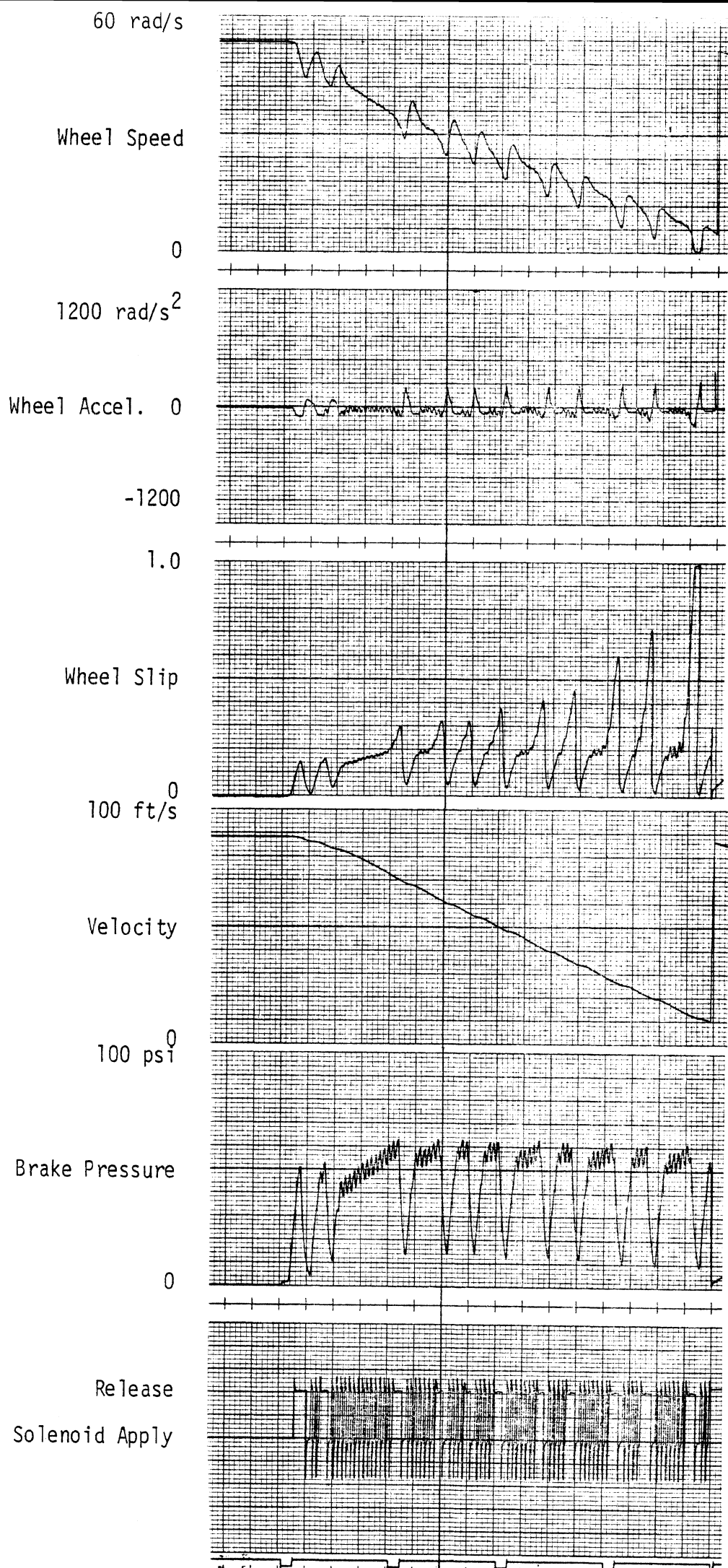


Figure A1. Bendix, 5000 lb., High Mu.

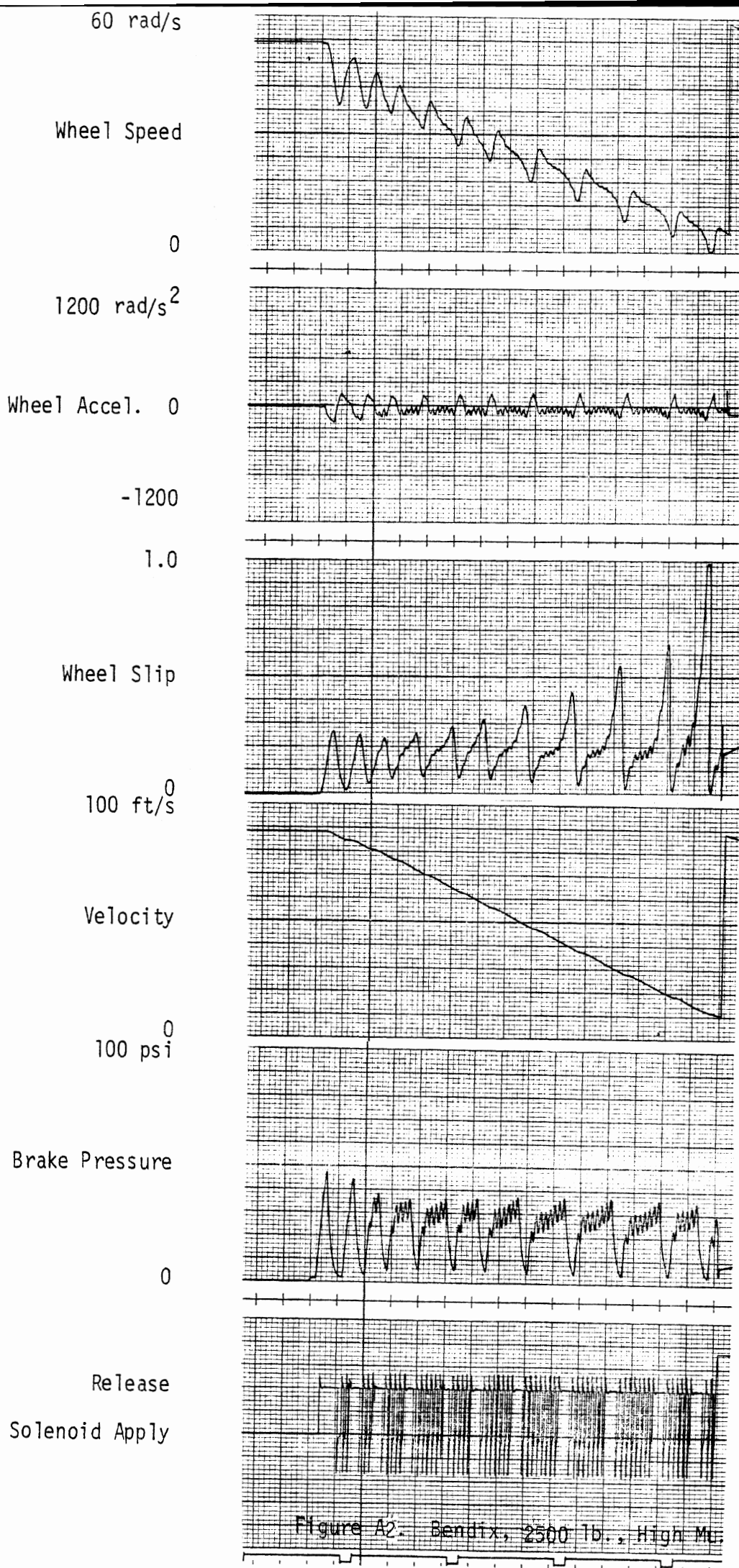


Figure A2: Bendix, 2500 lb., High Mt.

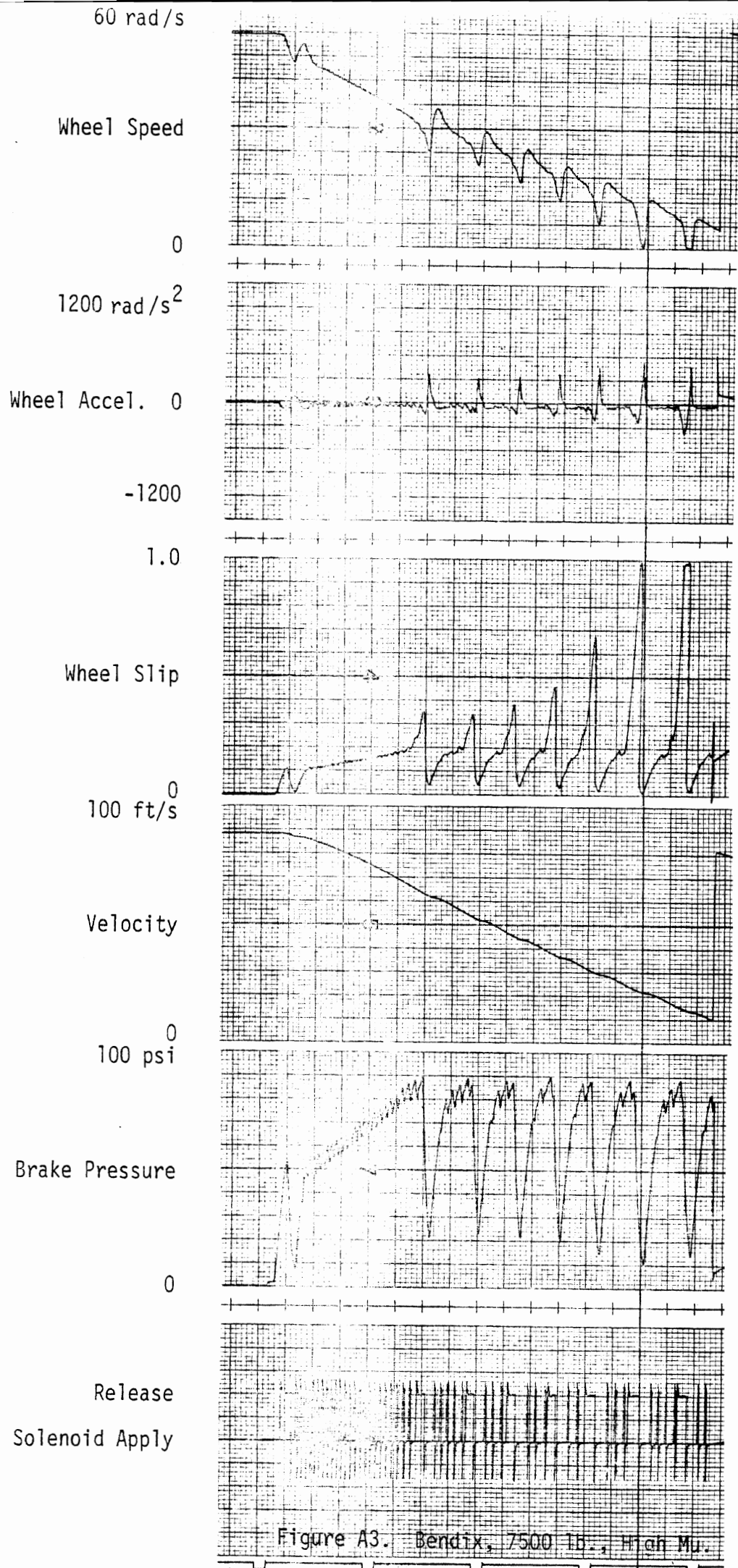


Figure A3. Bendix, 7500 lb., High Mu.

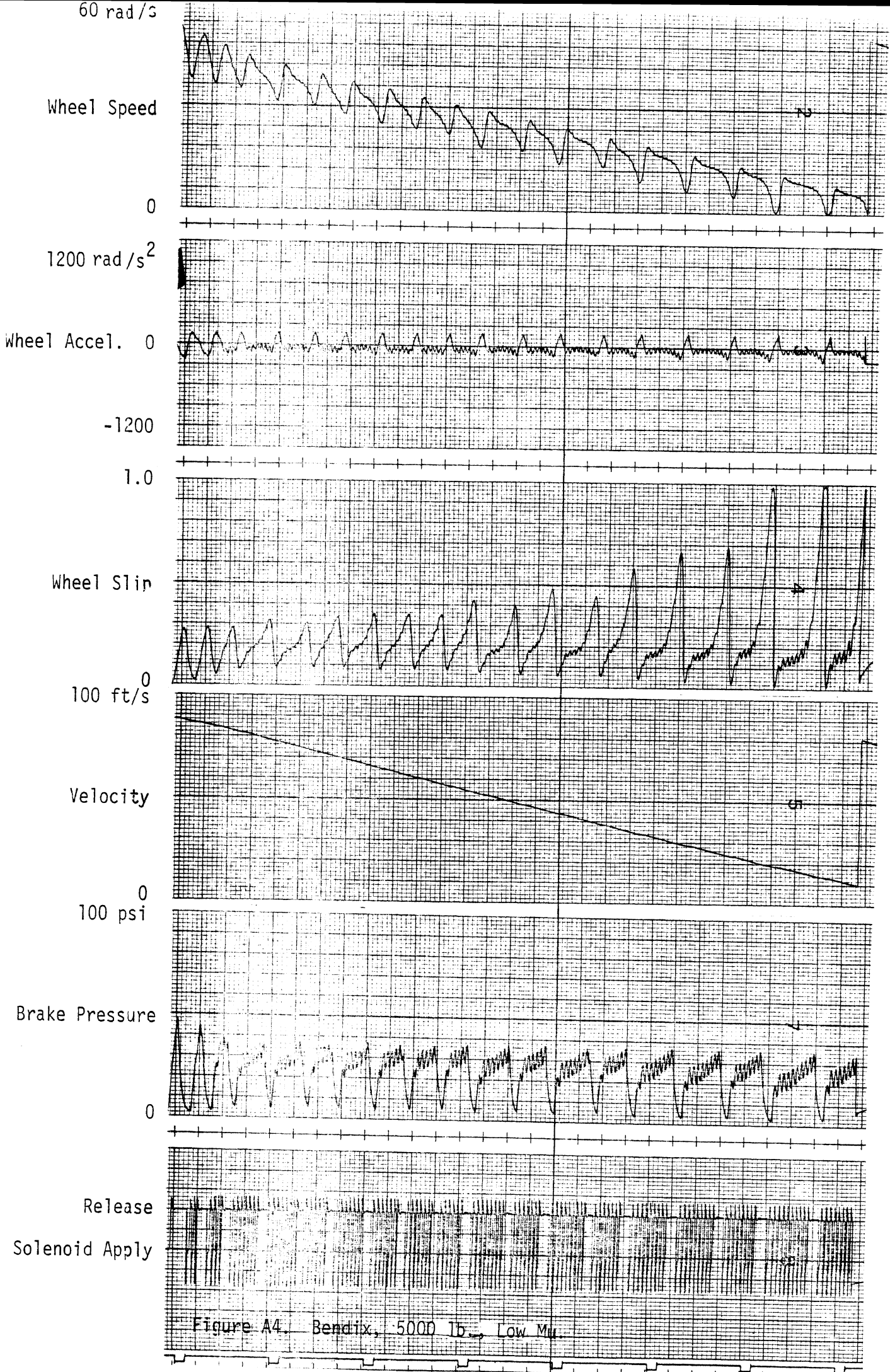
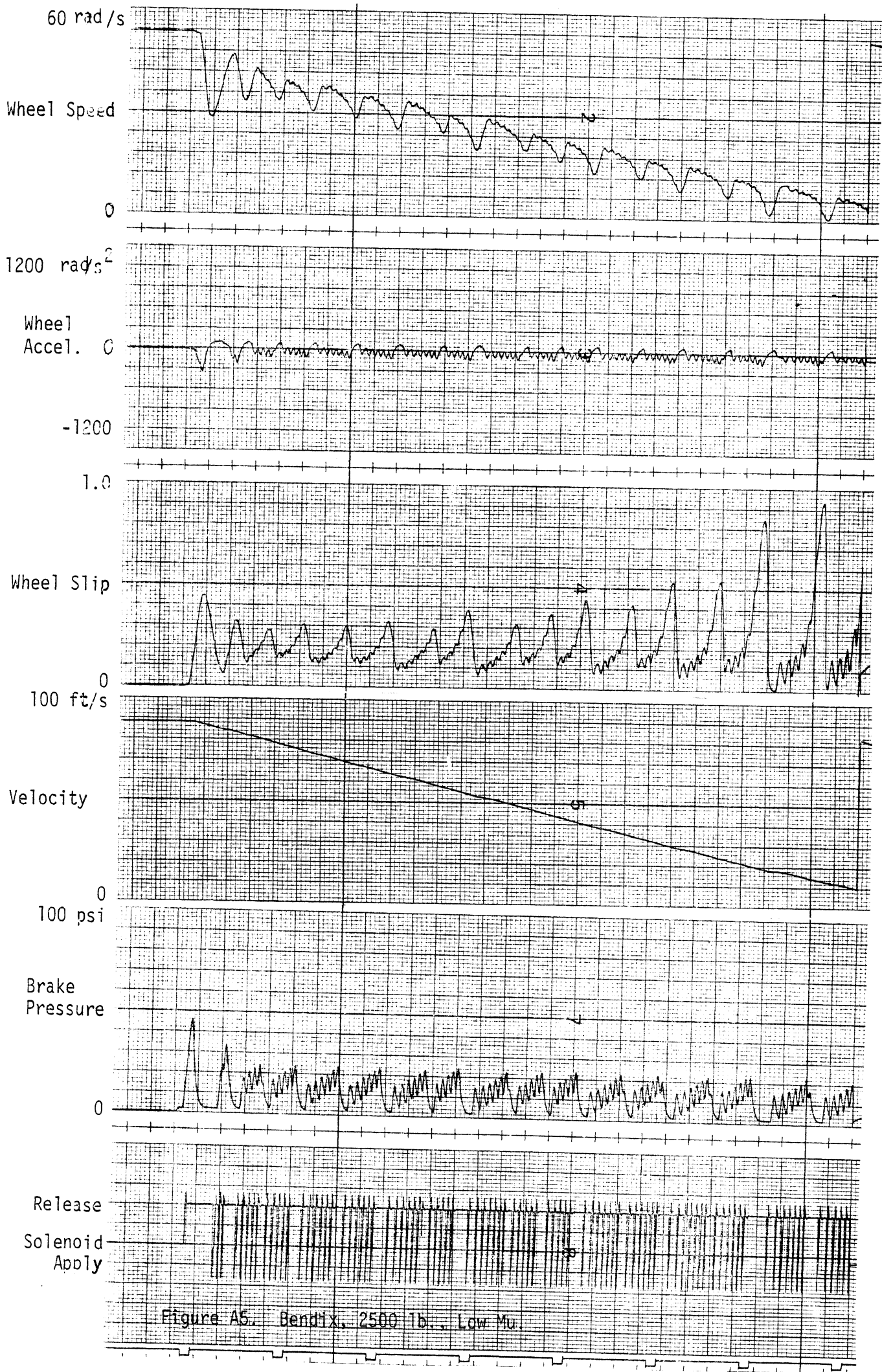


Figure A4. Bendix, 5000 lb., Low Mu.





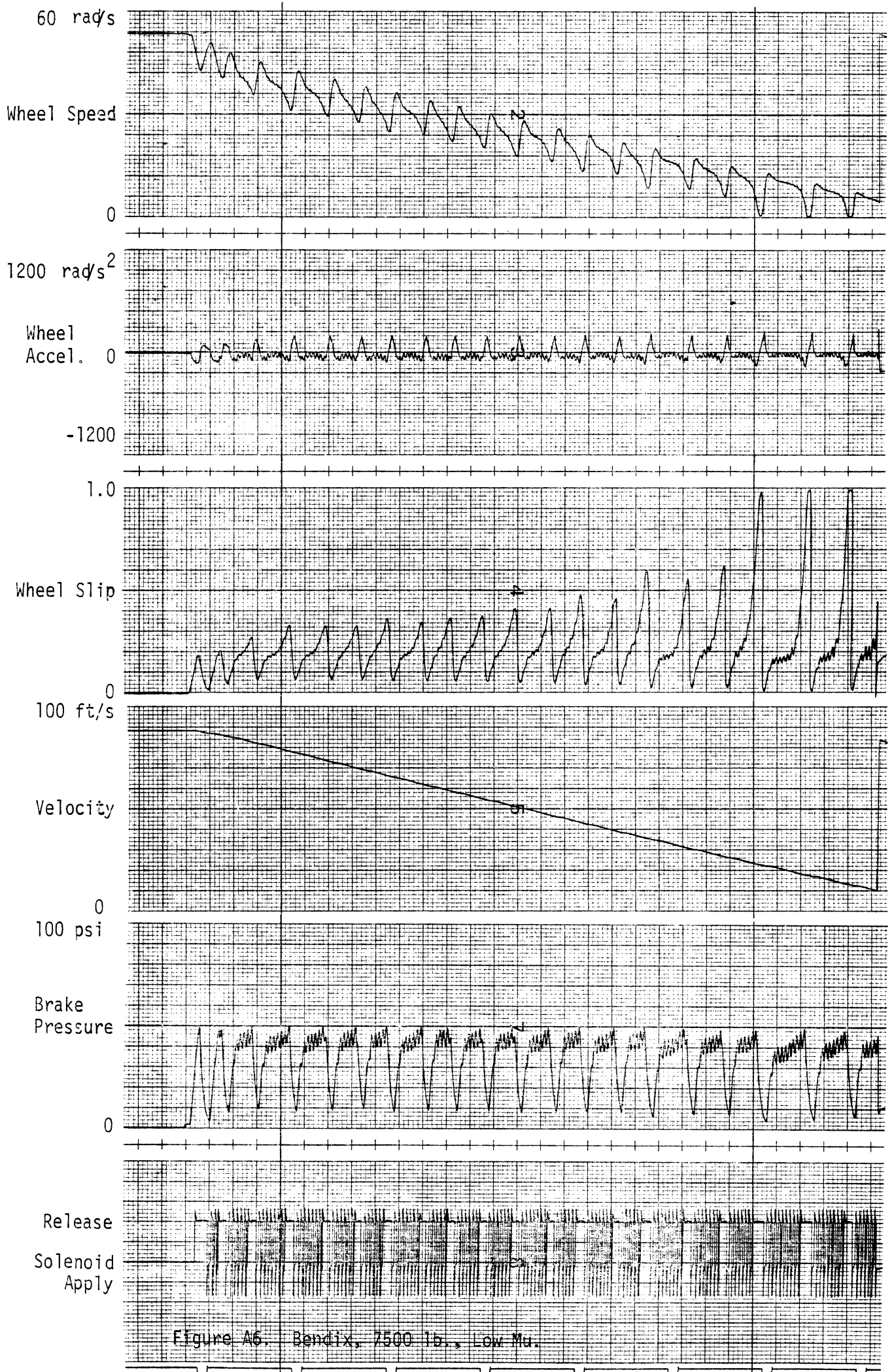
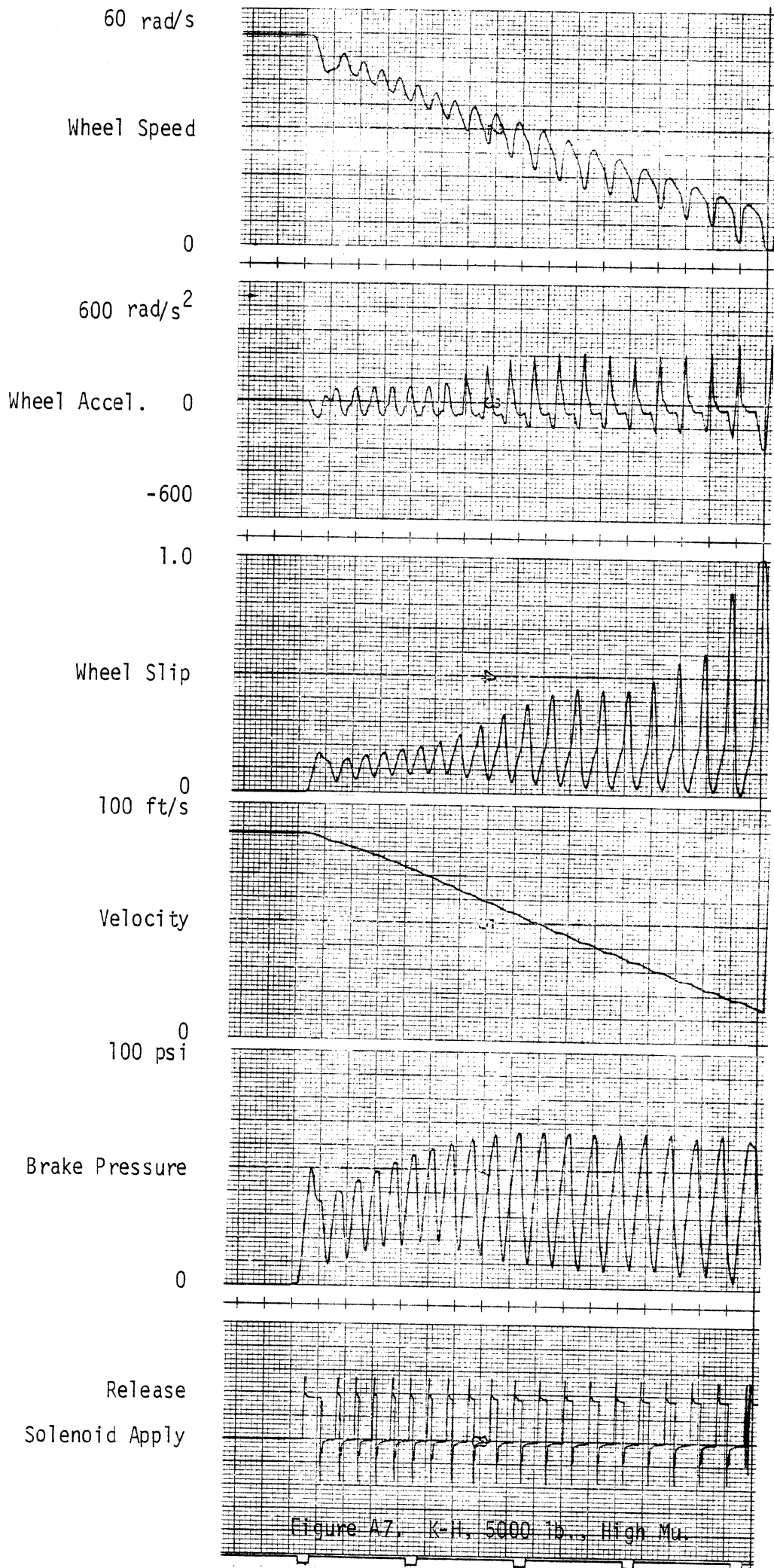


Figure A6. Bendix, 7500 lb., Low  $\mu$ .



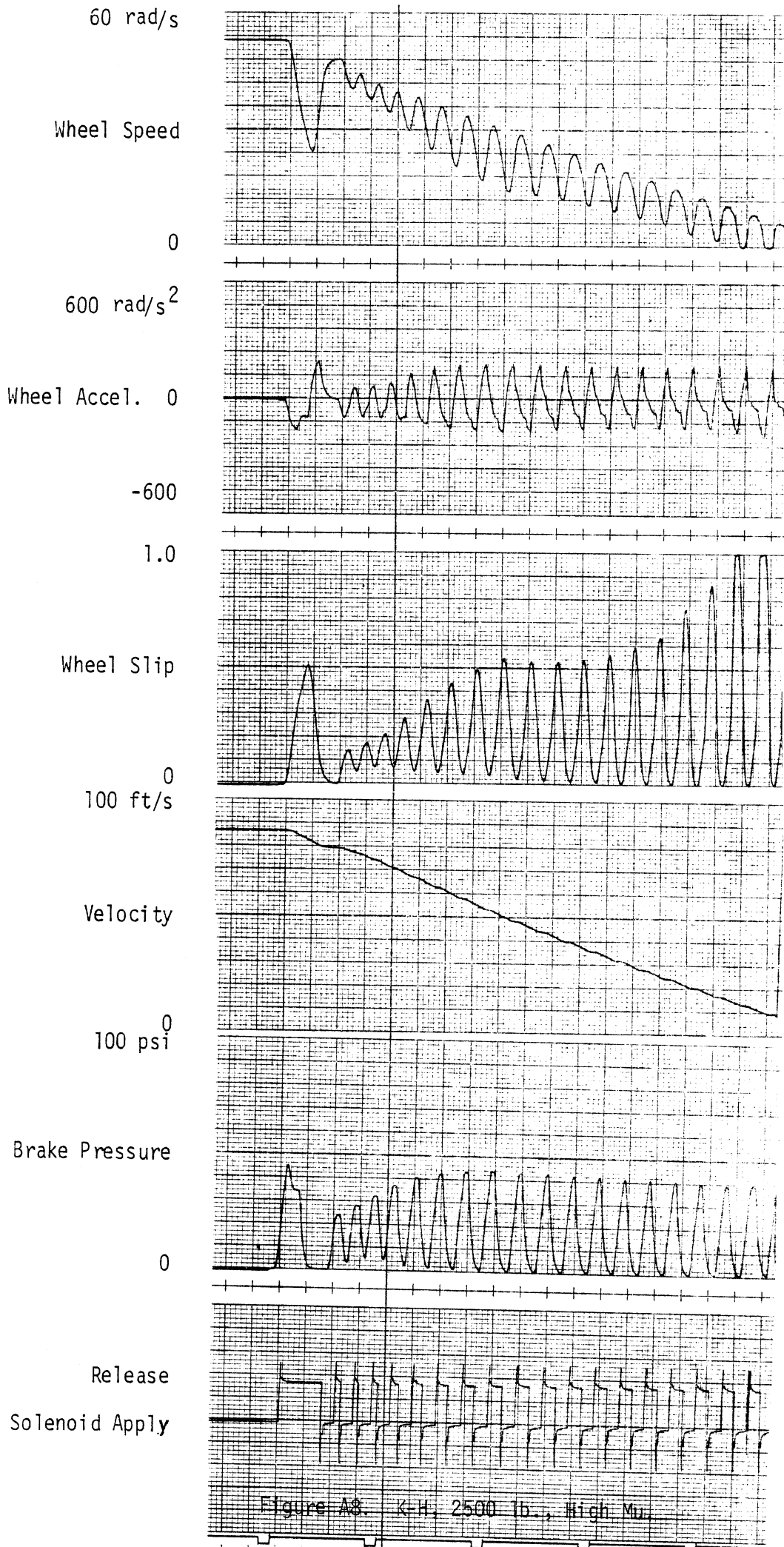
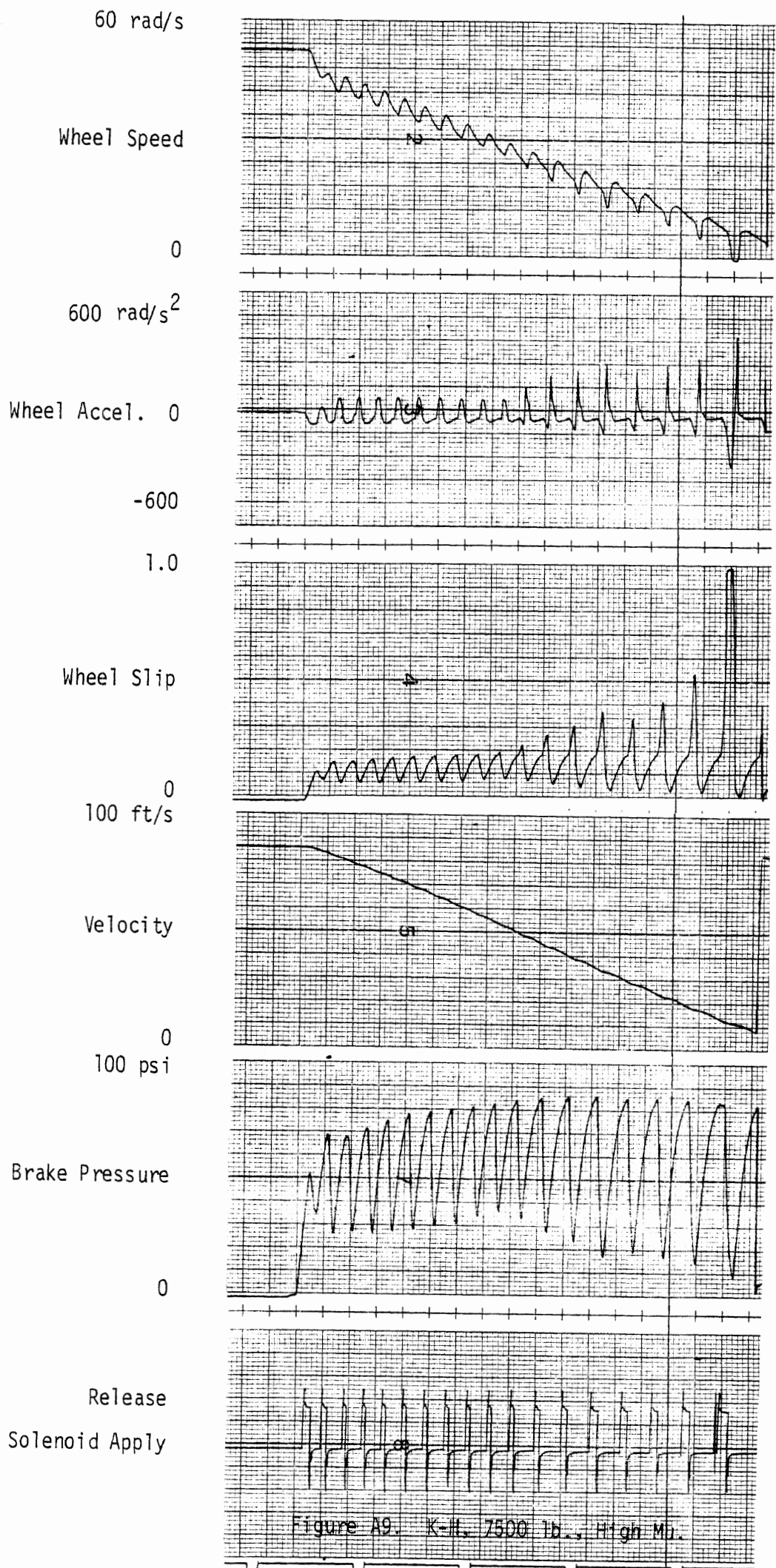
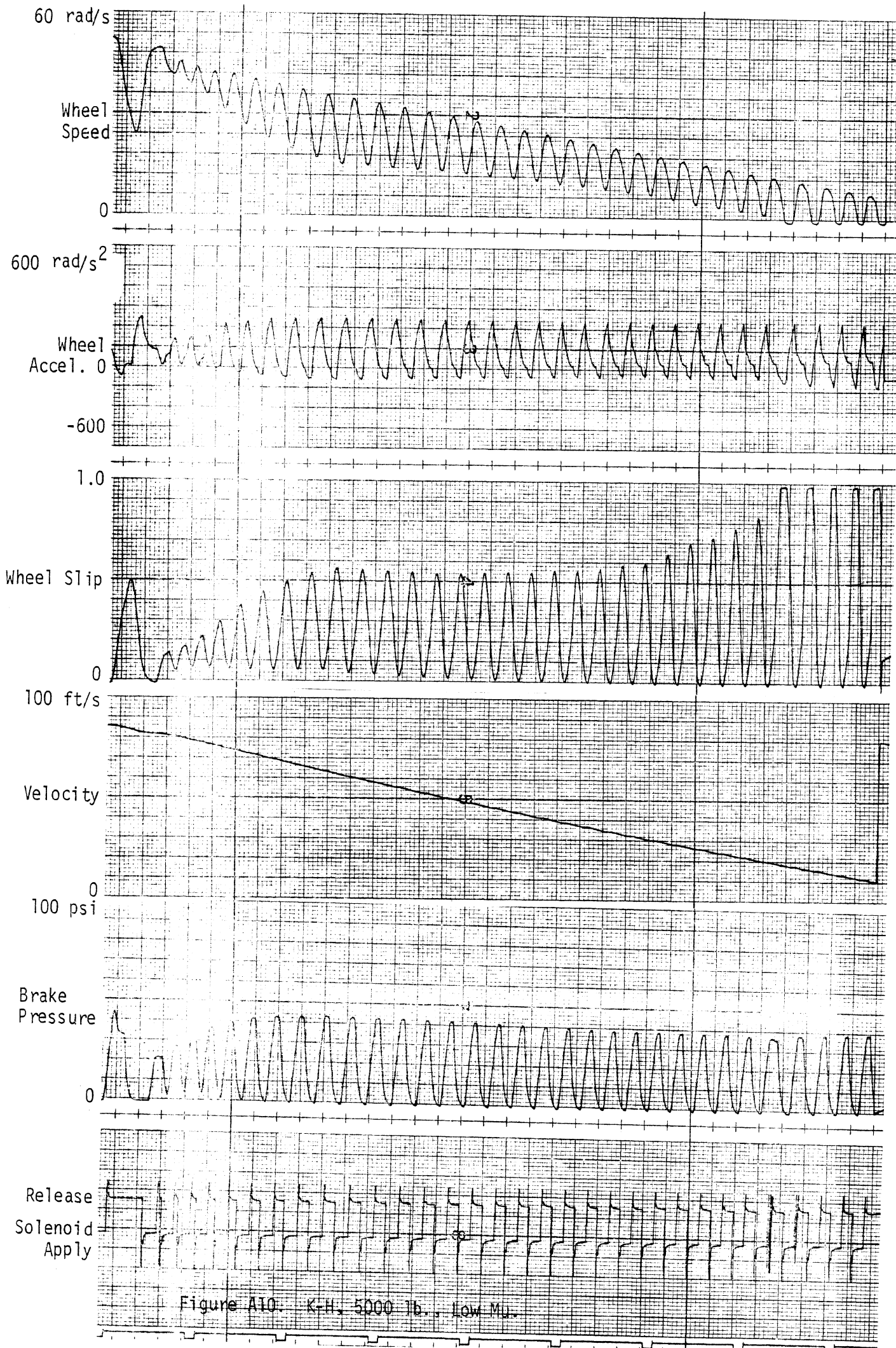


Figure A8. K-H, 2500 lb., High Mu.





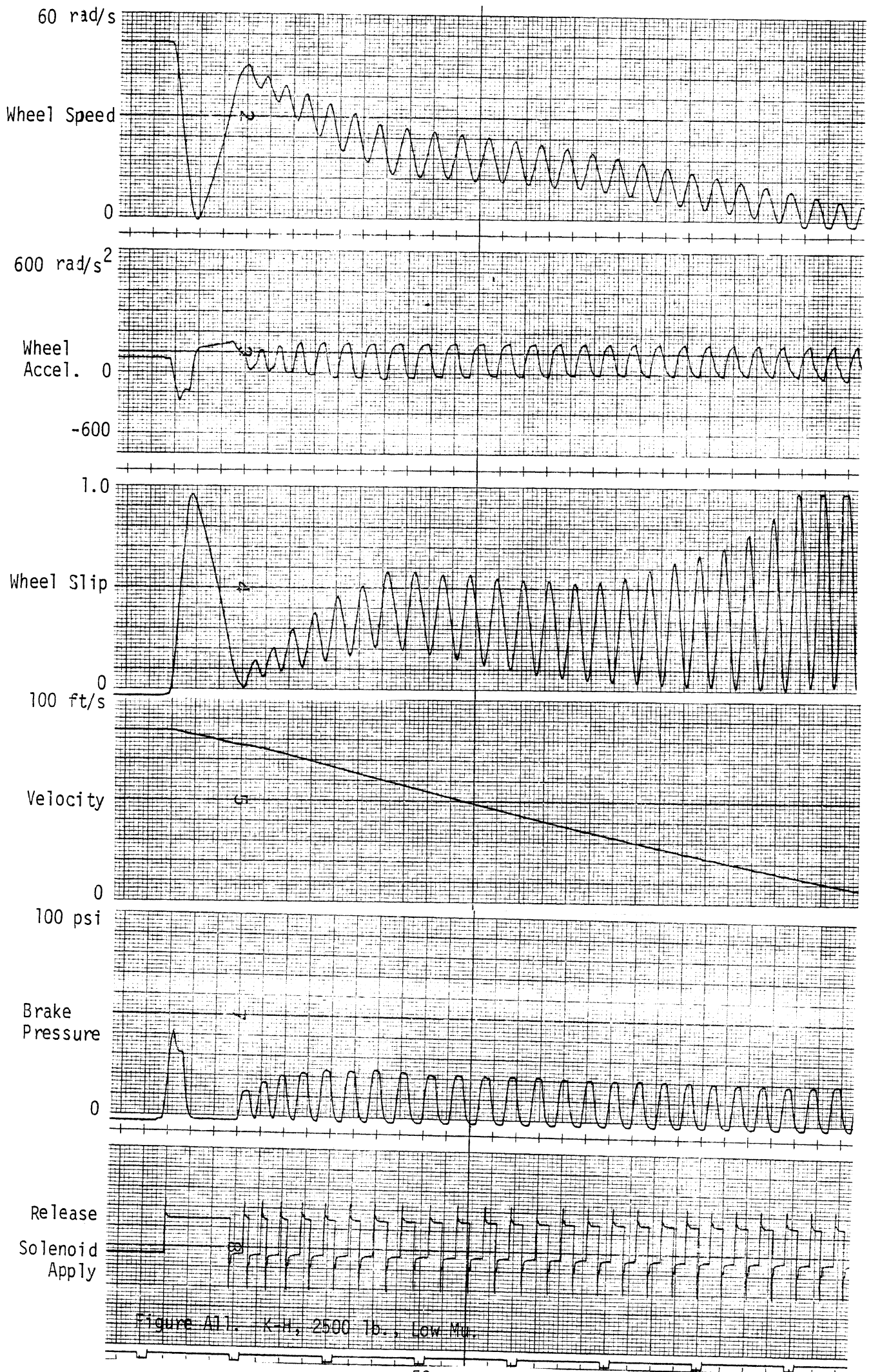


Figure A11. K-H, 2500 lb., Low Mo.

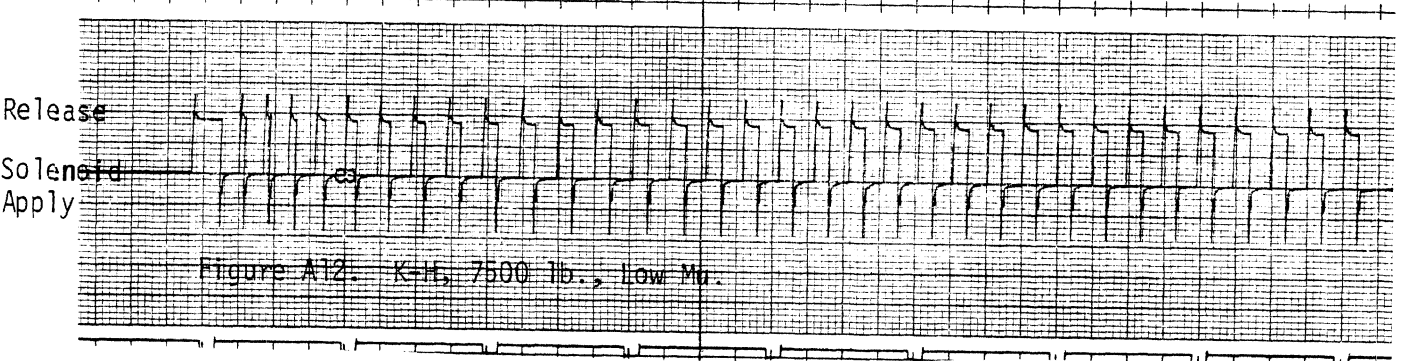
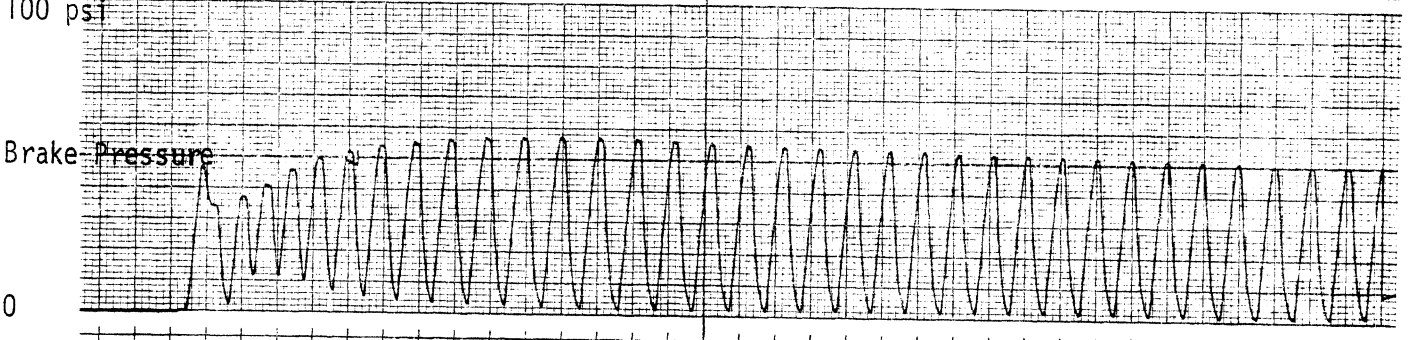
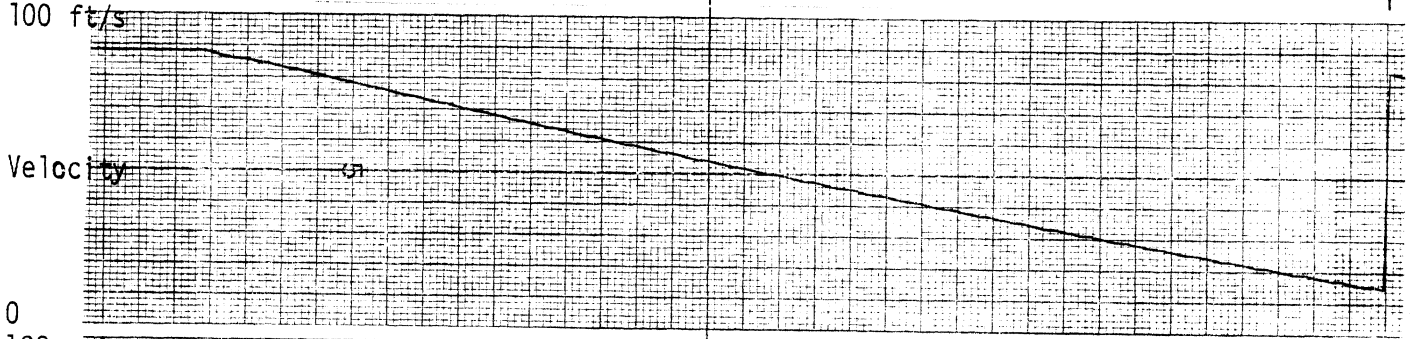
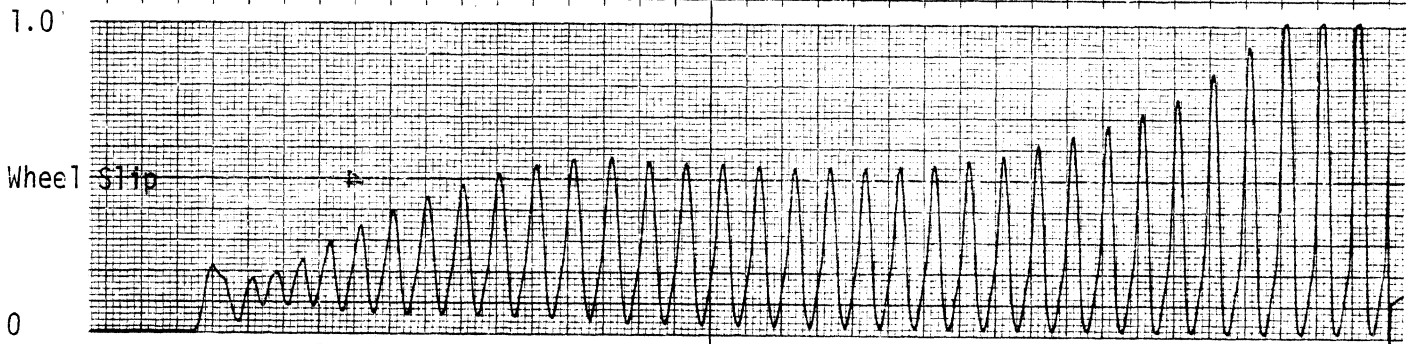
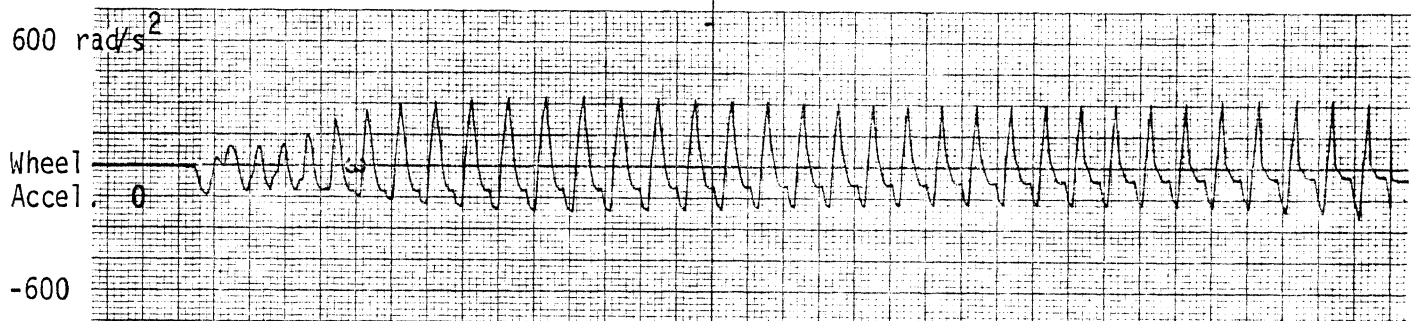
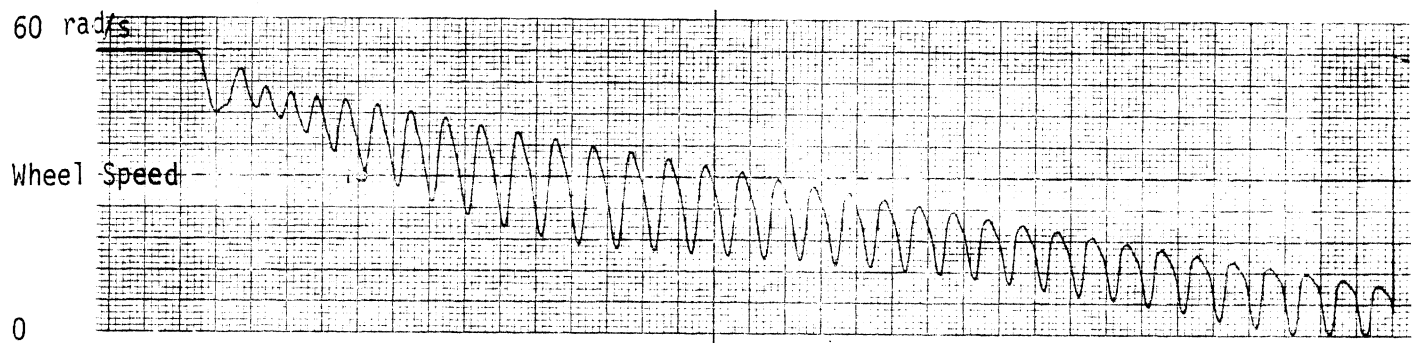
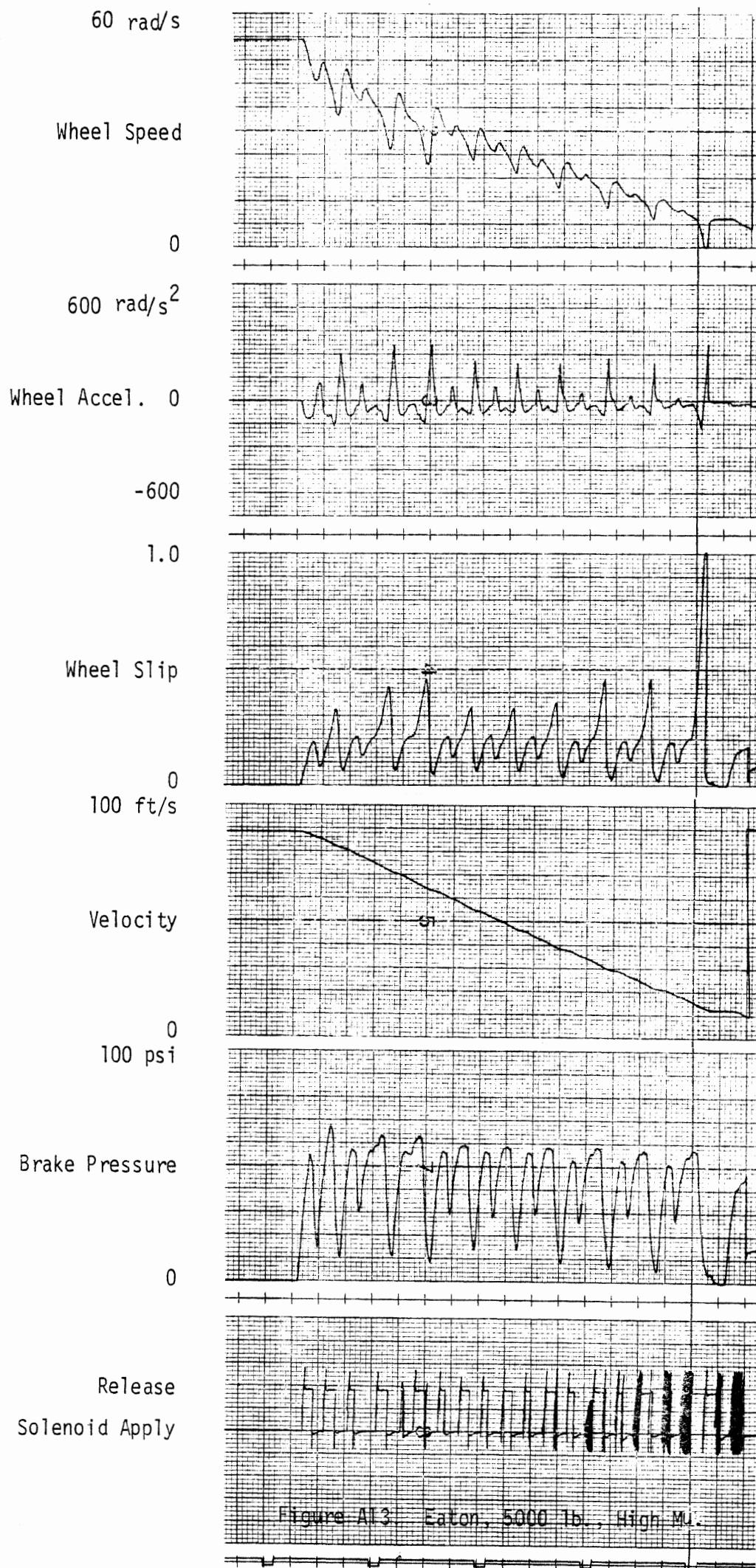


Figure A12. K-H, 7500 lb., low Mr.





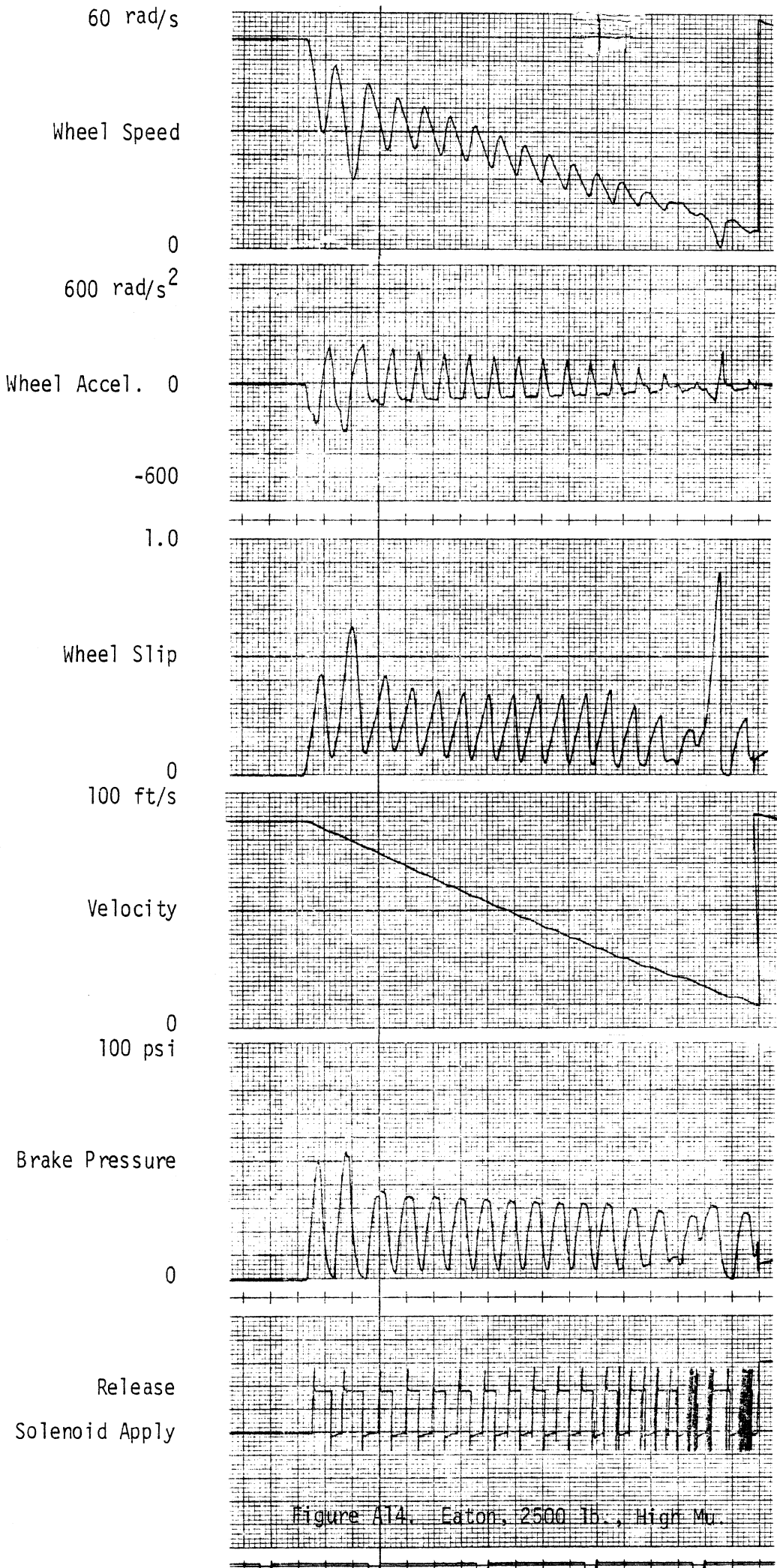


Figure A14. Eaton, 2500 lb., High Mu.

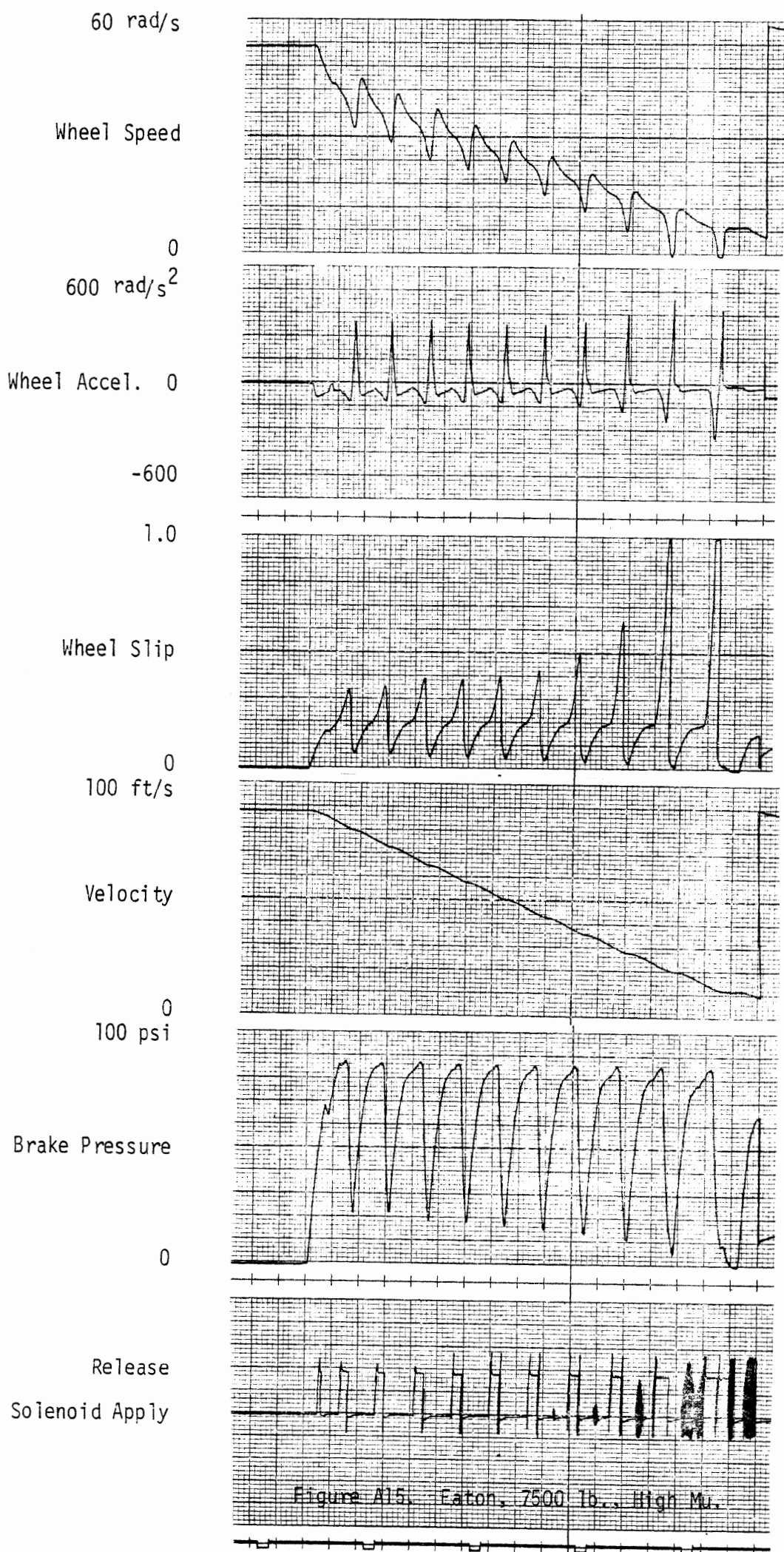


Figure A15. Eaton, 7500 lb., High Mu.

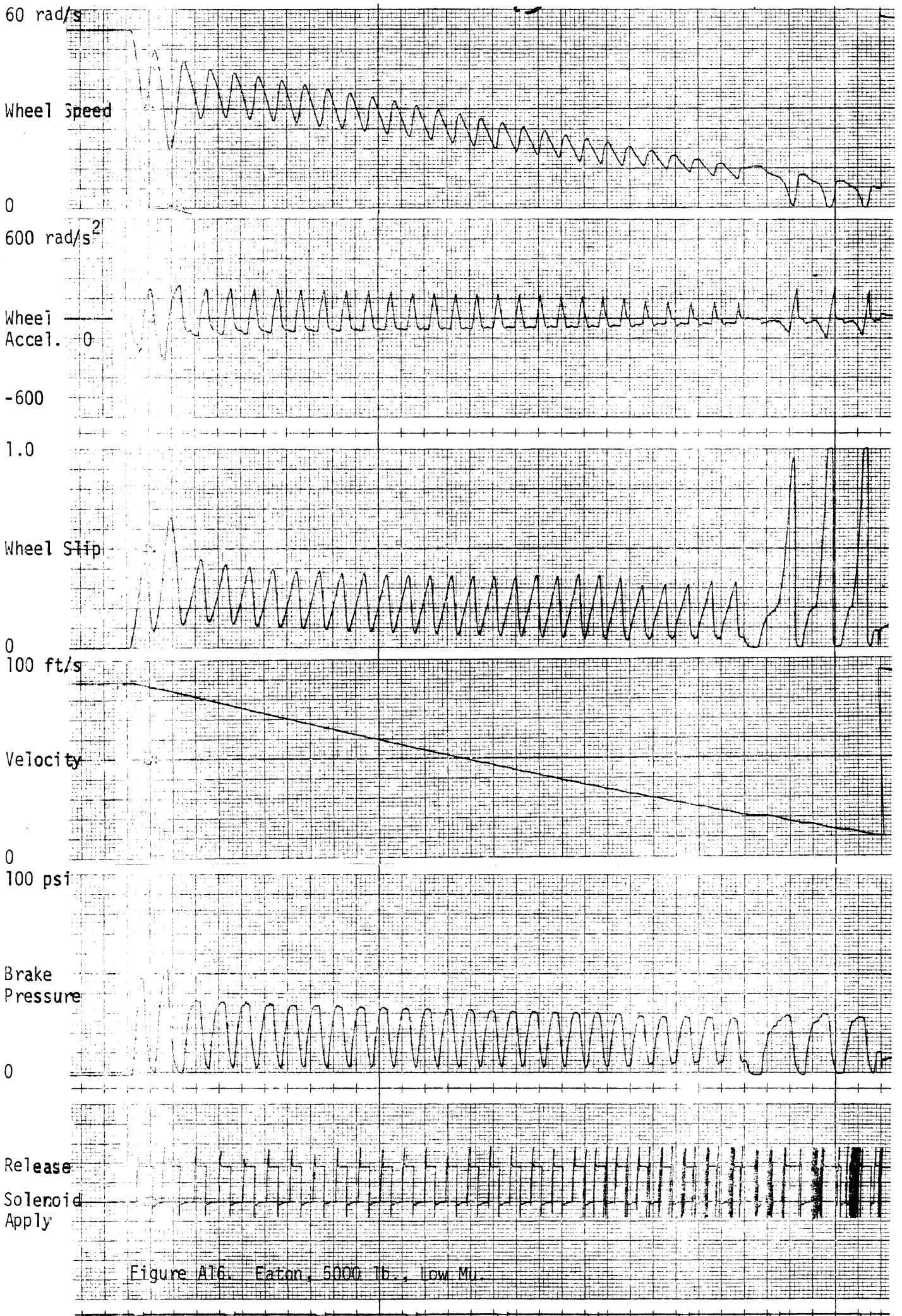


Figure A16. Eaton, 5000 lb., low M<sub>u</sub>.

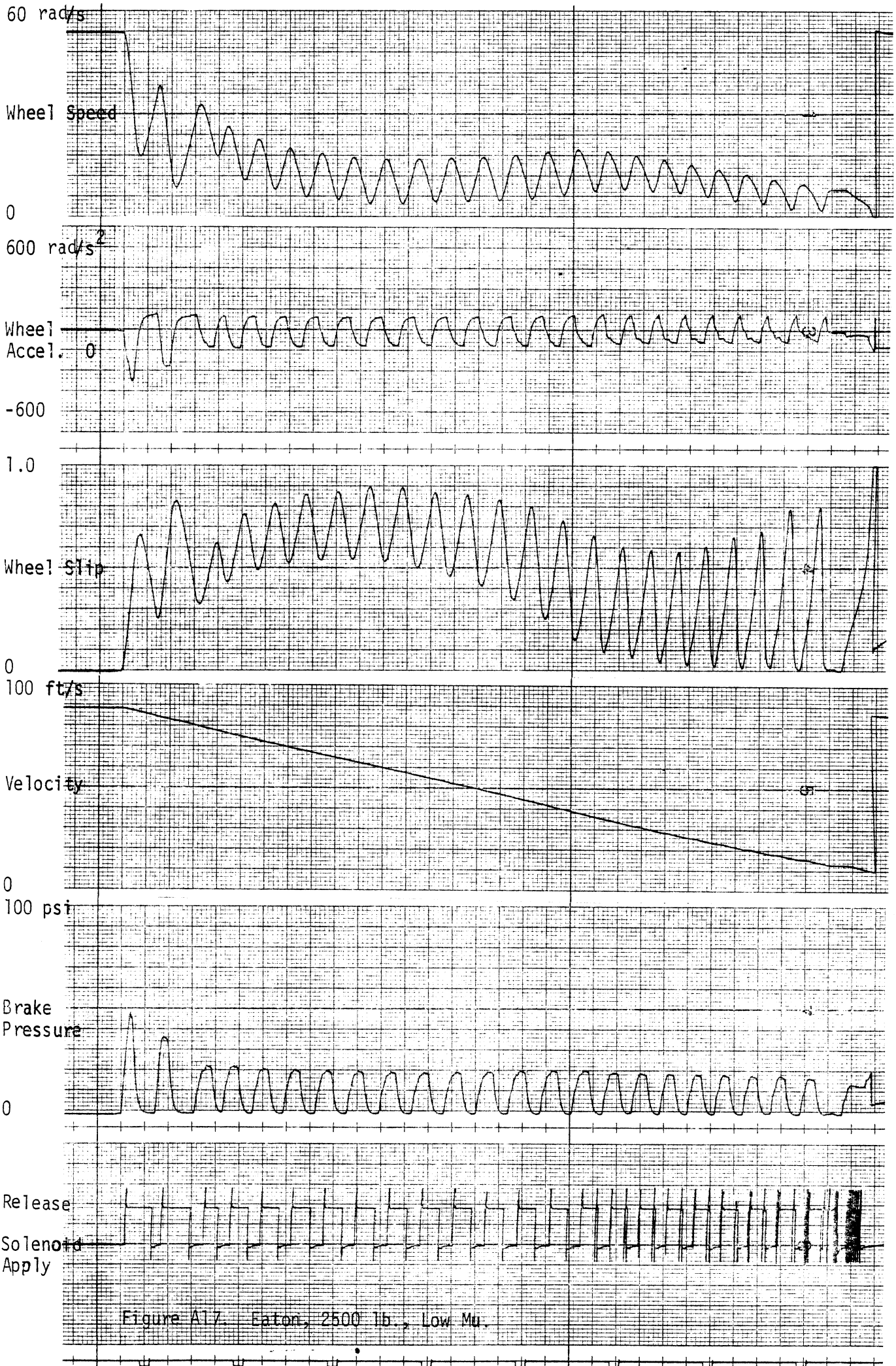
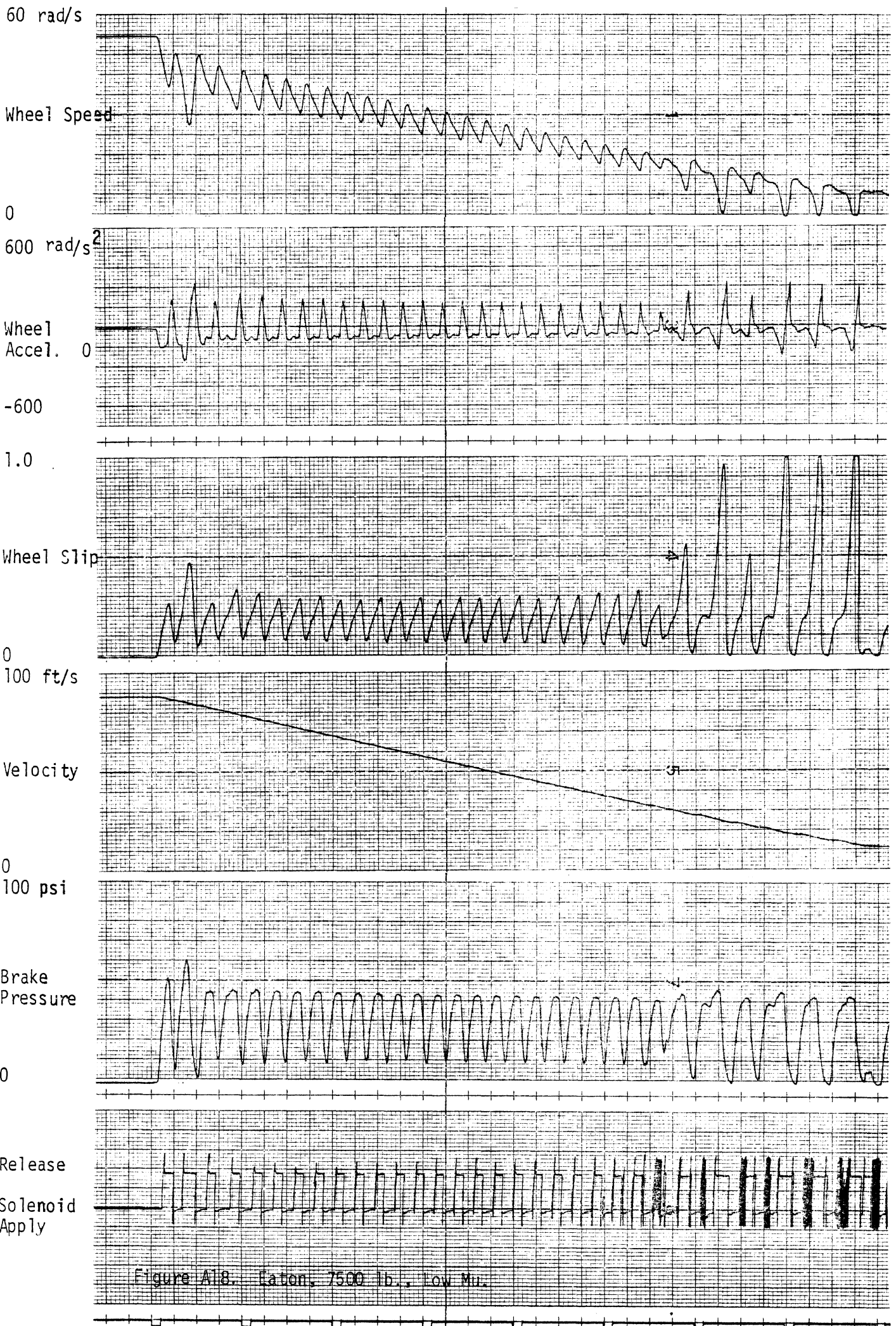


Figure A17. Eaton, 2500 lb., Low Mu.



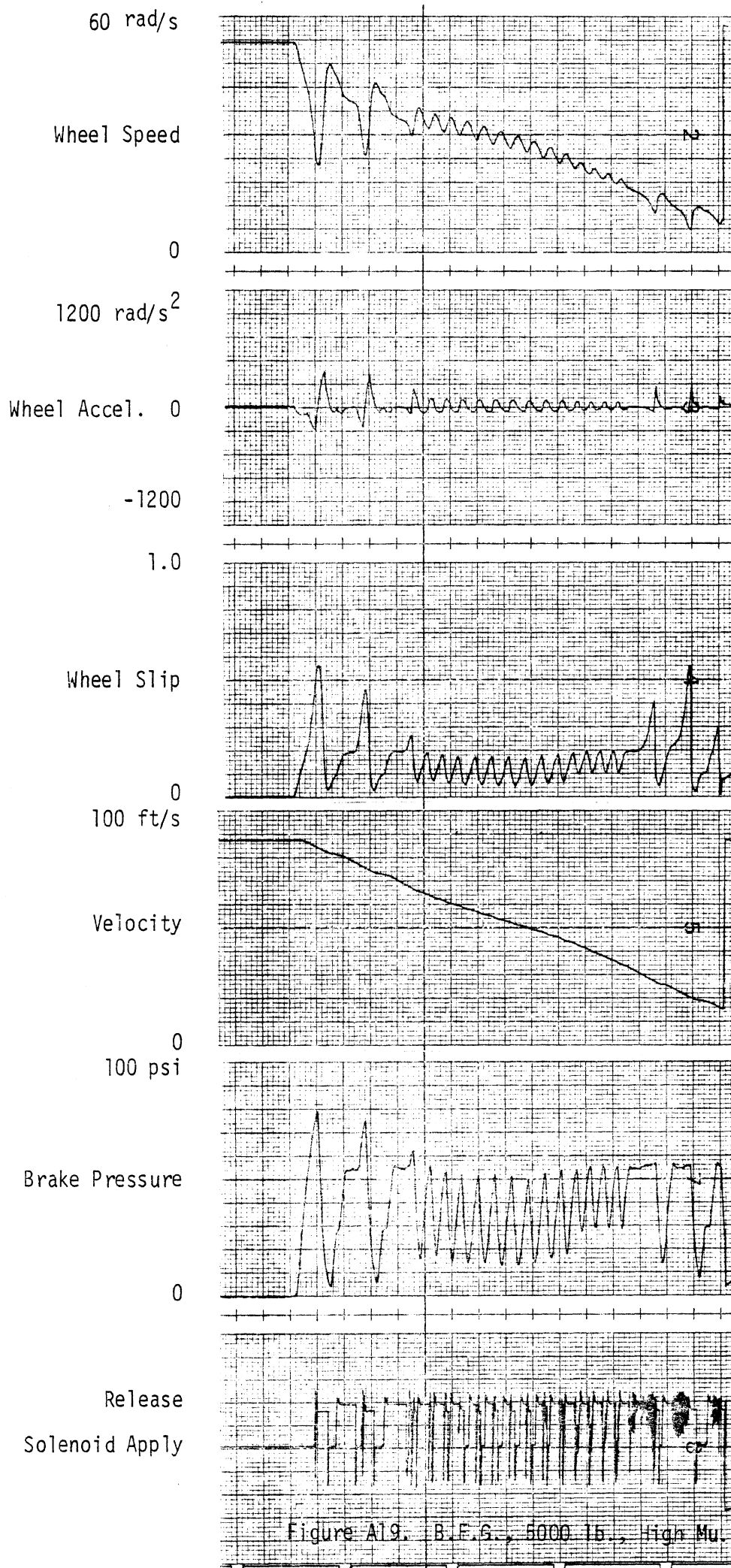


Figure A19. B.F.G., 5000 lb., high Mu.

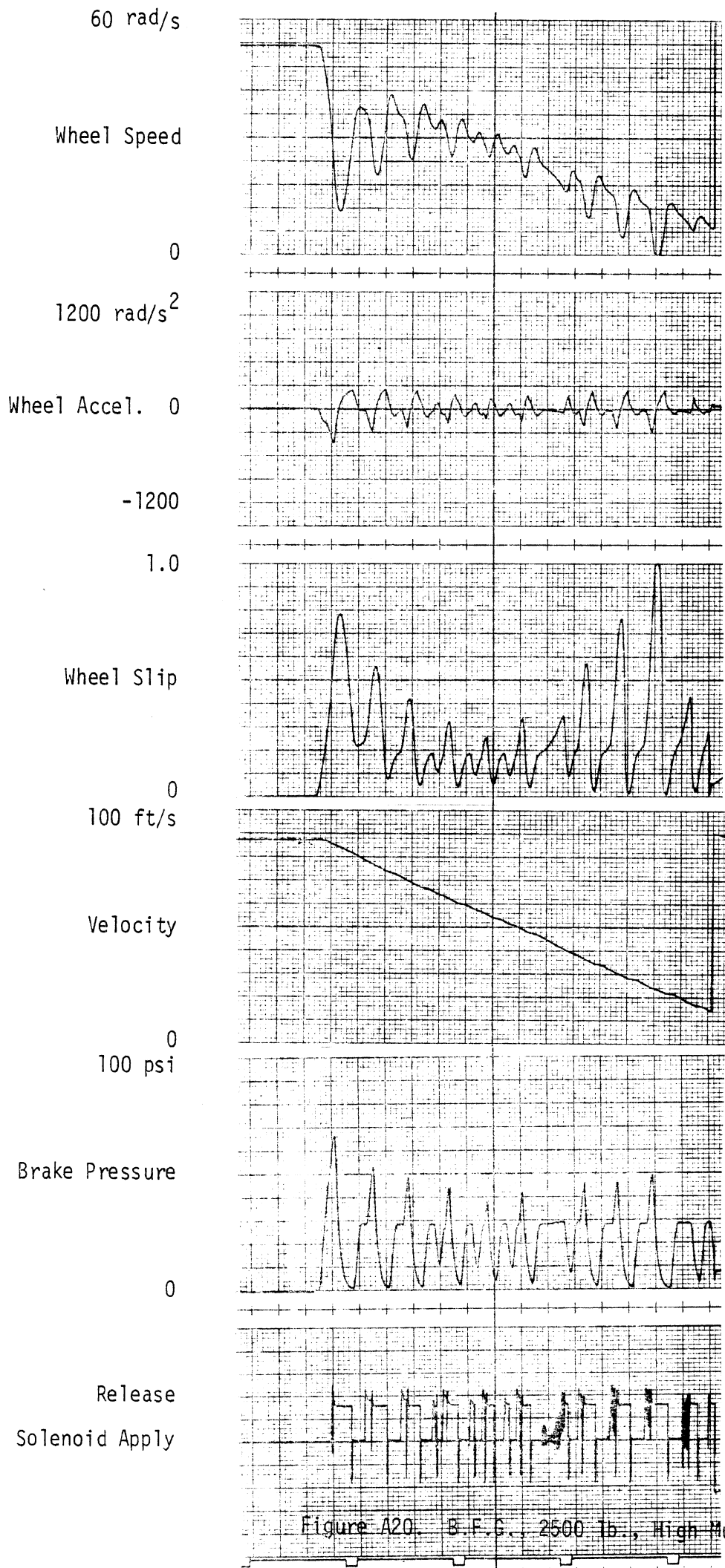


Figure A20. B.F.G., 2500 lb., High Mu.



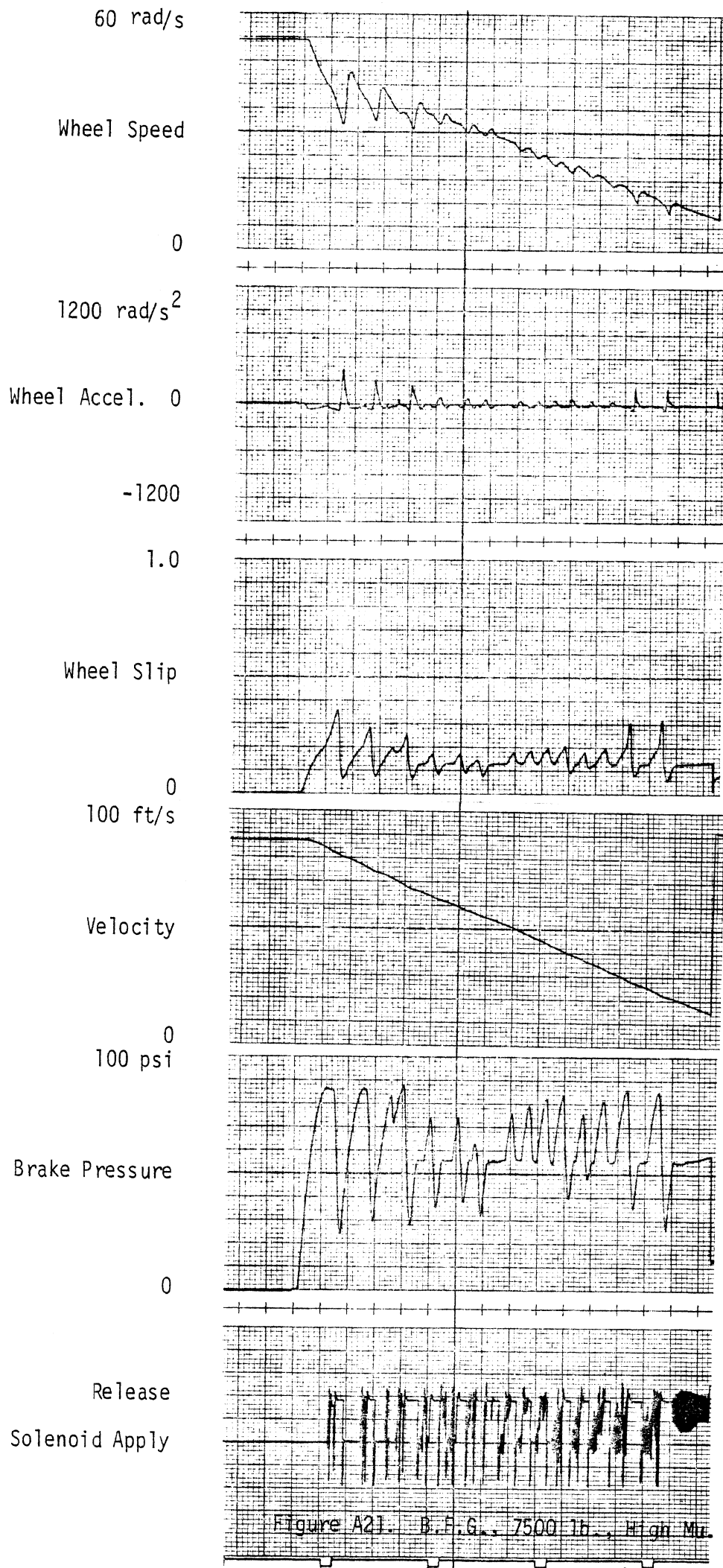


Figure A21. B.F.G., 7500 lb., High Mu.

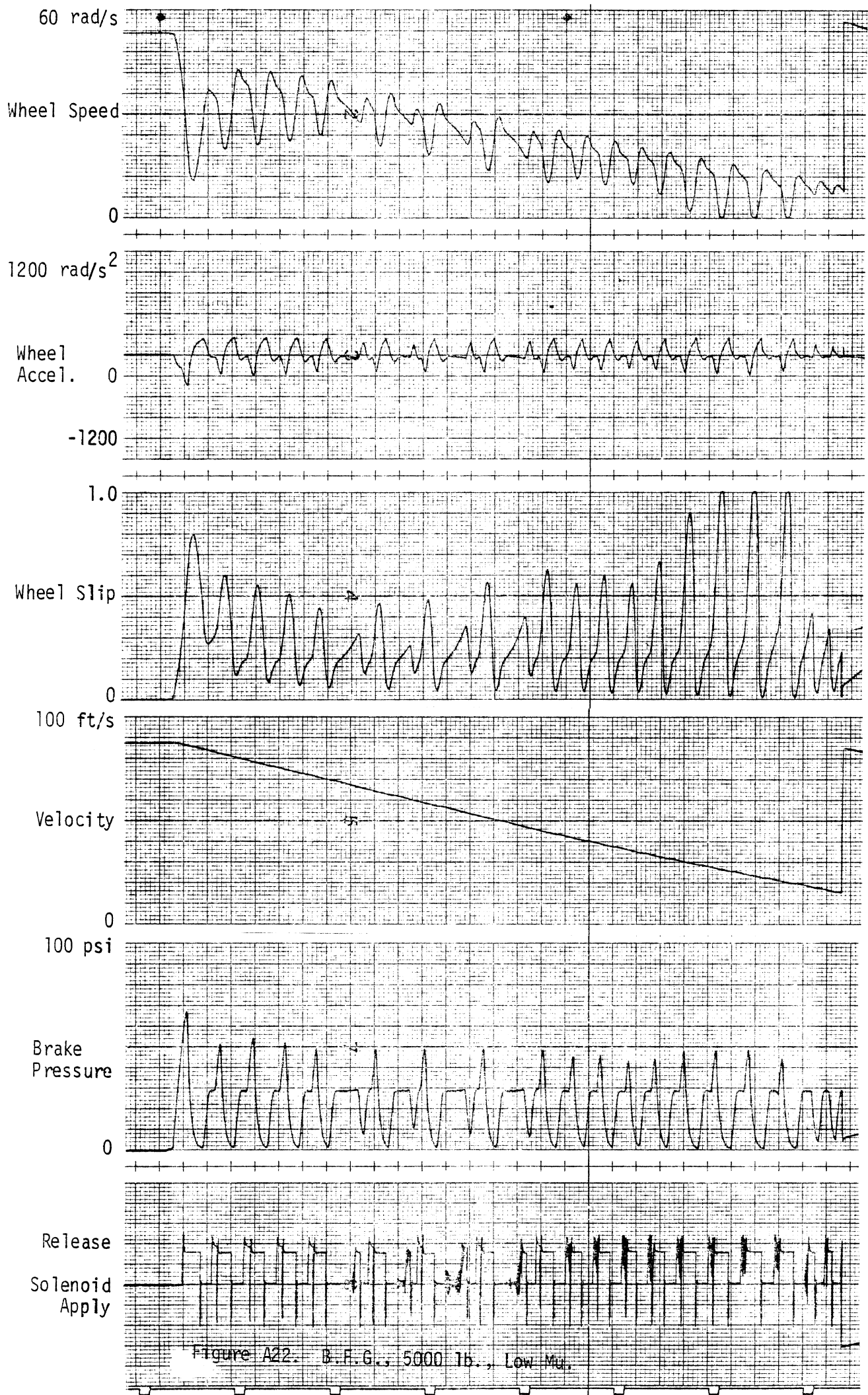
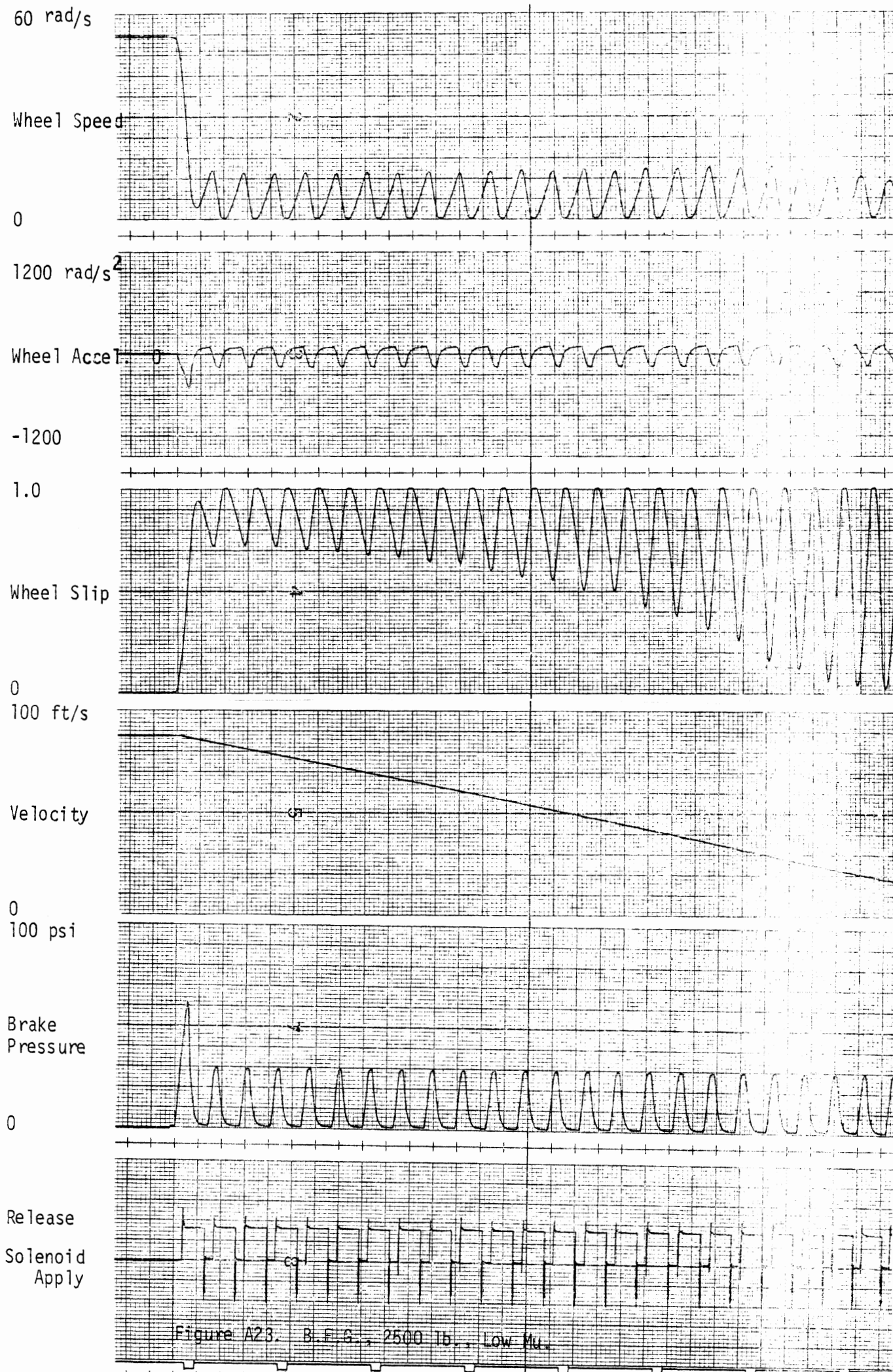


Figure A22. B.F.G., 5000 lb., Low Mu.



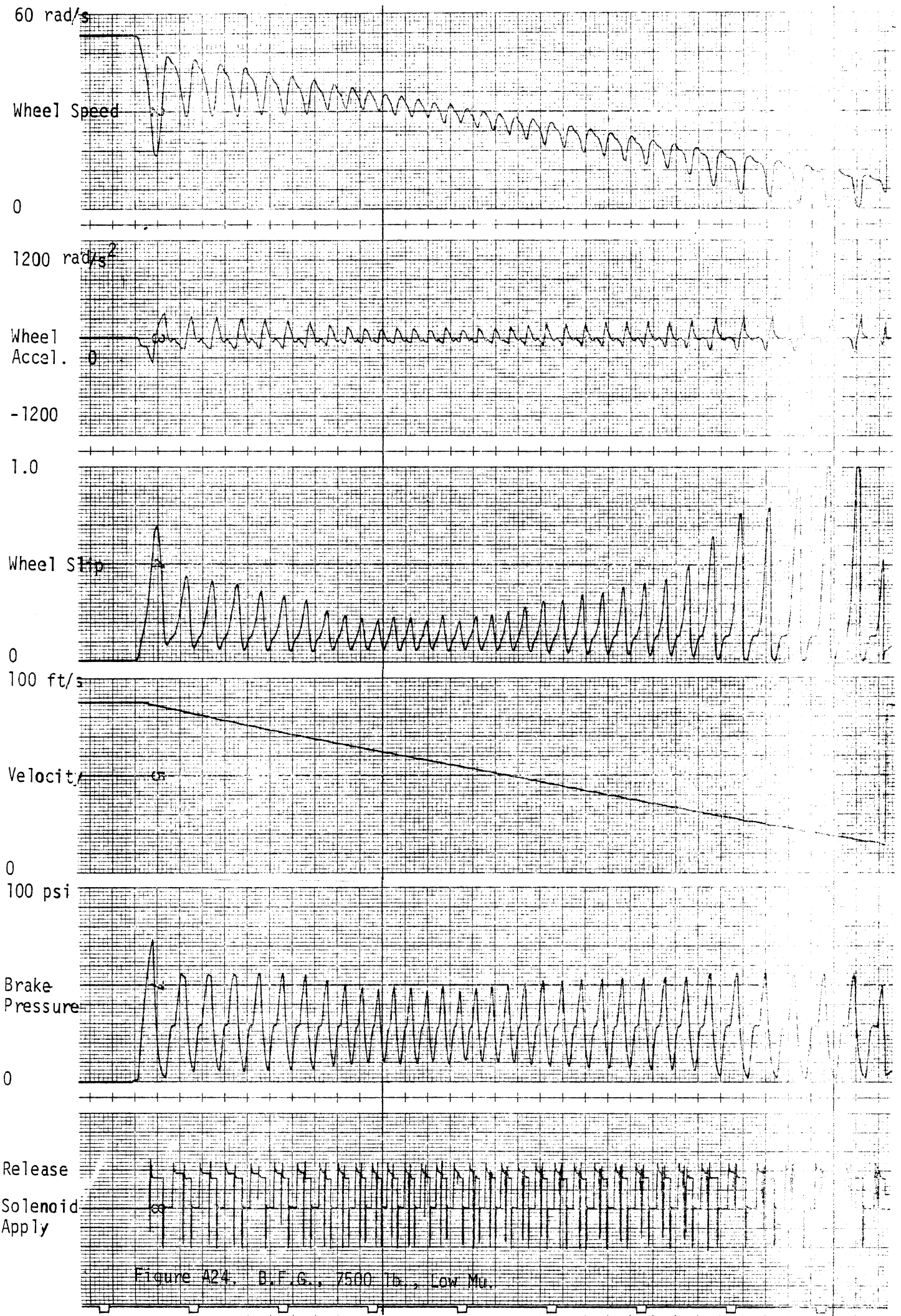


Figure A24. B.F.G., 7500 lb., Low Mu.

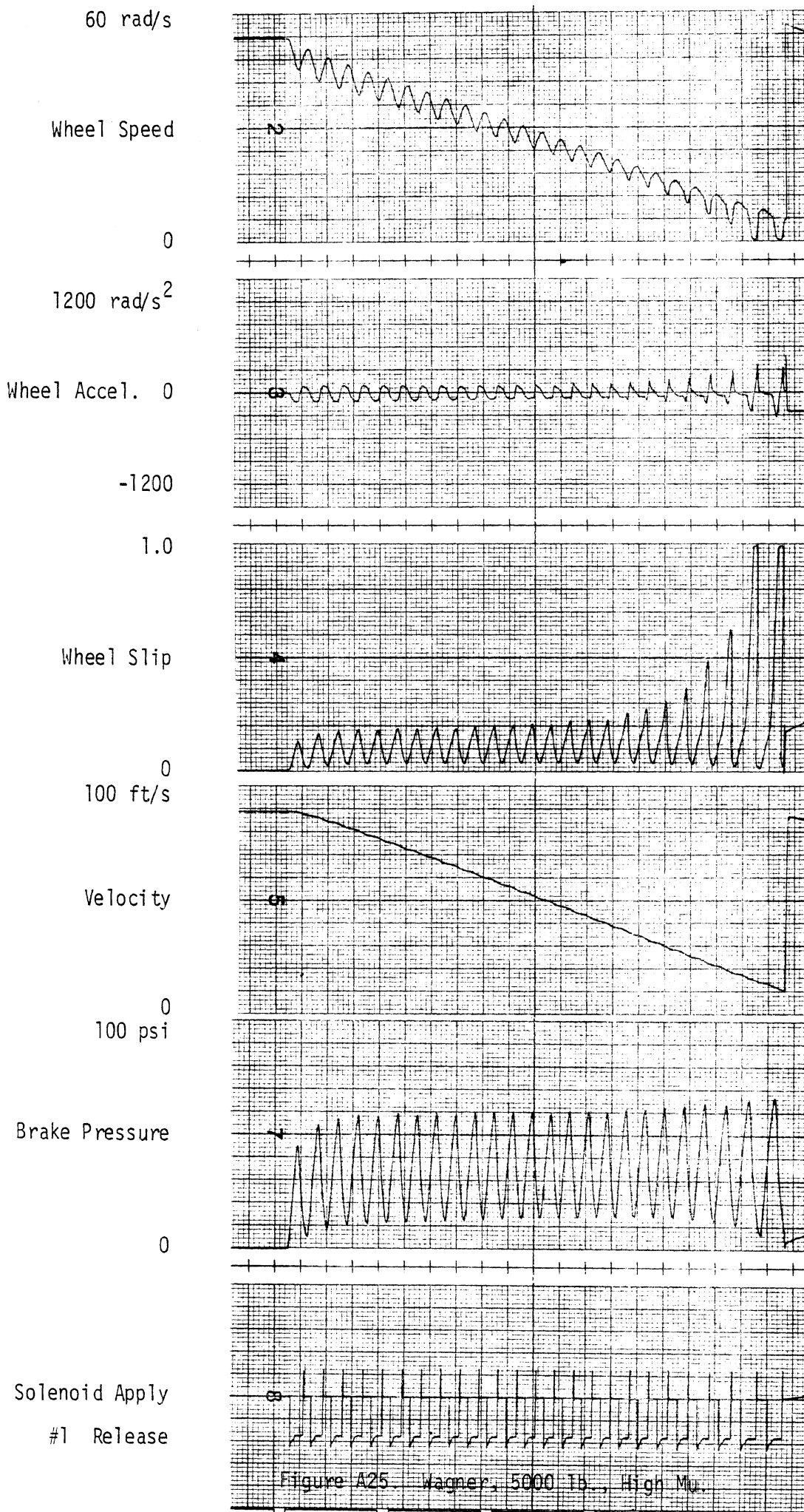


Figure A25. Wagner, 5000 lb., High Mu.

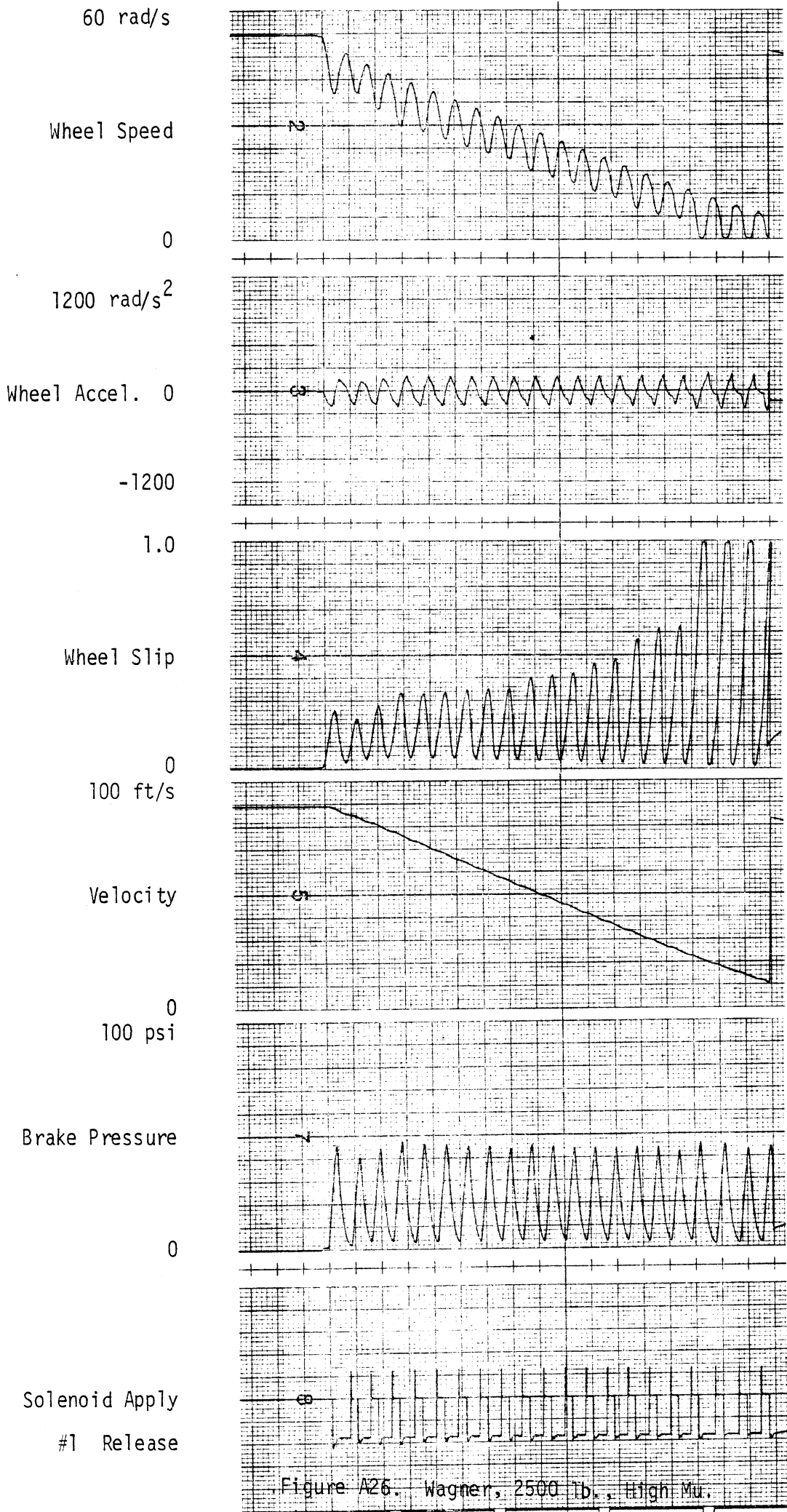


Figure A26. Wagner, 2500 lb., High Mu.

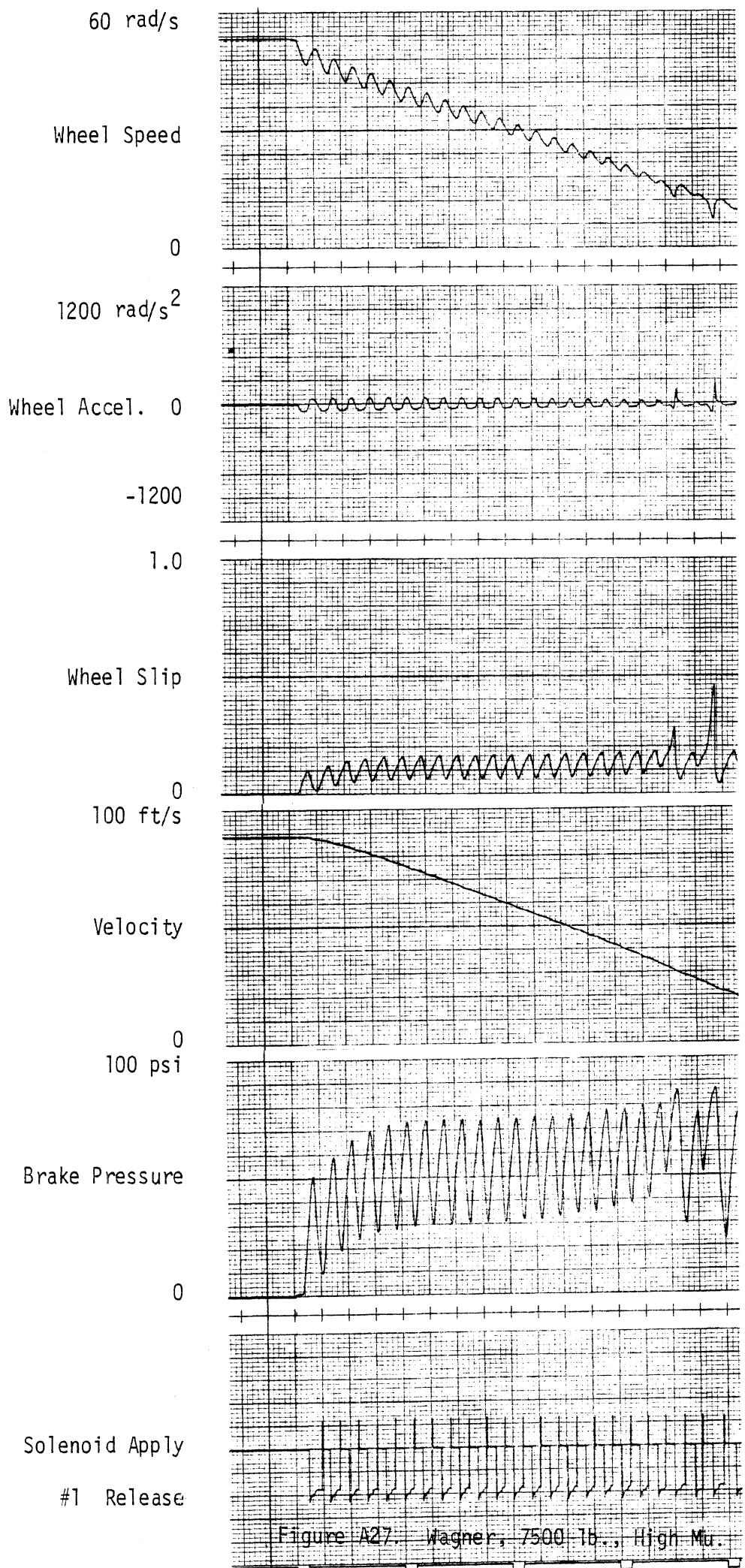


Figure A27. Wagner, 7500 lb., High Mu.

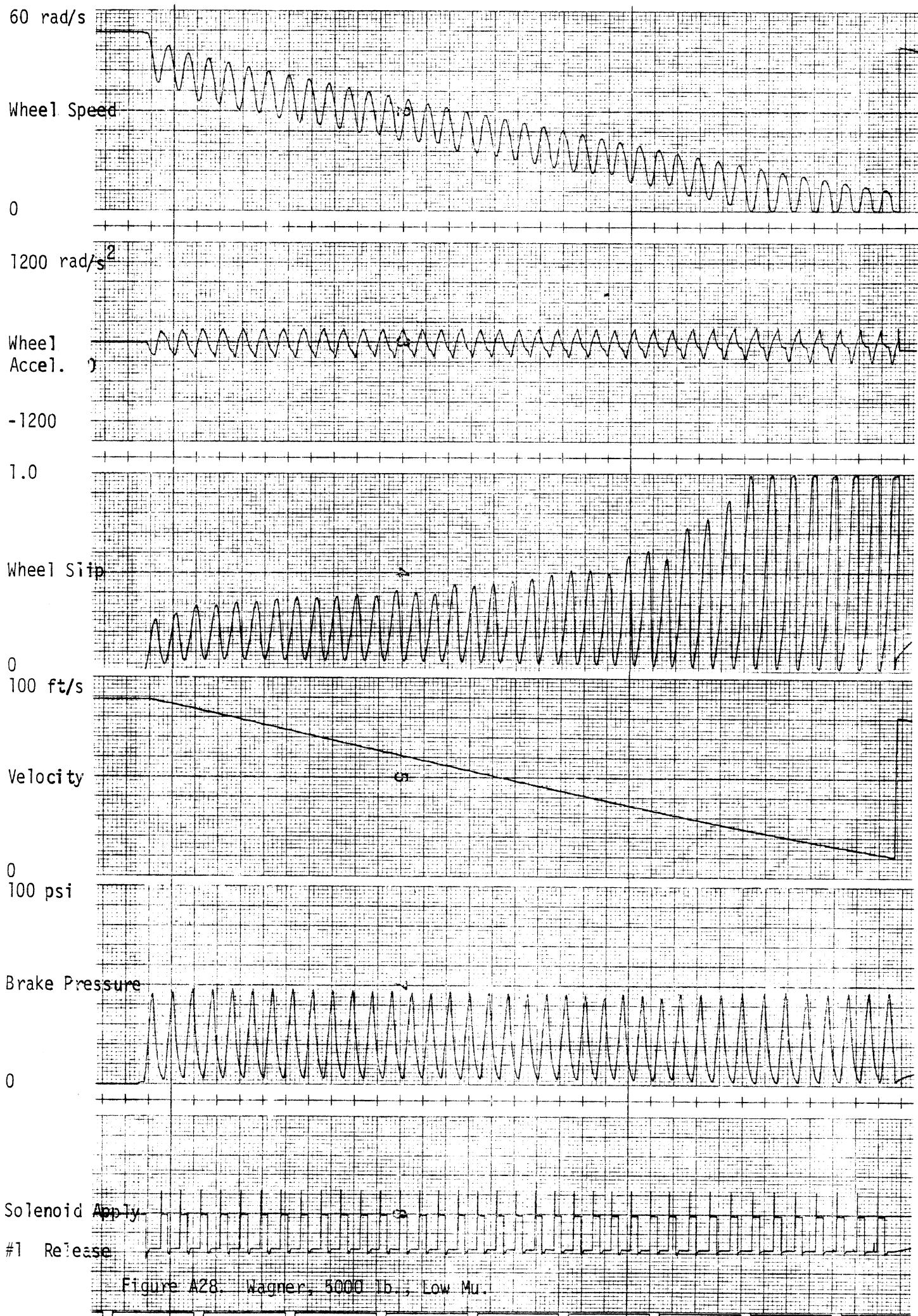
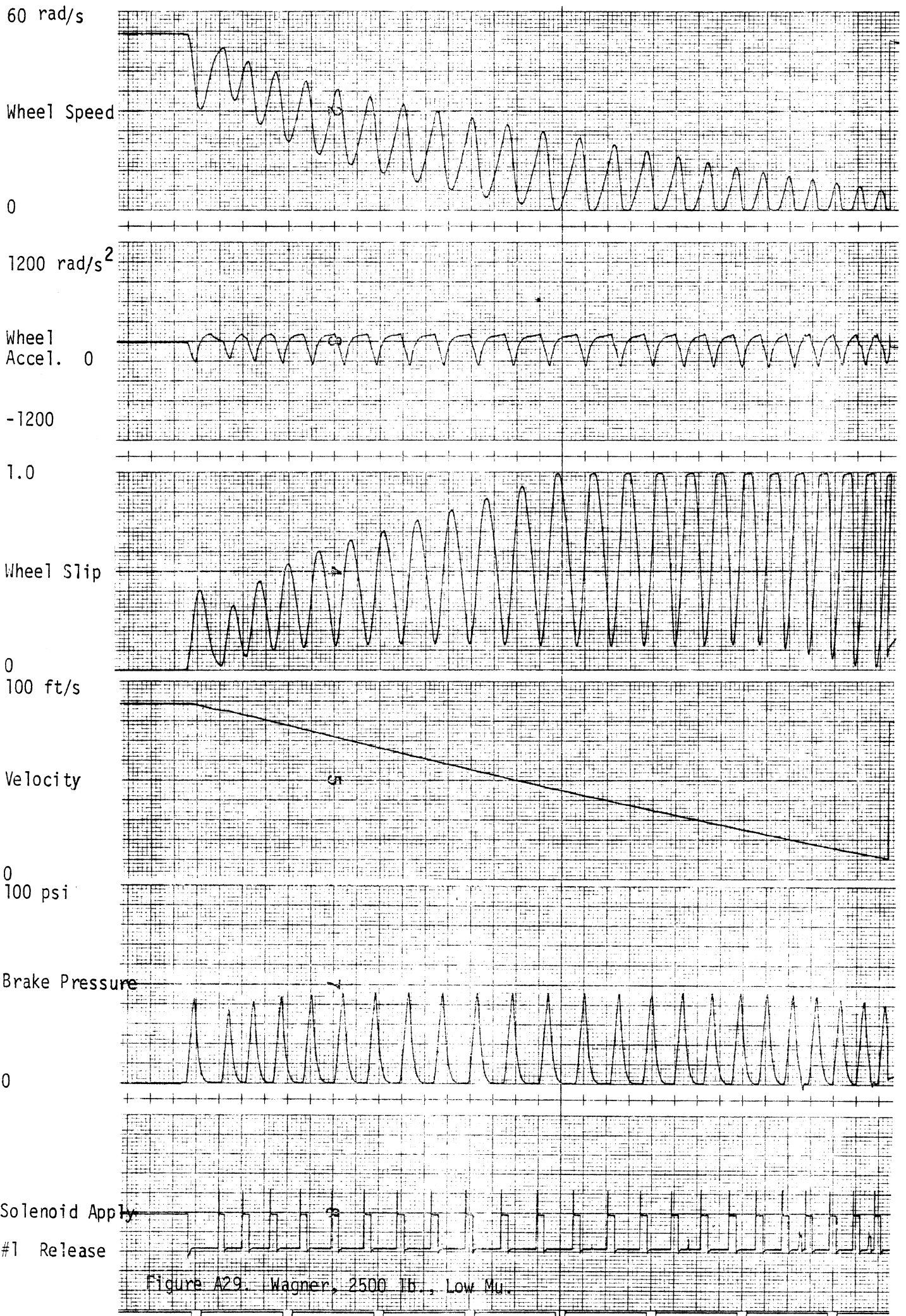
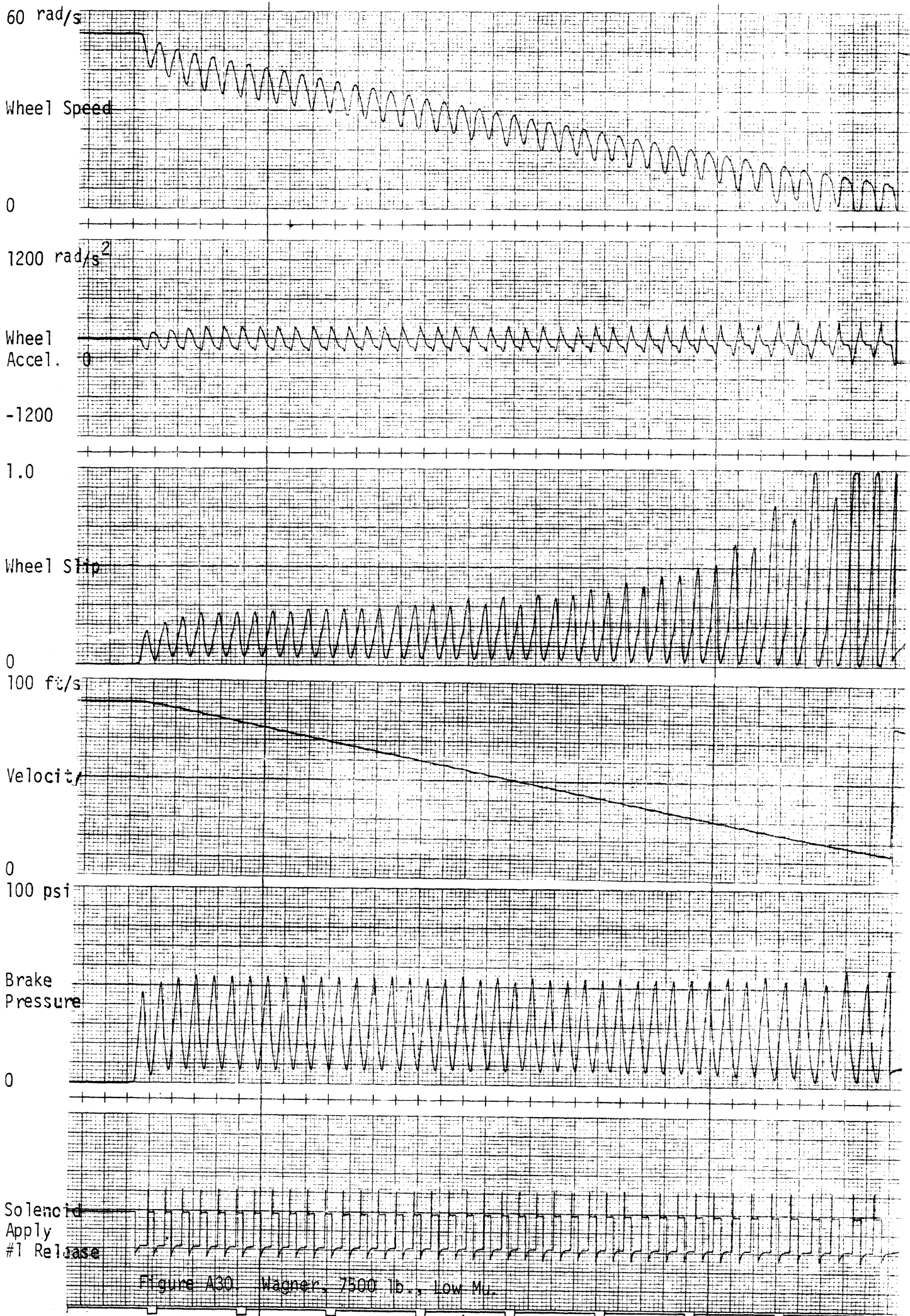


Figure A28. Wagner, 5000 lb., Low Mu.







## APPENDIX B

### EXAMPLE REGRESSION ANALYSIS USING THE DIGITAL ANTISKID LIBRARY DATA

The linear regressions shown in Section 3.3 of the report and within this appendix serve to provide simple and reasonable mathematical approximations or representations of the antiskid control logic under specific operating conditions. Furthermore, the forms of the derived mathematical expressions are, in general, compatible with the antiskid logical expressions used by the Phase III antiskid digital computer program.

Two example regressions are shown in this appendix using the data available in the digital library. These regressions are procedurally identical to the ones performed in Sections 3.3 except for: 1) the data used here is taken from the digital library and is subject to small quantization effects, and 2) the regressions shown here are performed for several cycles from a single test result — not for the same cycle over different tests, as was the case for the analog test results of Section 3.3.

The first example regressions are performed for the brake release (OFF) condition, followed by a second series of regressions for the re-apply (ON) condition. The data of file #110 (K-H system) is used for the example regressions. A partial listing of file #110 is shown in Table B-1.

Using the data from the second - tenth cycles, candidate regression variables at either brake release (OFF) or re-apply (ON) conditions are first recorded for each cycle as shown in Table B-2. Column 1 shows the cycle #, followed by  $\omega_0$  (wheel speed spin-up value for each cycle),  $\omega_{off}$  (wheel speed at brake release),  $\dot{\omega}_{off}$  (wheel acceleration at brake release),  $\omega_{on}$  (wheel speed at re-apply),  $\dot{\omega}_{on}$  (wheel acceleration at re-apply),  $t_{on}$  (time elapsed during each cycle from spin-up to re-apply), and  $t_{off}$  (time elapsed from spin-up to brake release).

The linear regression of  $\omega_{off}$  on  $\omega_0$ ,  $\dot{\omega}_{off}$ , and  $t_{off}$  for the data in Table B-2 yields,

Table B-1. Listing of Digital Library File #110.

```
>                                     *** KELSEY-HAYES ANTISKID SYSTEM ***
>INITIAL VELOCITY = 88 FT/SEC      LOAD = 5000 LBS
>WHEEL INERTIA = 150 INCH-LBS-SEC2  MU-PEAK = .80    MU-LOCK = .50
>REPEAT #2          BRAKE GAIN = 1500 INCH-LBS/PSI
```

Table B-1. Listing of Digital Library File #110 (Continued).

```

>
>          *** KELSEY-HAYES ANTISKID SYSTEM ***
>
>          WHEEL      WHEEL      BRAKE      WHEEL      FRICIT
> TIME      SPEED      ACCEL      PRESS      SLIP      VELOC      COEFF      SOL 1      SOL 2
> (SEC)     (RAD/S)    (RAD/S2) (PSI)     (PCT)     (FT/S)
>
>0.0       52.79       4.4        0.0        0.2       88.00      0.006      0.08      0.0
>0.01      52.76       -7.0       1.2        0.3       88.00      0.008      0.08      0.04
>0.02      52.73       0.8        0.8        0.3       87.98      0.010      0.08      0.04
>0.03      52.70       1.6        0.7        0.3       87.98      0.011      0.10     -0.02
>0.04      52.70       0.4        0.8        0.3       87.98      0.012      0.08      0.0
>0.05      52.69       0.6        0.8        0.3       87.98      0.012      0.08      0.0
>0.06      52.69       -6.6       1.5        0.4       87.98      0.013      0.08      0.02
>0.07      52.64       -7.6       1.8        0.4       87.98      0.016      0.08      0.04
>0.08      52.43      -30.8       5.1        0.8       87.98      0.031      0.10      0.02
>0.09      52.01     -51.0       9.5        1.6       87.96      0.064      0.08     -0.02
>0.10      51.35     -74.9      15.0       2.8       87.94      0.112      0.08      0.0
>0.11      50.48     -90.5      20.8       4.4       87.88      0.175      0.08      0.0
>0.12      49.51    -100.1     26.5       6.2       87.82      0.246      0.08     -0.02
>0.13      48.47    -103.4     31.9       8.1       87.70      0.321      0.10      0.0
>0.14      47.38    -106.6     37.4      10.0       87.60      0.399      0.08      0.04
>0.15      46.30    -105.7     42.4      11.9       87.46      0.475     10.04     -0.02
>0.16      45.24     -99.4     46.7      13.8       87.30      0.549      9.42      0.02
>0.17      44.26     -87.5     49.9      15.4       87.10      0.616      8.68     -0.02
>0.18      43.57     -47.0     48.8      16.6       86.88      0.661      8.70      0.04
>0.19      43.28      -8.5     45.9      16.9       86.68      0.676      8.88      0.0
>0.20      43.31     19.1     42.3      16.6       86.46      0.663      8.88     -0.02
>0.21      43.57     25.6     39.7      15.9       86.24      0.635      8.80      0.04
>0.22      43.88     31.6     37.1      15.1       86.06      0.603      8.78      0.02
>0.23      44.16     24.1     35.9      14.4       85.86      0.574      8.80     -0.02
>0.24      44.34     11.4     35.3      13.9       85.68      0.553      8.84      0.04
>0.25      44.42      6.1     35.5      13.5       85.50      0.539      8.84      0.0
>0.26      44.44      0.5     35.4      13.3       85.32      0.531      8.80      0.0
>0.27      44.42     -1.9     35.3      13.2       85.16      0.526      8.80      0.04
>0.28      44.42     13.3     33.3      13.0       84.98      0.519      8.82      0.0
>0.29      44.74     47.4     27.3      12.2       84.82      0.486      8.86      0.04
>0.30      45.38     73.0     21.3      10.8       84.66      0.430     -14.34     -0.02
>0.31      46.16     75.5     16.6      9.2        84.56      0.364     -3.08      0.04
>0.32      46.96     76.8     12.0      7.5        84.44      0.296     -3.16      0.0
>0.33      47.69     67.9      9.0      5.9        84.36      0.235     -0.04      0.04
>0.34      48.20     31.8      9.5      4.9        84.30      0.191      0.04      0.02
>0.35      48.35    -10.4     13.0      4.5        84.22      0.178      0.06      0.0
>0.36      48.02   -48.5     18.4      5.1        84.14      0.201      0.06     -0.02
>0.37      47.38   -73.4     24.0      6.3        84.10      0.249      0.08      0.04
>0.38      46.56   -86.6     30.5      7.8        83.98      0.309      0.06      0.02
>0.39      45.65   -92.0     34.5      9.5        83.88      0.378      0.08     -0.02
>0.40      44.71   -97.0     39.3     11.2       83.74      0.446      0.08      0.06
>0.41      43.90   -67.0     40.3     12.6       83.60      0.503      0.08      0.04
>0.42      43.36   -39.2     40.0     13.6       83.42      0.540      0.08     -0.02
>0.43      43.02   -27.8     40.6     14.1       83.26      0.559      0.08      0.02
>0.44      42.79   -15.1     39.6     14.3       83.06      0.570      0.08      0.04
>0.45      42.67    -9.1     39.0     14.4       82.88      0.572     10.08      0.0
>0.46      42.59    -1.7     38.3     14.4       82.70      0.571      9.56      0.0
>0.47      42.79     43.8     32.1     13.7       82.52      0.547      8.72      0.0
>0.48      43.38     73.8     25.1     12.4       82.36      0.491      9.06      0.06
>0.49      44.21     85.9     19.4     10.5       82.20      0.419     -3.63      0.0

```

Table B-1. Listing of Digital Library File #110 (Continued).

\*\*\* KELSEY-HAYES ANTISKID SYSTEM \*\*\*

>	WHEEL > TIME > (SEC)	WHEEL SPEED (RAD/S)	WHEEL ACCEL (RAD/S <sup>2</sup> )	BRAKE PRESS (PSI)	WHEEL SLIP (PCT)	VELOC (FT/S)	FRICT COEFF	SOL 1 (VOLTS)	SOL 2
>	>0.50	45.05	83.2	14.7	8.7	82.08	0.345	-0.98	0.02
>	>0.51	45.84	70.0	11.5	7.0	81.98	0.277	-0.92	0.02
>	>0.52	46.33	29.4	12.7	5.9	81.90	0.233	0.12	0.04
>	>0.53	46.34	-22.2	17.6	5.8	81.82	0.229	0.98	0.0
>	>0.54	45.90	-63.7	23.7	6.6	81.74	0.261	0.96	0.04
>	>0.55	45.20	-77.4	28.8	7.9	81.66	0.315	0.96	0.0
>	>0.56	44.36	-87.5	34.7	9.5	81.54	0.377	0.96	0.02
>	>0.57	43.45	-89.4	38.8	11.2	81.42	0.446	0.96	0.04
>	>0.58	42.54	-86.9	43.0	12.9	81.26	0.514	0.98	0.0
>	>0.59	41.75	-67.2	44.9	14.4	81.08	0.571	0.98	0.0
>	>0.60	41.20	-38.6	44.4	15.3	80.88	0.608	0.98	0.0
>	>0.61	40.88	-26.9	44.5	15.7	80.68	0.626	0.98	0.0
>	>0.62	40.64	-16.4	45.0	16.0	80.48	0.637	10.10	0.02
>	>0.63	40.55	2.9	43.1	16.0	80.28	0.635	9.58	0.02
>	>0.64	40.82	39.4	35.6	15.2	80.08	0.604	8.74	0.06
>	>0.65	41.51	77.8	27.8	13.5	79.88	0.539	-5.20	0.06
>	>0.66	42.38	92.3	21.4	11.5	79.72	0.459	-4.96	0.04
>	>0.67	43.30	89.3	16.2	9.5	79.60	0.377	-0.16	0.0
>	>0.68	44.09	61.0	14.4	7.7	79.48	0.306	0.02	-0.02
>	>0.69	44.44	13.9	17.0	6.9	79.36	0.272	0.98	0.02
>	>0.70	44.27	-39.2	22.8	7.1	79.30	0.282	0.98	0.0
>	>0.71	43.73	-66.4	28.3	8.2	79.20	0.324	0.98	0.04
>	>0.72	42.96	-79.1	33.6	9.7	79.10	0.384	0.98	0.04
>	>0.73	42.11	-85.9	38.5	11.3	78.96	0.449	0.10	0.02
>	>0.74	41.22	-87.4	43.3	13.0	78.80	0.517	0.98	0.0
>	>0.75	40.33	-82.6	47.3	14.6	78.62	0.584	0.98	-0.02
>	>0.76	39.58	-62.3	48.9	16.0	78.40	0.639	0.98	0.02
>	>0.77	39.08	-34.2	48.2	16.9	78.22	0.672	0.98	0.02
>	>0.78	38.78	-25.2	48.4	17.3	77.98	0.687	11.58	0.04
>	>0.79	38.57	-13.4	47.8	17.5	77.74	0.696	10.00	0.04
>	>0.80	38.57	13.8	44.0	17.3	77.54	0.687	9.24	0.06
>	>0.81	39.06	69.6	35.4	16.0	77.30	0.636	8.64	-0.02
>	>0.82	39.89	92.0	27.8	13.9	77.10	0.556	-3.38	0.0
>	>0.83	40.84	95.4	21.5	11.7	76.96	0.466	-2.12	0.0
>	>0.84	41.75	85.2	16.9	9.6	76.80	0.380	-0.92	0.0
>	>0.85	42.42	37.4	17.6	8.0	76.72	0.318	0.02	0.04
>	>0.86	42.54	-14.6	21.8	7.6	76.62	0.303	0.96	0.04
>	>0.87	42.14	-53.3	27.5	8.4	76.52	0.332	0.14	0.0
>	>0.88	41.48	-73.4	33.0	9.6	76.40	0.384	0.98	-0.02
>	>0.89	40.69	-82.4	38.1	11.3	76.28	0.448	0.98	0.0
>	>0.90	39.83	-85.4	43.0	13.0	76.12	0.516	0.98	-0.02
>	>0.91	38.96	-84.6	47.4	14.7	75.92	0.583	0.98	-0.02
>	>0.92	38.11	-78.6	51.2	16.3	75.72	0.648	0.98	0.02
>	>0.93	37.39	-56.6	52.6	17.6	75.50	0.702	0.98	0.04
>	>0.94	36.95	-31.3	51.9	18.4	75.28	0.731	0.98	-0.02
>	>0.95	36.66	-24.4	52.1	18.7	75.04	0.746	10.22	0.0
>	>0.96	36.47	-10.6	50.7	18.9	74.80	0.752	9.70	0.04
>	>0.97	36.71	52.2	42.8	18.1	74.54	0.720	8.78	0.0
>	>0.98	37.43	80.9	34.7	16.2	74.34	0.646	-16.02	0.02
>	>0.99	38.38	100.2	26.8	13.9	74.14	0.552	-3.82	0.04

Table B-1. Listing of Digital Library File #110 (Continued).

```

>
>          *** KELSEY-HAYES ANTISKID SYSTEM ***
>
> TIME      WHEEL      WHEEL      BRAKE      WHEEL      VELOC      FRICT      SOL 1      SOL 2
> (SEC)     (RAD/S)    (RAD/S2) (PSI)     (PCT)     (FT/S)    COEFF      (VOLTS)
>
>1.00      39.35         90.6        21.4       11.5       73.98      0.456      -0.66      0.04
>1.01      40.24         66.4        17.7        9.3       73.84      0.370      -0.02      0.04
>1.02      40.76         19.7        19.8        8.0       73.74      0.318      0.04      0.04
>1.03      40.69        -38.0        25.2        8.1       73.62      0.320      0.06      0.04
>1.04      40.19        -68.2        31.0        9.1       73.52      0.360      0.08      0.06
>1.05      39.46        -84.6        36.3       10.5       73.40      0.420      0.06      0.02
>1.06      38.63        -84.8        41.1       12.3       73.26      0.488      0.06      0.0
>1.07      37.78        -84.8        45.8       14.0       73.08      0.558      0.08      0.0
>1.08      36.92        -81.2        50.1       15.8       72.90      0.628      0.06      0.02
>1.09      36.11        -78.0        54.8       17.3       72.66      0.691      0.06      0.04
>1.10      35.38        -61.6        56.1       18.8       72.44      0.748      0.08      -0.02
>1.11      34.90        -38.5        55.5       19.6       72.18      0.781      0.08      0.04
>1.12      34.62        -23.2        55.4       20.0       71.94      0.795      9.98      0.0
>1.13      34.45          8.3        52.3       20.0       71.66      0.797      9.48      0.06
>1.14      34.84         66.0        43.4       18.8       71.44      0.750      8.50      0.04
>1.15      35.68         94.7        34.6       16.6       71.20      0.662      -5.70     0.0
>1.16      36.66        101.6       27.1       14.1       71.00      0.559      -4.34     0.0
>1.17      37.66         95.6       21.0       11.5       70.84      0.459      -0.13     0.04
>1.18      38.50         63.8       19.2        9.4       70.70      0.373      0.02      0.02
>1.19      38.87          6.2       21.8        8.4       70.58      0.334      0.06      0.0
>1.20      38.63        -44.3       27.9        8.8       70.48      0.350      0.08      0.0
>1.21      38.08        -67.8       33.4       10.0       70.36      0.399      0.10      0.0
>1.22      37.28        -77.8       38.8       11.7       70.22      0.464      0.06      0.04
>1.23      36.46        -82.8       44.0       13.4       70.06      0.535      0.08      0.0
>1.24      35.62        -82.4       48.7       15.2       69.88      0.605      0.08      -0.02
>1.25      34.80        -77.5       52.7       16.9       69.66      0.674      -0.04     0.04
>1.26      34.02        -73.4       56.5       18.5       69.44      0.736      0.08      0.02
>1.27      33.34        -59.2       58.7       19.8       69.20      0.791      0.08      0.0
>1.28      32.78        -54.8       58.5       20.9       68.94      0.796      11.80     0.06
>1.29      32.29        -46.9       57.6       21.8       68.66      0.793      10.02     0.04
>1.30      31.92         -6.6       53.8       22.4       68.42      0.791      9.30      0.02
>1.31      32.33         89.6       44.0       21.1       68.14      0.795      8.70      -0.02
>1.32      33.52        124.4       35.0       17.9       67.92      0.711      -5.22     0.04
>1.33      34.73        115.0       27.4       14.7       67.70      0.583      -4.60     0.04
>1.34      35.81         99.0       21.3       11.8       67.52      0.467      -0.14     0.0
>1.35      36.65         63.1       18.9        9.5       67.38      0.377      0.02      0.0
>1.36      36.98          3.0       22.6        8.5       67.28      0.339      0.06      0.04
>1.37      36.72        -47.0       28.9        9.1       67.18      0.360      0.08      -0.02
>1.38      36.10        -67.9       34.5       10.4       67.04      0.414      0.08      0.02
>1.39      35.34        -82.4       40.8       12.1       66.88      0.482      0.06      0.04
>1.40      34.54        -80.3       45.1       13.9       66.72      0.554      -0.22     0.0
>1.41      33.70        -80.4       49.9       15.7       66.54      0.627      0.08      0.0
>1.42      32.92        -73.9       53.8       17.5       66.34      0.695      0.08      0.04
>1.43      32.17        -69.5       57.5       19.0       66.08      0.753      0.06      0.04
>1.44      31.48        -72.1       60.5       20.5       65.84      0.798      0.08      0.0
>1.45      30.71        -75.2       60.4       22.1       65.58      0.792      0.08      -0.02
>1.46      29.96        -71.9       59.7       23.7       65.32      0.786      10.10     0.0
>1.47      29.24        -60.5       58.1       25.2       65.06      0.780      9.64      0.0
>1.48      29.06         30.6       48.9       25.4       64.80      0.779      8.82      0.0
>1.49      29.88        134.3       39.2       23.0       64.56      0.788      8.68      -0.02

```

Table B-1. Listing of Digital Library File #110 (Continued).

```

>
>>> KELSEY-HAYES ANTISKID SYSTEM >>>
>
>TIME      WHEEL      WHEEL      BRAKE      WHEEL      VELOC      FRICT
>(SEC)     SPEED      ACCEL      PRESS     SLIP       (FT/S)     COEFF      SOL 1      SOL 2
>          (RAD/S)   (RAD/S2) (PSI)     (PCT)
>
>1.50      31.60      176.5      30.7       18.2       64.30      0.725     -14.80     -0.02
>1.51      33.13      130.7      24.0       14.0       64.12      0.556     -4.02      -0.02
>1.52      34.28      101.9      18.4       10.8       63.96      0.429     -0.46      0.04
>1.53      35.15       68.8      15.3        8.4       63.82      0.331      0.02     -0.02
>1.54      35.56       11.6      17.9        7.2       63.72      0.285      0.06      0.04
>1.55      35.34      -43.3      24.5        7.6       63.64      0.302      0.06     -0.02
>1.56      34.75      -65.9      30.4        9.0       63.52      0.357      0.06      0.02
>1.57      34.03      -78.0      36.4       10.7       63.40      0.427      0.08      0.0
>1.58      33.20      -80.6      41.7       12.6       63.24      0.504      0.08      0.0
>1.59      32.39      -79.2      46.8       14.6       63.06      0.581      0.08      0.04
>1.60      31.58      -76.0      51.3       16.5       62.88      0.654      0.06      0.02
>1.61      30.83      -71.4      55.3       18.2       62.66      0.722      0.08      0.02
>1.62      30.14      -64.3      58.8       19.7       62.42      0.784      0.08     -0.02
>1.63      29.41      -66.8      61.8       21.4       62.16      0.795      0.08      0.0
>1.64      28.40     -101.4      62.6       23.7       61.90      0.786      0.08      0.04
>1.65      27.40     -97.1      61.6       26.1       61.64      0.777     10.20      0.04
>1.66      26.39     -90.4      60.3       28.5       61.40      0.768      9.68      0.0
>1.67      25.87      -2.0      51.1       29.6       61.14      0.763      8.86      0.0
>1.68      26.38     103.1      40.9       28.0       60.90      0.770      8.66      0.06
>1.69      27.91     201.0      32.3       23.5       60.64      0.787      8.84     -0.02
>1.70      30.14     198.5      25.2       16.9       60.40      0.674     -11.24     -0.02
>1.71      31.76     129.1      19.6       12.3       60.20      0.486      -4.12      0.0
>1.72      32.84      79.7      15.5        9.0       60.08      0.358     -0.32      0.04
>1.73      33.58      51.4      13.1        6.9       59.98      0.272      0.02      0.04
>1.74      33.80      -7.8      17.0        6.1       59.92      0.241      0.06      0.0
>1.75      33.48     -52.7      23.9        6.9       59.82      0.273      0.06      0.04
>1.76      32.84     -70.0      29.5        8.5       59.72      0.337      0.06      0.04
>1.77      32.09     -78.1      35.5       10.4       59.60      0.414      0.08      0.0
>1.78      31.30     -78.6      40.9       12.4       59.44      0.494      0.08      0.0
>1.79      30.52     -76.9      46.0       14.4       59.28      0.573      0.08      0.0
>1.80      29.75     -74.0      50.7       16.3       59.06      0.648      0.08      0.0
>1.81      29.00     -69.5      54.9       18.0       58.86      0.718      0.08     -0.02
>1.82      28.32     -63.6      58.6       19.6       58.62      0.782      0.08     -0.02
>1.83      27.61     -85.0      61.6       21.3       58.36      0.795      0.08      0.04
>1.84      26.56    -120.2      64.4       24.0       58.10      0.785      0.08      0.04
>1.85      25.26    -129.1      64.5       27.4       57.84      0.772     11.12     -0.02
>1.86      23.95    -129.5      63.6       30.9       57.60      0.759      9.90      0.04
>1.87      22.85     -69.2      56.9       33.7       57.36      0.748      9.10     -0.02
>1.88      22.64      33.6      46.4       34.0       57.12      0.747      8.68      0.0
>1.89      23.52     138.2      36.6       31.2       56.88      0.758      8.82      0.06
>1.90      25.36     230.9      28.9       25.4       56.62      0.779      8.92     -0.02
>1.91      27.98     238.0      22.3       17.4       56.36      0.690      8.86      0.04
>1.92      29.83     134.5      17.1       11.7       56.18      0.464     -3.76      0.06
>1.93      30.92      85.6      12.8        8.2       56.06      0.326     -0.92      0.06
>1.94      31.61      48.4      11.2        6.1       55.98      0.238      0.0        0.02
>1.95      31.82      -7.6      14.8        5.3       55.90      0.208      0.06      0.04
>1.96      31.50     -48.6      21.1        6.1       55.84      0.242      0.08      0.0
>1.97      30.90     -67.3      27.5        7.8       55.74      0.310      0.08     -0.02
>1.98      30.16     -74.3      33.6        9.3       55.64      0.389      0.08      0.0
>1.99      29.39     -73.9      39.0       11.9       55.50      0.473      0.08     -0.02

```



Table B-2. Candidate Regression Variables (File #110).

<u>Cycle #</u>	<u><math>\omega_0</math></u>	<u><math>\omega_{\text{off}}</math></u>	<u><math>\dot{\omega}_{\text{off}}</math></u>	<u><math>\omega_{\text{on}}</math></u>	<u><math>\dot{\omega}_{\text{on}}</math></u>	<u><math>t_{\text{on}}</math></u>	<u><math>t_{\text{off}}</math></u>
2	48.3	42.7	- 9.1	44.2	85.9	.14	.10
3	46.3	40.6	-16.4	41.5	77.8	.12	.09
4	44.4	38.8	-25.2	39.9	92.0	.13	.09
5	42.5	36.7	-24.4	37.4	80.9	.12	.09
6	40.8	34.6	-23.2	35.7	94.7	.13	.10
7	38.9	32.8	-54.8	33.5	124.0	.13	.09
8	37.0	30.0	-71.9	31.6	176.0	.14	.10
9	35.6	27.4	-97.1	30.1	198.0	.16	.11
10	33.8	25.3	-129.0	29.8	134.0	.18	.11

$$\omega_{\text{off}} = -2.06 + 1.028 \omega_0 + 0.0157 \dot{\omega}_{\text{off}} - 49.3 t_{\text{off}}$$

with a coefficient of determination value,  $R^2$ , of 0.999. A comparison of  $\omega_{\text{off}}$  values with those predicted by the above regression equation is shown in Table B-3.

An alternative regression in which the above variables are first normalized by  $\omega_0$  yields the result,

$$\omega_{\text{off}} = 1.00 \omega_0 + 0.017 \dot{\omega}_{\text{off}} - 58.6 t_{\text{off}}$$

with an  $R^2$  value of 0.994. Clearly, either one of the above regressions could be used to represent the brake-release switching logic under these operating conditions.

For the brake re-apply (ON) condition, the regression of  $\omega_{\text{on}}$  on  $\omega_0$ ,  $\dot{\omega}_{\text{on}}$ , and  $t_{\text{on}}$  from Table B-2 yields the equation,

$$\omega_{\text{on}} = -10.9 + 1.06 \omega_0 - .010 \dot{\omega}_{\text{on}} + 33.8 t_{\text{on}}$$

with an  $R^2$  value of 0.999. The  $\omega_{\text{on}}$  data is compared with the predicted values from the above regression in Table B-4.

An alternative regression of  $\omega_{\text{on}}$  on  $\omega_{\text{off}}$  and  $(t_{\text{on}} - t_{\text{off}})$  yields the equation,

$$\omega_{\text{on}} = -1.24 + .981 \omega_{\text{off}} + 85.7 (t_{\text{on}} - t_{\text{off}})$$

with an  $R^2$  value of 0.994.

Ignoring the influence of the  $(t_{\text{on}} - t_{\text{off}})$  term, the regression simply becomes,

$$\omega_{\text{on}} = 6.71 + .852 \omega_{\text{off}}$$

with an  $R^2$  value of 0.972.

Again, it appears that quite reasonable approximations to the control logic can be derived with the use of linear regressions. However it should be emphasized that these regressions, such as the examples in this Appendix, only apply to specific operating conditions. If antiskid behavior over a

Table B-3.  $\omega_{\text{off}}$  vs. Regression Predictions.

<u><math>\omega_{\text{off}}</math></u>	<u>Regression Prediction</u>	<u>Cycle #</u>
42.7	42.5	2
40.6	40.8	3
38.8	38.8	4
36.7	36.8	5
34.6	34.6	6
32.8	32.6	7
30.0	29.9	8
27.4	27.6	9
25.3	25.2	10

Table B-4.  $\omega_{on}$  vs. Regression Predictions.

<u><math>\omega_{on}</math></u>	<u>Regression Prediction</u>	<u>Cycle #</u>
44.2	44.2	2
41.5	41.5	3
39.9	39.7	4
37.4	37.5	5
35.7	35.9	6
33.5	33.5	7
31.6	31.4	8
30.1	30.3	9
29.8	29.7	10

variety of operating conditions or transient load variations is to be accurately represented, then larger sets of data, representative of those different operating conditions, need to be included in the analysis. For example, extending the data set shown in Table B-2 to include the lighter and heavier wheel load data, and then performing regressions similar to those shown in the above examples. Adaptive features are available within the Phase III digital antiskid program [1] and could also be employed to alter the control logic under different operating conditions.